MULTISCALE HABITAT SUITABILITY MODELING FOR CANARY ROCKFISH (*SEBASTES PINNIGER*) ALONG THE NORTHERN CALIFORNIA COAST

By

Portia Naomi Saucedo

A Thesis Presented to

The Faculty of Humboldt State University

In Partial Fulfillment of the Requirements for the Degree

Master of Science in Natural Resources: Environmental and Natural Resource Sciences

Committee Membership

Dr. Jim Graham, Committee Chair

Dr. Brian Tissot, Committee Member

Dr. Joe Tyburczy, Committee Member

Dr. Alison Purcell O'Dowd, Graduate Coordinator

July 2017

ABSTRACT

MULTISCALE HABITAT SUITABILITY MODELING FOR CANARY ROCKFISH (*SEBASTES PINNIGER*) ALONG THE NORTHERN CALIFORNIA COAST

Portia N. Saucedo

Detailed spatially-explicit data of the potential habitat of commercially important rockfish species are a critical component for the purposes of marine conservation, evaluation, and planning. Predictive habitat modeling techniques are widely used to identify suitable habitat in un-surveyed regions. This study elucidates the predicted distribution of canary rockfish (*Sebastes pinniger*) along the largely un-surveyed northern California coast using data from visual underwater surveys and predictive terrain complexity covariates. I used Maximum Entropy (MaxEnt) modelling software to identify regions of suitable habitat for *S. pinniger* greater than nine cm in total length at two spatial scales. The results of this study indicate the most important environmental covariate was proximity to the interface between hard and soft substrate. I also examined the predicted probability of presence for each model run. MaxEnt spatial predictions varied in predicted probability for broad-scale and each of the fine-scale regions. Uncertainty in predictions was considered at several levels and spatial uncertainty was quantified and mapped. The predictive modeling efforts allowed spatial predictions outside the sampled area at both the broad- and fine-scales accessed. This approach demonstrates that single-species suitable habitat can be defined with species-specific

covariates. Further, this approach may be applicable to other rockfish species to aid fisheries management in the delineation of essential fish habitat as well as in conservation efforts in marine spatial planning.

ACKNOWLEDGEMENTS

I would like to thank my thesis committee: Brian Tissot and Joe Tyburczy. I'd also like to thank Tim Bean for his involvement with this project. Without the expertise and guidance of these individuals, this project would not have been possible. Thank you, Jim Graham, for being a stellar graduate advisor during my nontraditional stint at Humboldt State University.

Many thanks to the team at Marine Applied Research and Exploration for these data and support. Thank you to graduate students Melissa Kimble, Jonathan Centori, and Emily Cooper for being awesome peers through our struggle to acquire our respective degrees.

To Calypso, my loving daughter, thank you for being a wonderful light throughout this educational journey. Many thanks to my family and friends for supporting me in following my dreams since my earliest inklings of interest in marine science.

TABLE OF CONTENTS

LIST OF TABLES

LIST OF FIGURES

LIST OF APPENDICES

INTRODUCTION

Many marine fish species are experiencing overexploitation and habitat destruction. Worm et al. (2006) predicts that without immediate action to mitigate anthropogenic impacts some commercial fisheries may collapse beyond the point of recovery. Commercial and recreational fisheries rely upon the deep-water fish assemblages that dominate the rocky habitats along the California coast (Love and Yoklavich 2006). Despite some significant recoveries since the late 1990s, in northern California once robust rockfish populations are now only remnants of their original numbers due to direct and indirect anthropogenic pressures (PFMC 2003; Bloeser, 1999). The genus *Sebastes* is a diverse group of rockfishes which is currently comprised of 65 known species. Many of these rockfish species live over 100 years, are slow-growing, and experience late sexual maturity (Love et al. 2002). Because of these life-history characteristics coupled with fishing pressure targeting larger-bodied, more fecund individuals (Hixon et al. 2014), most rockfish populations are susceptible to and or are suffering from overfishing. There are over 40 species of rockfish that dominate these deep-water rocky habitats and six of these species, including the commercially important canary rockfish, *Sebastes pinniger*, have been classified as "overfished" by the National Marie Fisheries Service and Pacific Management Council (PMFC 2011). Most recently, *S. pinniger* catches have been reported at historical lows since the fishing increase of 1916 (Thorson and Wetzel 2015). To rebuild these depleted stocks, the US Sustainable Fisheries Act of 1996 title 16, section 1854e (16 U.S.C. § 1854[e]) emphasized the

significance of identifying the biological and physical habitat aspects that influence species distribution and abundance.

In California, *S. pinniger* is considered a "Species of Concern" and is monitored by both PFMC and the California Department Fish and Wildlife (CDFW)." *S. pinniger* is a fecund ovoviviparous iteroparous rockfish, with egg production being correlated with size: approximately 69,000 eggs at 27 cm total length; 489,000 eggs at 44 cm total length; and 1,113,000 eggs at 54 cm annually (NOAA 2017). *S. pinniger* is a relatively large demersal rockfish that can weigh up to approximately four kg and reach a total length of approximately 76 cm (Miller and Lea 1972). It is estimated that roughly 50 percent of *S. pinniger* adults are mature at 40 cm (seven to nine years of age) (NMFS 2014). *S. pinniger* is a long-lived rockfish species with an estimated lifespan of 84 years (Love et al. 2002; Andrews et al. 2007). Adults are a bright orange-yellow with olive-gray mottling and have three prominent orange stripes that run diagonally across the head. The fins of this species are distinctive. The anal fin is pointed and slanted anteriorly and the caudal fin bares a strong indentation in its center (Love et al. 2002). Juveniles (less than approximately 35 cm) are large-headed, thin-bodied, bare some brass-colored modeling with gray/white background, are marked with a dark brown-black spot on the posterior end of the dorsal fin (Love et al. 2002), and are found in high densities in kelp forests (Carr 1991). Juveniles move from shallow (11 m) to deeper waters during the end of summer (Love et al. 2002). Adults hover in loose groups above rocky bottoms to 30 m above the seafloor in mid-water aggregations in areas of substantial current flow (Love & Yoklavich 2006; Lamb and Edgell, 1986). *S. pinniger* is most commonly found from

central California to Alaska at depths of 80 – 200 m (Love et al. 2002). Some individual fish have been tagged and shown to move long distances (approximately 700 km) along the western coast of the United States (Love et al. 2002). *S. pinniger* generally show site fidelity to rocky outcroppings, although information on the geospatial distribution of canary rockfish in untrawlable habitat in Northern California is currently sparse (CDFG 2008; PFMC 2005).

Assessment of fish populations using Remote Operated Vehicles (ROVs) and human-occupied submersibles are now standard methods by which to gather detailed data on rockfishes in both untrawlable and trawlable areas (Stein et al. 1992, Auster et al. 2003, Busby et al. 2005, Wakefield et al. 2005). Used in tandem with ROVs/submersibles, remotely-sensed acoustic imagery and video data are common methods by which data are collected to produce benthic habitat maps (Jordan et al., 2005; Lundblad et al., 2006; Wilson et al., 2007; Lucieer, 2008). Multi-beam sonar imagery of the sea floor makes it possible to differentiate hard and soft benthic sediments via specific intensities of reflected sound at various spatial resolutions. Utilizing GPS and high-resolution sonar systems in combination with ROV imagery transect data allows for the correlation of specific habitat types with rockfish presence over large bathymetric regions (Able et al. 1987; Yoklavich et al. 1995; Greene et al. 1995; Clarke et al. 1996; Fox et al. 1999; Hughes; Nasby-Lucas et al. 2002).

Habitat suitability for a given species is a measure of how appropriate the area is for the species to occur (Elith et al. 2006). Modeling approaches approximate the distribution of suitable habitat for a given species (Peterson et al. 2011) through

correlative trends between a suite of environmental covariates and species presence (Elith et al. 2011). The environmental covariates, spatial scale of the study region, and quantity of species occurrences impact all habitat modeling methods (Phillips et al. 2005; Elith et al. 2006, Barve et al. 2011). Additionally, it is important to include environmental conditions that may be encountered in the study region (Barve et al. 2011).

Modeling techniques to geospatially predict species distribution have been broadly used in several different ecosystems including terrestrial (Franklin, 2009), freshwater (Olden and Jackson, 2002), and in the marine environment (Valavanis et al., 2008; Ready et al., 2010). Modeling techniques vary greatly in how they treat variable contribution, prediction products, etc. (Elith et al., 2006; Franklin, 2009).

In addition, the scale at which a given species is modeled can impact model performance. Multi-scale analyses allow for the delineation of suitable versus non-suitable habitat for any given organism due to the differing influences at both fine- and broad-scales (Guisan and Thuiller 2005). A study region that is too small may result in inconsistent model outputs, whereas a study region that is too large may result in an overestimate of suitable habitat (VanDerWal et al. 2009).

Habitat type and complexity are key components in determining the spatial distribution of fish assemblages in marine ecosystems (Caley & St John 1996; Friedlander & Parrish 1998; Gratwicke & Speight 2005; Luckhurst & Luckhurst 1978; Risk, 1972; Roberts & Ormond 1987). Habitat associations with the physical substrate and biogenic structures are reportedly species-specific for rockfish (*Sebastes spp*.)

(Richards 1986; Stein et al. 1992; Auster et al. 2003; Auster et al. 2005; Love et al. 2006), and for *S. pinniger* specifically, reported habitat associations vary geographically.

Yoklavich et al. (2000 and 2002) reported *S. pinniger* was associated with benthic habitat that transitioned from areas of low (mud/sand) to high relief, such as in areas with vertical rock walls, ridges, and boulder fields, at depths of 75-175 m, whereas Johnson et al. (2003) reported observing *S. pinniger* over both complex and soft substrates in mixed species aggregations and actively swimming at depths exceeding 36 m in southeastern Alaska. Tissot et al. (2007) reported *S. pinniger* adults to be habitat generalists, as they were observed aggregating over a variety of seafloor types at Heceta Bank, Oregon, whereas the 1992 findings by Stein et al. that found *S. pinniger* most associated with boulder and cobble fields in the same region.

In previous studies, environmental covariates used to model the suitable habitat of rockfish species have included depth, slope, aspect, Bathymetric Positioning Index, surface area to planar area, terrain ruggedness, curvature, and specific substrate types based on a classification of backscatter data (Wilson et al. 2007).

Depth is an important covariate to include in habitat modeling, as many rockfish are found at specific depths (Love et al. 2002); depth is also relevant to assessments at several spatial scales along the continental margins (Greene et al. 1999; Wilson et al 2007).

Slope is a measure of the change in depth over a horizontal distance and is expressed in degrees and has been used in many marine-based studies (Whitmire et al. 2004; Roberts et al. 2005; Lundbald et al. 2006; Wilson et al. 2007). Slope is thought to

be an important factor in determining benthic habitat and may contribute to current flow amplification (Mohn and Beckman 2002), which may be an important predictive layer for *S. pinniger* as they have been observed oriented toward currents.

Aspect (orientation), measured in degrees from north, reflects the orientation of the seabed at any given location. Although aspect has not been as widely used in studies of the marine environment as other variables (i.e. slope), aspect is an important factor to consider in the marine habitat because it can provide insight on the exposure to water circulation (Wilson et al. 2007).

Bathymetric Positioning Index (BPI) is a variation of the Topographic Positioning Index that is used for terrestrial analyses. BPI characterizes bathymetric data from the Digital Elevation Model (DEM) for each pixel as either a negative (i.e. canyon) or a positive (i.e. rock outcrop) value. BPI was developed by Weiss (2001) and has become a common metric in marine habitat research (Weiss 2001; Iampeitro and Kvitek 2002; Iampietro et al. 2004; Young et al. 2010; Wedding and Yoklavich 2015). BPI can be calculated with user-defined scales to elucidate broad- and fine-scale variations in bathymetric position.

Surface area to planar area (Rugosity) computes a ratio between the three-dimensional surface area and the planar area of the surface and has been used to study marine regions (Guinotte & Andrews 2012). A tool, implemented by Jeff Jenness in the Benthic Terrain Modeler extension for ArcGIS, triangulates a surface grid to yield a surface area dataset (Jenness 2003). The output values represent ratios between the

surface area and planar area; a value of zero indicates a perfectly flat area with low no relief (or complexity) whereas three indicates an area of high relief.

Terrain Ruggedness (VRM), represents the variability in aspect and slope with a single value. The values reported range from 1 (complete variation in terrain) to 0 (no terrain variation). Orthogonal dispersion within a specific neighborhood is calculated to measure the three-dimensional orientation of grid cells (Valentine et al. 2004). VRM has been used to delineate habitat of marine organisms in previous studies (Beck 2000; Kostylev et al. 2005).

Curvature describes benthic terrain features relative position by calculating the curvature of a raster surface (Moore et al 1991). Curvature measurement is an important environmental covariate to consider because of the link between seabed characteristics and current strength (Wilson et al. 2007).

Habitat complexity, particularly the interface between rock and soft substrata, has been found to be an important covariate of suitability in for rockfish species in temperate waters (Young et al. 2010). Many marine studies have utilized Euclidean distance interpolation measurements between data points and benthic features to generate predictions of values at unknown locations (Friedlander & Parrish 1998, Pittman et al. 2004, Dorenbosch et al. 2005, Pittman et al. 2007, Young et al. 2010). This approach, however, is not ideal as spatially distributed data often have geographically complex connectivity where distances cannot be determined from Euclidean distance measurements (Greenberg et al. 2011). Euclidean distance measurements represent the connectivity between points and or features using one-dimensional lines (i.e. roads,

streams). Conversely, cost distance (cost of a least cost path) is the sum of the cost values associated with the cells of a path (O'Brien et al. 2006). A cost distance environmental covariate can represent a bidirectional surface from once location to another, where the interface itself is the lowest "cost" (Bolstad 2012).

Several recent advancements have been made in seafloor mapping techniques and modeling approaches, which have supported robust predictions for individual fish species (Young et al. 2010). Numerous modeling techniques have been used to correlate biotic and abiotic features with regard to demersal fish (O'Brian and Rago, 1996; Olden, J. D. & D. A. Jackson, 2002; Leathwick et al., 2006; Wedding and Yolklavich 2015). Many of these studies have shown relationships between abundance and abiotic/biotic variables tend to be non-linear and have adopted the use of modeling techniques that reflect this. Many of the modeling techniques currently being used require presence/absence or abundance data from geographic regions systematically surveyed (Guisan and Zimmermann, 2000). The unavailability of species absence data, however, is common problem in that it comes from museum specimens or is unverifiable at sites where species are present, but not observed (Gu and Swihart 2004). Moreover, when absence data is used it may lead to the misidentification of unsuitable habitat when species are unseen rather than truly absent from a region of interest (Baldwin 2009).

Presence-only modeling techniques are gaining popularity to predict marine fish distributions (Maravelias et al., 2003; Ready et al., 2010; Jones et al., 2013; Garcia-Alegre et al., 2014). Maximum Entropy modeling is implemented in MaxEnt, an open source general-purpose machine-learning software package (Phillips et al.,2006). MaxEnt

has been shown to outperform other presence-only modeling techniques (Elith et al., 2006; Tittensor et al., 2009) and has been used to successfully study the distribution of marine species at several spatial scales (Ready et al., 2010; Hermosilla et al., 2011; Pittman & Brown, 2011, Jones et al., 2013, Bohrer do Amaral et al. 2015). This method predicts the distribution of a species from presence-only data and environmental covariates with an algorithm that applies the principle of maximum entropy. Through this principle (Jaynes 1957), a set of constraints (here, the environmental data associated with *S. pinniger* occurrence data) that are representative of the incomplete information pertaining to species distribution are used to approximate the unknown probability through maximizing entropy (Phillips et al. 2006).

MaxEnt has been criticized for its tendency toward overfitting the data by way of clustering predicted distributions around occurrence points (Anderson & Gonzalez 2011; Warren & Seifert 2011; Radosavljevic & Anderson 2014). Consequently, a user-defined regularization parameter (β) is now available within current releases of the MaxEnt software, allowing the user to specify the β value instead of having to use the default value of one. Changing the β value can smooth out complexities in the response curves that do not accurately represent the phenomenon being modeled. A response curve is a is a curve that shows the difference among different feature types (Philips et al. 2006). The goal of this type of modeling is to find a balance between fitting the data and creating a simple, parsimonious model (Burnham and Anderson 2002). Modifying the β value can change the fit of the response curve to the data inputs and previous research has found that a β value two to four times higher than the default of may be preferentially selected

to reduce overfitting (Radosavljevic and 2014). MaxEnt performance is indicated by a positively sloped diagonal line. The area under the line, or Area Under the Curve (AUC), measures performance with range between one (perfect performance) and zero (model predictions are the exact opposite of observations), with a value of 0.5 representative of random guessing (Handley and McNeil 1982). AUC has been widely used to evaluate the performance of habitat suitability models with pseudo-absences or "background" points (Fielding and Bell 1997). Relying upon the AUC metric alone to evaluate model performance should be done cautiously, as it operates under the assumption that under- and over-prediction are equivalent, ignores the predicted probability values and the goodness-of-fit of the model, and provides no information on the spatial distribution of model errors (Lobo et al. 2008). Additionally, comparative statistical testing and measurements that interact with MaxEnt were developed by Warren et al. (2008) in the ENMTools software (Warren et al. 2010; Warren and Seifert 2011) to select the most parsimonious, best fit models based on Akaike's Information Criterion (AIC) scores.

Many studies that explore suitable habitat mainly consider the strengths and weaknesses of different modeling approaches for a certain time and space (Convertino et al. 2012) and leave out uncertainty analyses. Beale and Lennon (2012) point out that in predictive modeling uncertainty in the data is rarely evaluated and Gould et al. 2014 make the point that uncertainty should be considered in any modelling process. Uncertainty relating to species occurrence data can originate from various sources including taxonomic misidentification, spatially and temporally biased sampling efforts, and inexact spatial data (Gould et al. 2014).

My primary objectives of this study were to: (1) Elucidate the suitable habitat of *S. pinniger* based on several seafloor descriptors of the surveyed sites with predictive distribution models at the broad-scale (20-meter resolution) and the fine-scale (two meter resolution); (2) Identify various sources of uncertainty in these models, such that future improvements could be made to the methodology I utilized. The results of this study will provide a greater insight into the habitat variables influencing *S. pinniger* and add to the knowledge base to further develop spatially explicit management strategies; they can also help inform population recovery mitigation, and stock assessments by identifying regions with bathymetry most suitable to support them (Thorson and Wetzel 2016).

MATERIALS AND METHODS

Study Region

The study region was along the northern California coast between 42°00 N latitude (northern county line of Del Norte County) and 38°46 N latitude (southern county line of Mendocino County) (Figure 1). This portion of the west coast of California is made up of large rocky banks, canyons, seamounts, and long stretches of sand/mud substrates (Whitmire and Clarke 2007); for over a half century, this area has supported recreational and commercial fishing (Love et al. 2002).

Data used in this study originated from two surveying efforts: the North Coast Marine Protected Area (NCMPA) survey and the Coastal Impact Assistance Program (CIAP) survey. These efforts were conducted September 9, 2014 through October 12, 2014. The objectives of NCMPA survey efforts included 1) baseline characterization of selected Marine Protected Areas (MPAs) across the north coast study region 2) assessment of the initial ecological changes in fishes, macrofaunal invertebrates, and associated seafloor habitats in those MPAs during the first year following designation 3) recommendations for future monitoring efforts in the region (Lauermann et al. 2017). The objectives of CIAP survey efforts included 1) estimating macro invertebrate and fish species density/relative abundance inside and outside of MPAs; 2) determining size frequency distribution of ecologically important commercial and recreational species to one centimeter resolution using stereo cameras 3) providing spatial data to allow

examination of the distribution of observed species in relation to other spatial datasets such as high resolution bathymetry, spatially derived habitat classifications and fisher effort 4) providing an archive of high quality video transects that capture the baseline ecological conditions for California's MPAs (Lauermann 2015).

The survey efforts were largely within the bounds of California state waters (3 nautical miles from shore) and extended from depths of 20 m to >100 m within and outside the boundaries of Marine Protected Areas (MPAs). The coverage of the study region was limited to the available acoustic multibeam bathymetry data boundaries. All sampling locations were positioned and based on habitat interpretations from multibeam bathymetry data (Monterey Bay Aquarium Research Institute Mapping Team, Northern California Multibeam Survey; Seafloor Mapping Lab, California State University Monterey Bay [SFML-CSUMB]) and focused on a broad range of bathymetric ecosystem features including mid-depth rock, soft-bottom subtidal, and deep-water canyons (Lauermann et al. 2017).

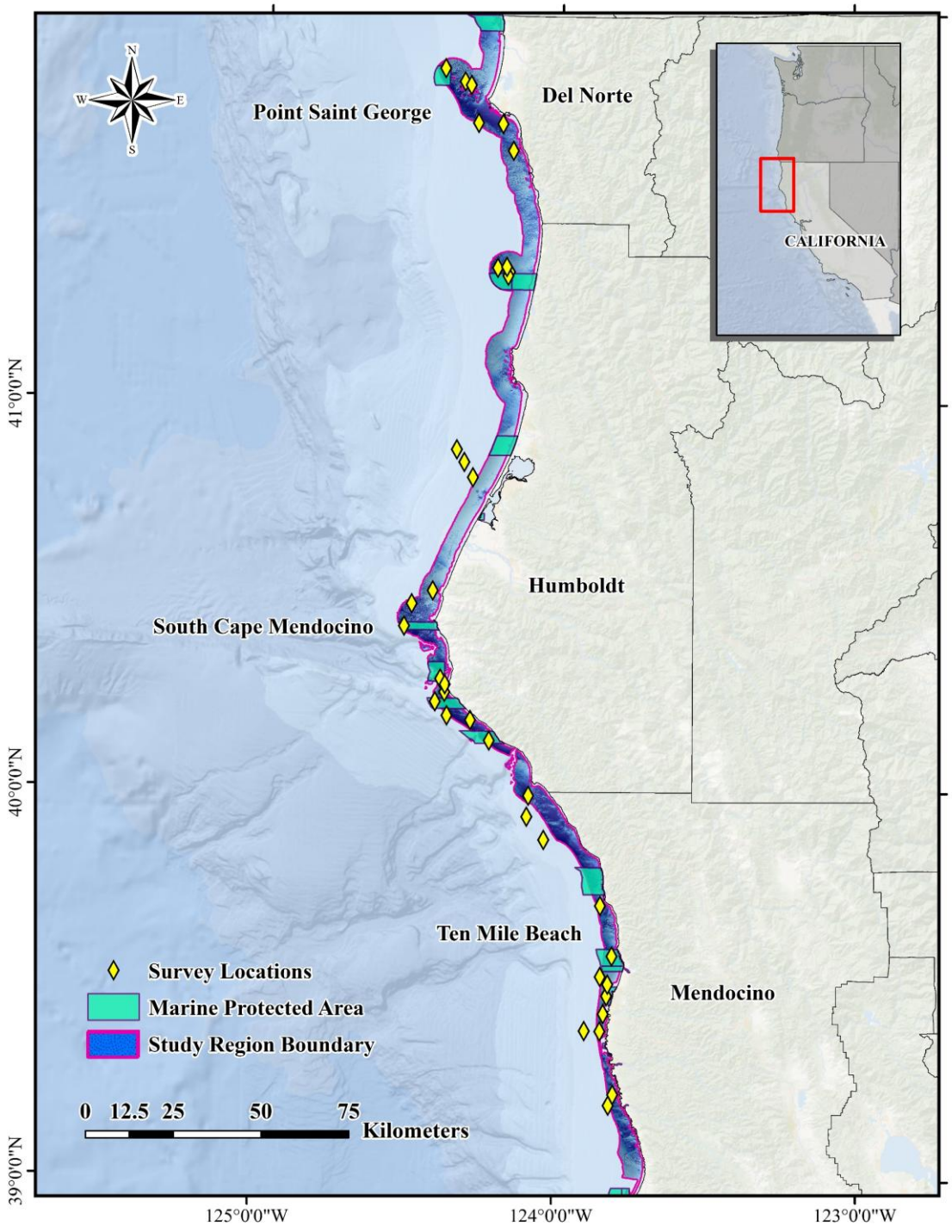

Figure 1. All survey locations collected autumn of 2014 along the northern California study region with reference to California's three northernmost counties.

Data collection

The visual underwater surveys of habitat, demersal fish species, and invertebrates were conducted by Marine Applied Research and Exploration using a Deep Ocean Engineering Vector M4 Remote Operated Vehicle (ROV) at each survey location in the study region. The ROV was equipped with a three-axis autopilot including a rate gyro-damped compass card. To maintain a consistent velocity, they used an automatic forward speed control. Two Tritech® 500 kHz ranging sonars (used to measure distance across a range of 0.1–10 m using a 6° conical transducer) were used as the principal system for measuring transect breadth and averaged five times per second at one-second intervals.

To reference the ROV position relative to the research vessel's Wide Area Augmentation Global Positioning System, they used an ORE Offshore Trackpoint III® ultra-short baseline acoustic positioning system with ORE Offshore Motion Reference Unit pitch and roll sensor. A KVH magnetic compass-determined the research vessel's heading. The ROV coordinates relative to the research vessel was calculated at two-second intervals by the Trackpoint III® positioning with an angular accuracy of 0.1 degrees. Using HYPACK® 2013 hydrographic survey and navigation software, the ship-relative position was corrected to real world position and recorded in meters as X and Y position using the World Geodetic System 1984 Universal Transverse Mercator coordinate system. All measurements (including depth, water temperature, ROV heading, sonar distance and forward/downward camera tilt) collected were averaged over a one-second period and recorded in synchronously with the position data. The ROV was

flown at a mean depth of 0.2 meters above the substrate at a speed ranging from 0.5 to 0.75 knots.

The ROV was equipped with two color cameras (one facing forward and one downward-facing toward the substrate) and digital video was recorded with SONY® DSR 45 digital video tape recorders and Pioneer DVR510 digital video disc recorders. To generate on-screen displays of GPS time, they used a Horita® GPS3 and WG-50. ROV tracked position and sensor data was recorded directly by HYPACK® as a time-linked text file. Outputs of Society of Motion Picture and Television Engineers linear time-code were recorded on the SONY® DSR audio tracks at an interval of 1/30th of a second (see Lauermann et al. 2017 and Karpov et al. 2006 for further information on ROV and methods).

Prior to at-sea operations, planned survey lines within each of the survey sites were selected and placed across the width of the site parallel to the prevailing line of constant depth. The locations of the survey lines were chosen by selecting the desired number of planned lines and then evenly distributing them across the site in a grid (Figure 2). Survey lines were numbered in accordance with the distance along the site boundary running from shallow to deeper depths. One or more survey grids were collected at each survey site (Table 1).

Overall, 110.4 km of transects were surveyed during 61 individual ROV dives. A total of 91.5 hours of video, 16,965 digital stills, and 196 survey lines were collected at

36 study sites (Table 1).

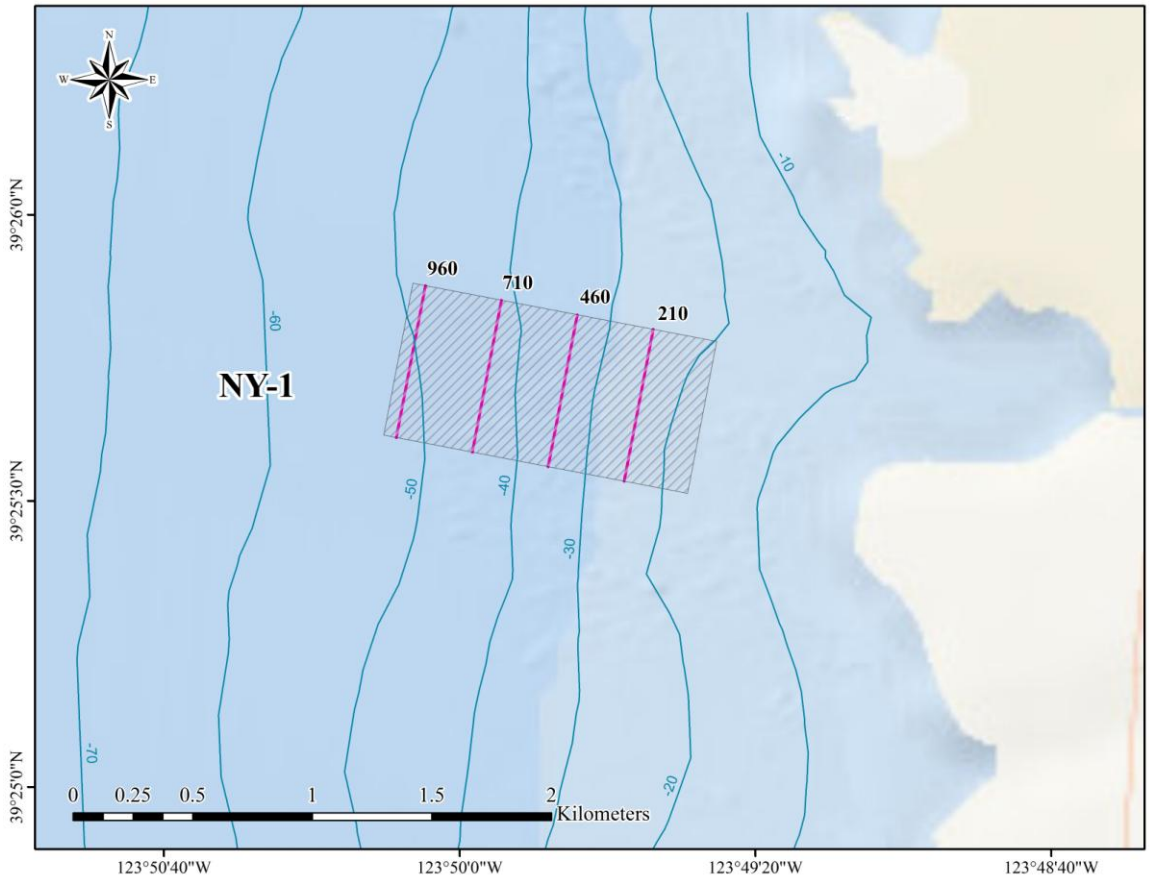

Figure 2. Example of a planned survey. The lines within the hash-marked box were surveyed. This example is from the survey site at Noyo Harbor (NY-1), California, USA.

Table 1. ROV survey and site locations both inside and outside of MPAs, as specified.

Survey Location	*Site Code*	*MPA*
Point Saint George	PSG1	inside
	PSG2	outside
	PSG3	outside
	PSG4	outside
Crescent City	CC1	outside
	CC2	outside
Reading Rock	RR1	inside
	RR2	outside
	RR3	outside
	RR4	outside
Eureka	EU1	outside
	Dump Site	outside
South Cape Mendocino	SC1	outside
	SC2	outside
	SC3	inside
Mattole Canyon	MC1	inside
	MC2	outside
Sea Lion Gulch	SL1	outside
	SL2	inside
	SL3	outside
	SL4	outside
Big Flat	BF1	inside
Tolo Bank	TO1	outside
	TO2	outside
	TO3	outside
Ten Mile Beach	TM1	inside
	TM2	outside
	TM3	outside
	TM4	outside
	TM5	outside
MacKerricher	MK1	outside
	MK2	inside
	MK3	outside/inside
Noyo	NY1	outside
Cabrillo	CB1	outside
	CB2	outside
Albion	AB1	outside
	AB2	outside

Species abundance data

I collected observations of demersal fishes from non-overlapping forward-facing video. Taxonomic identifications were made by marine biologists trained in formal fish identification procedures, including myself. In addition to the geographic position of *S. pinniger* occurrences, I recorded data on estimated total length, number of individuals, and time of sightings. I chose to only include fish longer than nine cm for four reasons: (1) the method by which these data were processed allowed observers to group fish that were nine cm or less (estimated total length based upon scaling lasers set 10 cm apart) into groups containing several different species within a school; (2) standard definition video can be grainy and does not always lend to highly accurate identifications at the species level for juvenile fish; (3) previous research in tropical marine ecosystems has shown that models to assist in the determination of conservation management value of certain areas have performed better for larger bodied fish (Costa et al., 2014); and (4) larger individuals are likely to be more fecund and more important to consider in conservation efforts (Hixon et al. 2014).

Environmental covariates

I obtained bathymetric multi-beam acoustic data including backscatter intensity, downloaded from the California Seafloor Mapping Project Library. I selected seven environmental covariates based on ROV video observations, previous research (Lampietro et al. 2005, Young et al. 2010, Wedding & Yoklavich 2015), and scientific

literature (Love et al. 2002, Love & Yoklavich 2006). To account for inconsistencies that can arise from the breadth of the study region, I chose to model at both the broad- and fine-scale. All environmental covariates were processed in ArcGIS 10.3 in datum World Geodetic System 1984 (WGS 84), with the same spatial extent and the same resolution for both broad and fine-scale analyses. Environmental covariates evaluated for both broad- and fine-scale analyses included: depth, slope, curvature, aspect, broad-scale bathymetric positioning index (BPIb), fine-scale bathymetric positioning index (BPIf), surface area to planar area (Rugosity), Terrain Ruggedness (VRM), and a novel "Cost Distance" layer (Appendices A and B). Depth values came from two-meter Digital Elevation Models (DEM) from high-resolution multibeam data collected by the California Seafloor Mapping Program (http://seafloor.otterlabs.org/SFMLwebDATA_SURVEYMAP.htm). All covariates except for Cost Distance were derived from a digital elevation model and computed with the Benthic Terrain Modeler extension in ArcGIS. I calculated BPI using the Benthic Terrain Modeler extension at two commonly used scales: fine-scale BPI (BPIf) at a scale factor of 35 and broad-scale BPI (BPIb) at a scale factor of 200 (Martín-García et al. 2013). For the broad-scale region, I combined 26 individual DEMs and resampled to 20-meter pixel resolution by calculating the mean of all data values of the two-meter pixels that fell within the bounds of the 20-meter pixel. I kept the three fine-scale study regions at the native two-meter pixel resolution.

Following visual surveys, it became apparent that *S. pinniger* was most often observed at the interface between hard rock and soft (mud/sand) substrates. I determined

that this interface would be included as an environmental covariate. Many marine studies have included the rock and soft substrate interface as unidirectional environmental variables (Friedlander and Parrish 1998; Pittman el al. 2004; Pittman et al. 2007; Dorenbosch et al. 2005; Young et al. 2010). Here, I wanted to include a more robust bidirectional environmental covariate at the interface with a cost distance raster. I used a novel cost distance analyses to define the bathymetric substrate to allow the complex systems of connectivity to be interpolated. Cost distance (ArcGIS Spatial Analyst Extension), is a measure of the least accumulative cost distance for each cell to the nearest source over a cost surface. Cost distance methods determine the shortest weighted distance (accumulated travel cost) rather than the Euclidean approach of calculating the actual distance from one location to another (Bolstad 2012). Benthic substrate data was collected and classified by the Seafloor Mapping Laboratory, California State University Monterey Bay. I assessed the backscatter intensity values at a two-meter resolution and then classified them into two distinct categories at different depths to isolate hard rock from soft substrates. I converted the hard rock category of each raster to a vector to obtain an outline of the rock and soft substrate interface. Cost distance was calculated in ArcGIS with a cost surface raster of the same extent as each study region with all pixel values set equal to two and of the same resolution. I assigned a value of 1 to the line at the hard/soft benthic substrate interface. The resulting cost distance raster created has a value of zero (low cost) on the line of the hard/soft benthic substrate interface and increments to a value of one (high cost) the farthest away from the interface (See Appendices). I created the cost distance raster for the broad-scale study

regions by the same methodology at a two-meter pixel resolution for the fine-scale analyses. I converted the vector file to a raster format, resampled to a 20-meter resolution, then converted back to vector format to remain consistent with the other environmental layers.

Table 2. Covariates evaluated for the modeling efforts.

Measurement	*Description*	*Software*	*Reference*
Bathymetry	Digital Elevation Model (DEM) of the Bathymetry with a native resolution of two meters.	ArcGIS 10.3	Wilson et al. 2007
Cost Distance	Calculation of the least aggregate cost distance for each cell to the nearest source (rock/ soft substrate interface) over a cost surface.	ArcGIS 10.3; Spatial Analyst Extension	This work (novel)
Aspect	Slope orientation measured in continuous units (-1 to +1) with indices of eastness (E) and northness (N).	ArcGIS 10.3; Spatial Analyst Extension	Wilson et al. 2007
Slope	Maximum rate of change between pixels. Calculated in degrees (°).	ArcGIS 10.3; Spatial Analyst Extension	Wilson et al. 2007
Vector Ruggedness Measure (VRM)	A grid that combines variations in slope and aspect to represent terrain complexity.	ArcGIS 10.3; Benthic Terrain Modeler Extension	Eastman, J.R. 1999
Bathymetric Positioning Index (BPI)	Measurement of bathymetric data from a digital elevation Model (DEM) that characterizes features at within a local and regional context for broad-scale (BPIb); scale factor of 200, and fine-scale (BPIf); scale factor of 35.	ArcGIS 10.3; Benthic Terrain Modeler Extension	Weiss 2001; Wright et al. 2005; Wedding and Yoklavich 2015
Surface Area to Planar Area (Rugosity)	Ratio between the three-dimensional surface area and the planar area minus one, ranging from values of zero (no variation) to three (high variation).	ArcGIS 10.3; Benthic Terrain Modeler Extension	Jenness 2004
Curvature	Calculation of the change in slope that measures the concavity and convexity of the benthic substrate.	ArcGIS 10.3; Benthic Terrain Modeler Extension	Pittman et al. 2006

I ran Pearson's correlation tests in R (R Core Team, 2014) for all potential environmental covariates at both the broad- and fine-scales to decrease multicollinearity, avoid misrepresentation of modeled phenomena (Plant, 2012), and improve interpretation of results. Covariates exhibiting a threshold value greater than 0.7 I chose not to run within the same model (Dormann et al., 2013). Values bolded indicate a high degree of correlation (Table 3). The fine-scale Pearson's correlation results (not shown) showed similar correlative outcomes.

Table 3. Pearson's correlation results of the environmental covariates evaluated for the broad-scale modeling effort. Values range from 0-1, where a value of one indicates 100% correlation. Values bolded indicate high correlation.

	Cost Distance	*Aspect*	*Depth (m)*	*Slope (°)*	*VRM*	*Fine BPI*	*Broad BPI*	*Rugosity*	*Curv-ature*
Cost Distance	1.000		-	-	-	-	-	-	-
Aspect	0.088	1.000	-	-	-	-	-	-	-
Depth (m)	-0.079	0.026	1.000	-	-	-	-	-	-
Slope (°)	-0.042	-0.041	0.042	1.000	-	-	-	-	-
VRM	-0.126	-0.268	0.107	-0.041	1.000	-	-	-	-
Fine BPI	0.015	0.007	0.030	0.038	-0.053	1.000	-	-	-
Broad BPI	0.056	0.008	0.002	0.044	-0.137	**0.850**	1.000	-	-
Rugosity	0.015	-0.162	0.062	0.204	0.185	0.227	0.267	1.000	-
Curvature	0.023	-0.088	0.035	0.076	-0.093	**0.887**	**0.873**	-0.124	1.000

Maximum entropy models and validation

Of the nine environmental covariates evaluated, I chose the covariates for each region and each model based on the reported model contribution and permutation importance with MaxEnt version 3.3.3 software (MaxEnt 2012) and did not include covariates that were highly correlated within the same model run. I retained covariates in a leave-one-out stepwise fashion to identify and remove variables with the lowest predictive power (Parolo et al. 2008).

Although I largely adhered to the default parameters for MaxEnt, as they have displayed acceptable model fit (Phillips and Dudik 2008), I did make some modifications. To examine covariate importance, I applied a jackknife procedure. The jackknife procedure elucidates the most influential covariates of the output model in terms of the individual influence and influence on the model. Gains were calculated from the jackknife procedure for each of the environmental covariates which allowed me to compare the influence each covariate had on each model. Multiple *S. pinniger* occurrences were recorded within the same grid cell (fish near one another) in several locations throughout all study regions. Occurrences recorded in the same grid cell are referred to as "duplicate records" by default in MaxEnt. To maintain these records and add weight to areas where more than a single fish was observed, I disabled the default setting. The default regularization parameter (β) is set to 1 in MaxEnt. I tested β values ranging from 1 to 3 as suggested by Phillips, 2005 and elected to add additional β values of 4 and 5 to test for optimal model complexity and biological relevance.

The MaxEnt software has the option of being able to add an ancillary sampling probability surface called a bias grid (Dudík et al. 2005; Elith et al. 2010) that reflects sampling effort and provides weight to random background data used in the models. Geographical sampling bias can result in a model that reflects sampling effort rather than the accurate distribution of a species (Phillips et al. 2009). Previous research suggested that the best way of creating a bias layer to reduce geographical sampling bias was to represent the actual sampling intensity across the entire study region (Fourcade et al. 2014). Thus, I created the bias layer for the broad-scale analysis by using the study site

boundary areas with a pixel value of 2 and the remaining pixels were assigned a value of 1. This bias layer was implemented within the bias file option in MaxEnt with each of the broad-scale models.

ENMTools (www.ENMTools.com; Fielding and Haworth 1995; Warren et al 2008) was used to calculate the Akaike's information criterion (AIC) (Warren and Seifert 2011). The AIC is a statistic which is commonly used to compare models, where a lower AIC is indicative of a "better" model (Burnham and Anderson 2002). The change in AIC (ΔAIC) was calculated and represents the difference in AIC between the top performing model and each of the others. Akaike weights (ω_i) were calculated to assess the relative support that each given model had from the data, where a ω_i close to one reflects the best approximating model (Burnham and Anderson 2002). Area Under the Curve (AUC) is commonly used to evaluate the predictive performance of presence-only models (Handley and McNeil 1982; Fielding and Bell 1997; García-Alegra et al. 2014) and an AUC values that are close to one are considered to better fitting. Given that using AUC alone to evaluate model performance has been notable weaknesses, as it assumes that the costs of under-prediction and over-prediction are equivalent and that presence-only modeling can only result in under-prediction (Lobo et al. 2008; Peterson et al. 2008), I opted to incorporate other parameters to evaluation model performance.

To select the most parsimonious models among all covariate combinations for both fine- and broad-scale study regions, I used Area Under the Curve (AUC) (Zweig & Campbell 1993; Fielding & Bell 1997; Tittensor et al. 2009), ΔAIC and ω_i, as well as covariate response curves. I visually inspected response curves to diagnose overfitting in

models. In comparing different models, I diagnosed as overfitted those whose covariate response curves were jagged and erratic; I selected as the most parsimonious (best) model the one with the highest AUC and ω_i, lowest ΔAIC, and covariate response curves that were comparatively smooth and continuous.

In addition, I plotted the predicted probability of occurrence for each *S. pinniger* occurrence in each study region (Fitzpatrick et al. 2013) at both scales. The default MaxEnt algorithm assumes a baseline species prevalence of 0.5 (Phillips and 252 Dudík 2008), meaning equivalent to random. I examined the predicted probability of occurrence by extracting the reported values from each of the highest performing models outputs generated by MaxEnt associated with each *S. pinniger*. These values were plotted displaying the 25^{th} and 75^{th} percentiles around the median predicted probability of presence for the broad-scale region and for each of the fine-scale regions.

Uncertainty analysis

To evaluate uncertainty relating to species occurrence data I examined taxonomic misidentification, spatially and temporally biased sampling efforts, and inexact spatial data (Gould et al. 2014) at both scales.

The genera *Sebastes* can be taxonomically challenging to identify because of the large number of species within the genera, and morphological (Orr et al. 2000) and behavioral similarity. During identification, *S. pinniger* was found to be similar in appearance to other rockfish species including vermillion rockfish (*Sebastes miniatus*), yelloweye rockfish (*Sebastes ruberrimus*), and the sunset rockfish (*Sebastes crocotulus*)

newly discovered in 2008 (Hyde et al. 2008) (Figure 3). Observations of *S. pinniger* were made from standard definition video and still images stamped with a corresponding time code to match the point in the transect images were taken. Standard definition video can be grainy and unclear and clarity can be further diminished when the water column contains a high particulate load. To rule out the misidentification, observations were made by *experienced* marine biologists and any *S. pinniger* occurrences in question were not used in this study.

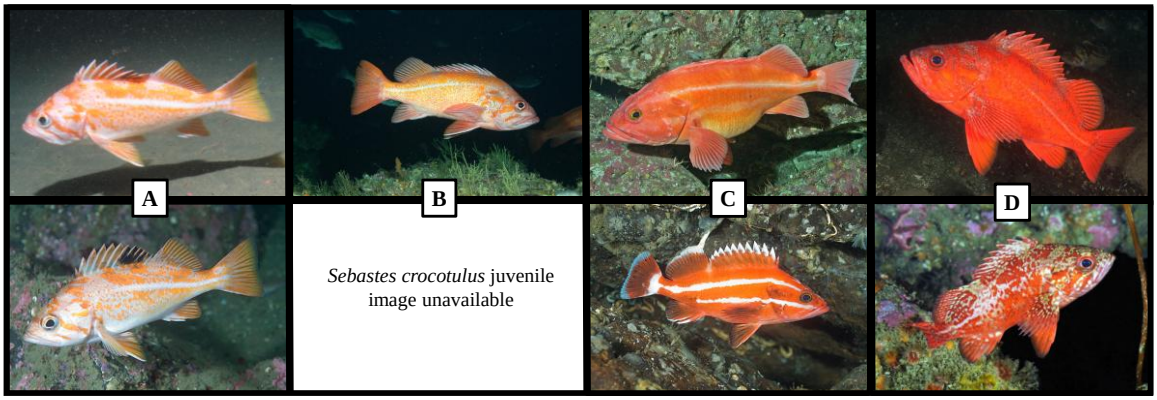

Figure 3. Red-colored rockfish species that are commonly confused with one another. Top images are adults and bottom images are juveniles. (A) *S. pinniger*, (B) *S. crocotulus*, (C) *S. ruberrimus*, and (D) *S. minatus*. Photographic credits: (A) CDFW and www.elasmodiver.com, (B) NOAA, (C) www.elasmodiver.com (D) Dan Hershman and David R. Andrew.

The bathymetric covariates used in this study have a reported accuracy of ± two m for horizontal position, ±0.02° for pitch/roll/heading, and a heave accuracy (vertical position) of ± five cm (SFML-CSUMB). Due the small reported uncertainty in these covariates, I did not incorporate this error into my uncertainty analyses. Instead, I focused on the larger source of uncertainty associated with the survey methodology.

The largest estimated source of uncertainty in this study came from the geographic position data. Uncertainty in GPS position was estimated to be +/-15 m for each fish occurrence. The hydrophone relaying the ROV position may have been impacted by current, debris collision, etc. (A. Lauermann, personal communication, January 14, 2015). To create a map of spatial uncertainty for the occurrence data, my models were run through numerous iterations of MaxEnt with the aid of BlueSpray, a Java based GIS software developed by SchoonerTurtles, Inc. (BlueSpray GIS Software, 2016). BlueSpray contains a module that permits batch processing of several MaxEnt models (O'Banion and Olsen 2014) as well as a Monte Carlo feature. The Monte Carlo feature contains a parameter which can be set to represent the cumulative "noise" or uncertainty in the data and then the model can be run repeatedly with noise injection to determine the distribution of the outputs from MaxEnt (O'Banion and Olsen 2014). I added the maximum predicted noise of range -15 m minimum to 15 m maximum for both the fine and broad-scale analyses. BlueSpray creates Receiver Operator Characteristic (ROC) curves, where the ROC is a measure of model efficacy for all possible thresholds, where sensitivity represents the fraction of true positives (y-axis) and specificity the fraction of false positives (x-axis) (Fielding and Bell 1997). BlueSpray also creates iteration and histogram figures to evaluate the uncertainty analyses performed.

RESULTS

Broad-scale

The broad-scale study region for this research spanned approximately 1,871 km^2 along the continental shelf off the coastline of the three northernmost counties of California: Del Norte, Humboldt, and Mendocino. A total of 1,061 occurrences of *S. pinniger* measuring more than nine cm total length were observed in this study, however, only 845 (Figures 9 - 11) were used in the broad-scale analysis due to 216 occurrences lacking environmental covariate data. I generated 28 predictive models for the broad-scale study region (Table 7).

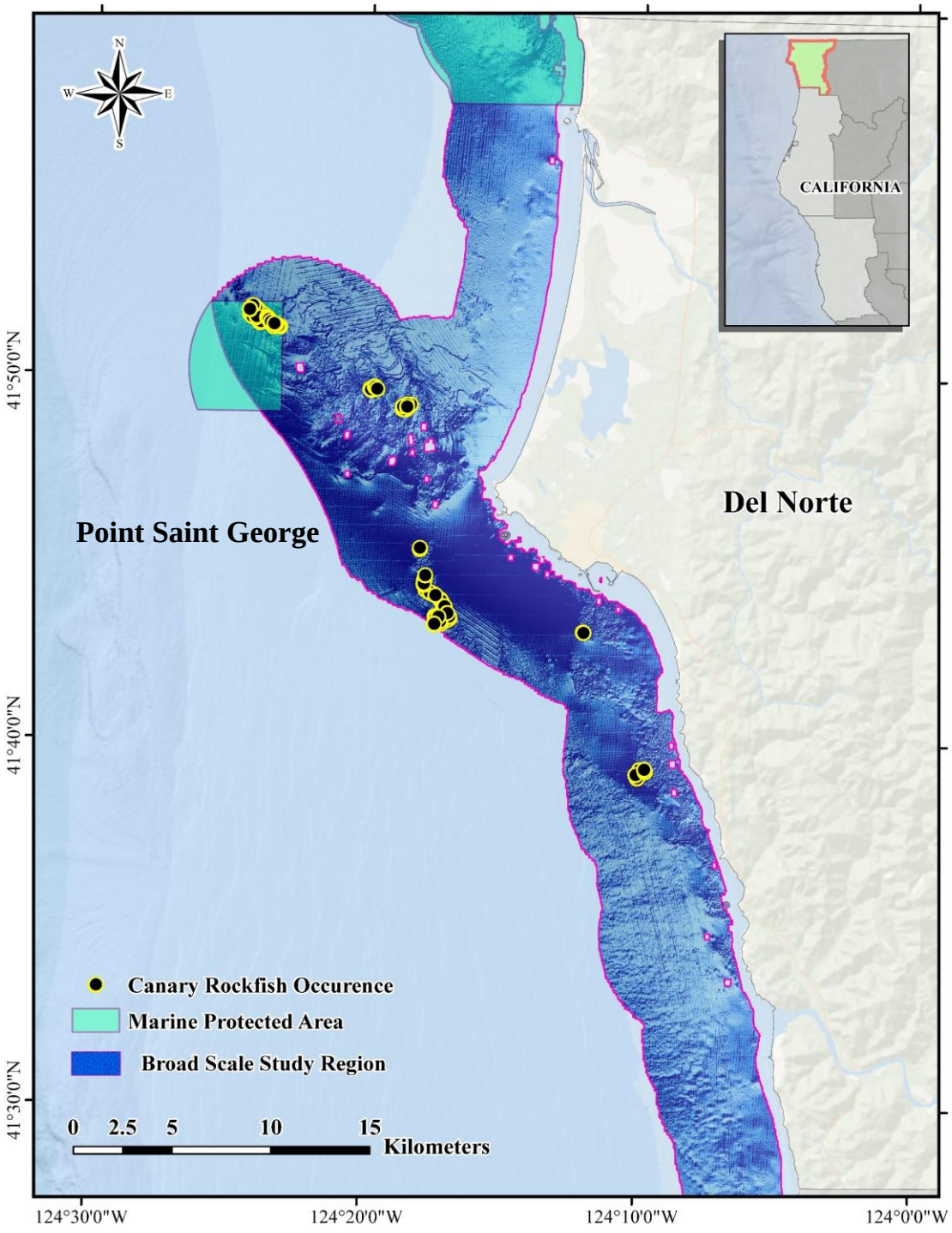

Figure 4. Map of the canary rockfish (*S. pinniger*) recorded occurrence recorded in the fall of 2014 during the survey cruises off the coast of Del Norte County, California, USA.

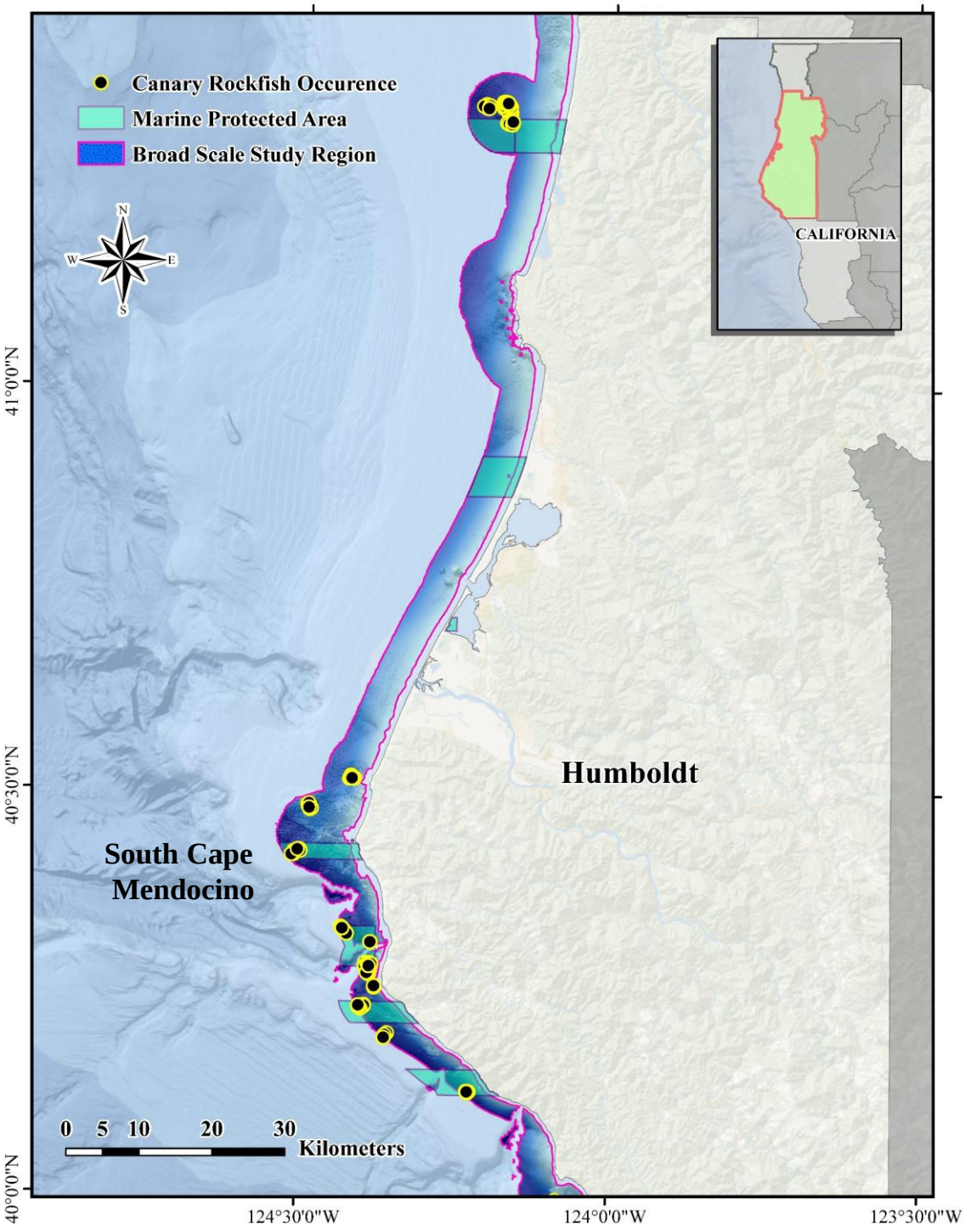

Figure 5. Map of the canary rockfish (*S. pinniger*) recorded occurrence recorded in the fall of 2014 during the survey cruises off the coast of Humboldt County, California, USA.

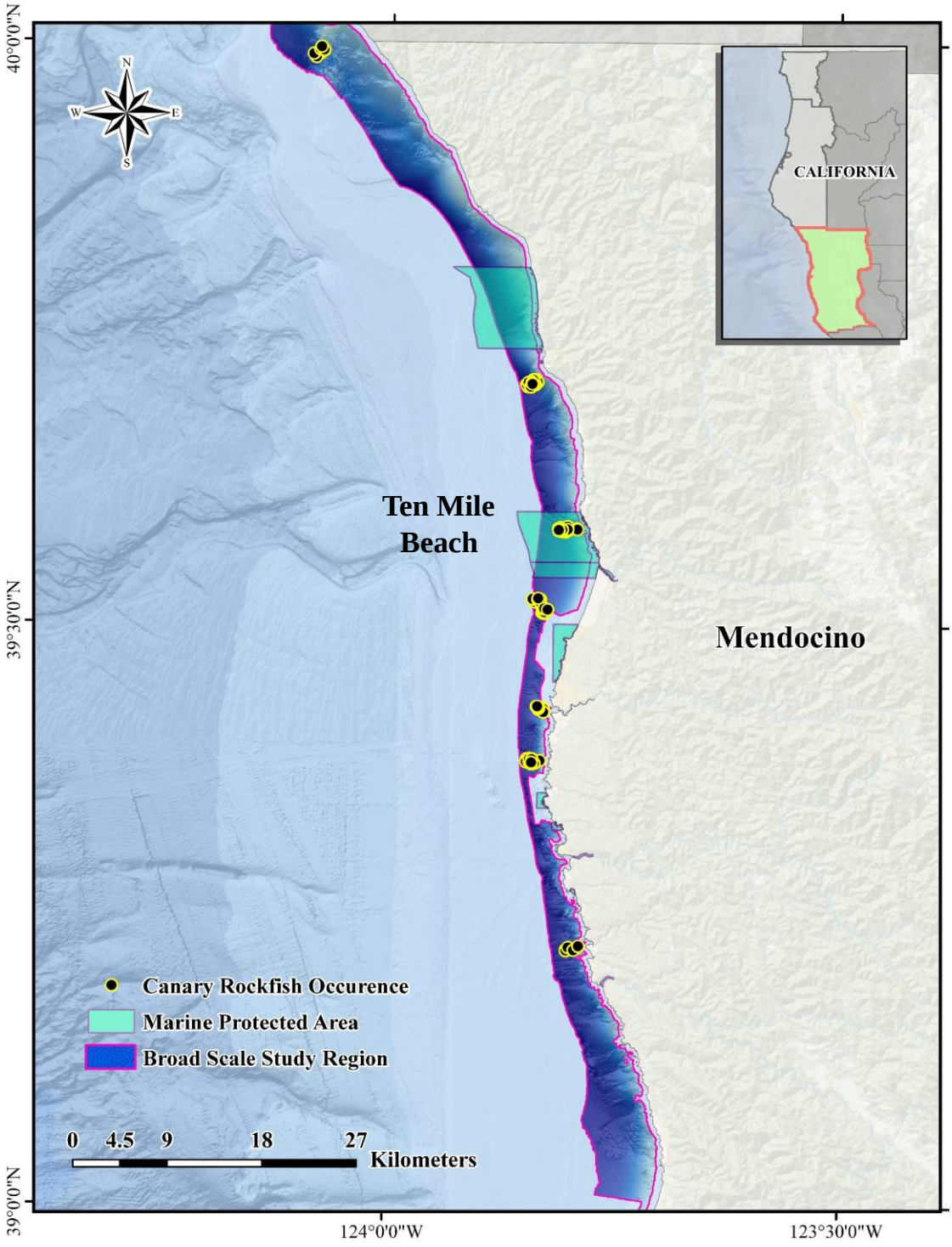

Figure 6. Map of the canary rockfish (*S. pinniger*) recorded occurrence recorded in the fall of 2014 during the survey cruises off the coast of Mendocino County, California, USA.

Results of the broad-scale predictive modeling effort indicated that the highest performing model was model 25, which accounted for 53.1% of weight in the table, used a β value of 1, AUC of 0.949, and included seven environmental covariates: cost distance, depth, VRM, rugosity, slope, aspect, and BPIb (Table 3). However, model 25 was not selected due to nonsensical response curves (highly jagged or multimodal) that appear to overfit the data instead of reflecting a plausible relationship between the covariate and the likelihood of fish occurrence (Radosavljevic and Anderson, 2014). The selected and most parsimonious model to predict suitable habitat of *S. pinniger* for the broad-scale region was model 16, which accounted for < 0.001% of weight in the table, used a β value of 4, AUC of 0.943, and included four environmental covariates: cost distance, depth, VRM, and rugosity. The habitat suitability map produced from model 16 predicted regions at the interface between rock and soft substrates and discriminated against areas where *S. pinniger* wasn't observed (i.e. sand flats) (Figures 7, 8, and 9) and was < 1% different from both AUC and ΔAIC values reported for model 25. Results of the jackknife test for model 16 indicate the most influential environmental covariates were cost distance, depth, VRM, rugosity, respectively (Figure 10). Areas of high suitability occurred where depth was approximately 60 to 64 meters and rugosity values were between 0.20 and 0.40 (Figures 11 and 12). Figures 11 and 12 show a comparative look at the response curves for model 16 versus the overfitted response curves of model 25.

Table 4. All model runs for the broad-scale region (Del Norte, Humboldt, and Mendocino Counties): relative contributions of the major environmental variables, regularization parameter (β), AUC, AIC, ΔAIC, and ωi.

Model	*Variable Contribution*	*β*	*AUC*	*AIC*	*ΔAIC*	ω_i
1	Cost Dist. (73.8%) Depth (26.2%)	1	0.939	22031.290	556.755	< 0.001
2	Cost Dist. (75.4%) Depth (24.6%)	2	0.937	22152.468	677.934	< 0.001
3	Cost Dist. (76.6%) Depth (23.4%)	3	0.935	22201.988	727.454	< 0.001
4	Cost Dist. (76.9%) Depth (23.1%)	4	0.934	22234.512	759.977	< 0.001
5	Cost Dist. (76.8%) Depth (20.4%) Rugosity (2.8%)	1	0.946	21525.517	50.9818	< 0.001
6	Cost Dist. (77.7%) Depth (19.8%) Rugosity (2.5%)	2	0.944	21673.880	199.346	< 0.001
7	Cost Dist. (78.8%) Depth (18.9%) Rugosity (2.3%)	3	0.943	21723.917	249.382	< 0.001
8	Cost Dist. (79.7%) Depth (18.2%) Rugosity (2.1%)	4	0.943	21783.658	309.124	< 0.001
9	Cost Dist. (71.6%) Depth (25.7%) VRM (2.7%)	1	0.941	21977.769	503.234	< 0.001
10	Cost Dist. (74.0%) Depth (24.3%) VRM (1.8%)	2	0.938	22122.007	647.473	< 0.001
11	Cost Dist. (74.0%) Depth (23.6%) VRM (2.3%)	3	0.936	22176.155	701.62	< 0.001
12	Cost Dist. (74.7%) Depth (23.4%) VRM (1.9%)	4	0.935	22219.672	745.138	< 0.001

Model	*Variable Contribution*	β	*AUC*	*AIC*	ΔAIC	ω_i
13	Cost Dist. (75.5%) Depth (20.5%) Rugosity (2.2%) VRM (1.7%)	1	0.948	21482.254	7.7192	0.011
14	Cost Dist. (75.9%) Depth (19.9%) VRM (2.2%) Rugosity (2.1%)	2	0.944	21638.899	164.365	< 0.001
15	Cost Dist. (77.2%) Depth (18.7%) VRM (2.1%) Rugosity (2.0%)	3	0.944	21692.878	218.344	< 0.001
16	Cost Dist. (77.0%) Depth (18.6%) Rugosity (2.4%) VRM (2.0%)	4	0.943	21747.024	272.49	< 0.001
17	Cost Dist. (75.5%) Depth (20.2%) VRM (1.5%) Rugosity (2.6%)	1	0.948	21508.703	34.1683	< 0.001
18	Cost Dist. (75.7%) Depth (19.8%) VRM (2.1%) Rugosity (2.1%) Slope (0.2%)	2	0.945	21642.209	167.674	< 0.001
19	Cost Dist. (76.8%) Depth (19.0%) VRM (1.9%) Rugosity (2.2%) Slope (0.1%)	3	0.944	21707.836	233.302	< 0.001
20	Cost Dist. (78.3%) Depth (17.9%) VRM (1.8%) Rugosity (1.9%) Slope (0.1%)	4	0.943	21753.621	279.086	< 0.001
21	Cost Dist. (74.9%) Depth (20.2%) VRM (1.3%) Rugosity (2.4%) Slope (0.7%)	1	0.949	21474.831	0.29614	0.458

Model	*Variable Contribution*	*β*	*AUC*	*AIC*	*ΔAIC*	ω_i
	Aspect (0.5%)					
22	Cost Dist. (77.9%) Depth (19.3%) VRM (1.1%) Rugosity (1.4%) Slope (0.1%) Aspect (0.2%)	2	0.945	21645.458	170.924	< 0.001
23	Cost Dist. (79.0%) Depth (18.2%) VRM (1.2%) Rugosity (1.2%) Slope (0.1%) Aspect (0.3%)	3	0.945	21700.597	226.062	< 0.001
24	Cost Dist. (80.8%) Depth (17.4%) VRM (0.6%) Rugosity (0.9%) Slope (0.1%) Aspect (0.1%)	4	0.944	21742.173	267.639	< 0.001
25	Cost Dist. (74.9%) Depth (20.2%) VRM (1.9%) Rugosity (2.3%) Slope (0.2%) Aspect (0.4%) BPIb (0.1%)	1	0.949	21474.535	0.000	0.531
26	Cost Dist. (74.9%) Depth (19.2%) VRM (1.1%) Rugosity (1.4%) Slope (3.0%) Aspect (0.4%) BPIb (0.1%)	2	0.946	21636.438	161.904	< 0.001
27	Cost Dist. (78.8%) Depth (18.2%) VRM (1.4%) Rugosity (1.2%) Slope (0%) Aspect (0.2%)	3	0.945	21688.552	214.017	< 0.001

Model	*Variable Contribution*	*β*	*AUC*	*AIC*	*ΔAIC*	ω_i
	BPIb (0.2%)					
28	Cost Dist. (80.7%) Depth (17.3%) VRM (0.7 %) Rugosity (1.0%) Slope (0%) Aspect (0.1%) BPIb (0.1%)	4	0.944	21742.488	267.953	< 0.001

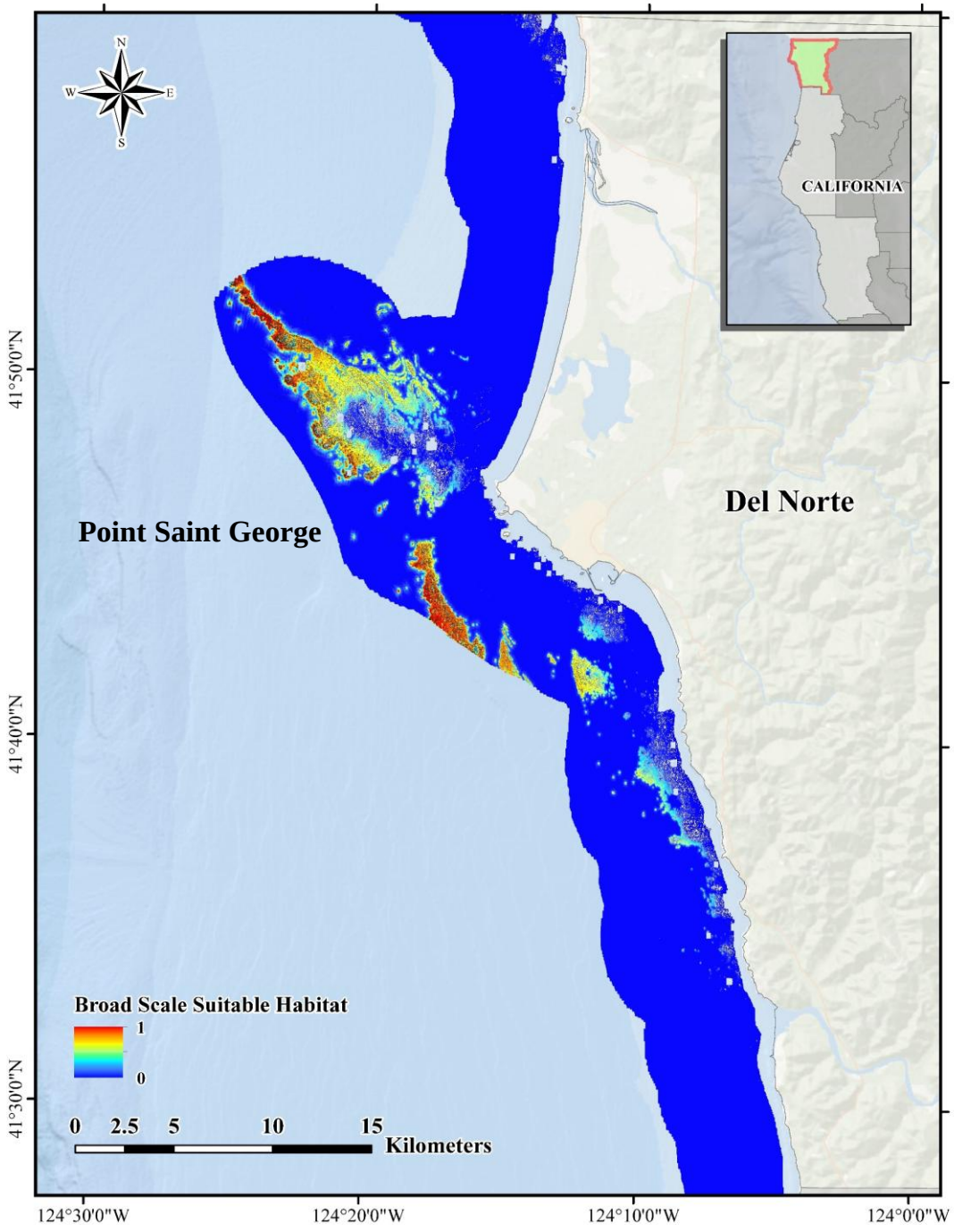

Figure 7. Map of the suitable habitat for the Del Norte County region based on the occurrence data for *S. pinniger* and the environmental variables of the most parsimonious model (model 16): cost distance, depth, VRM, and Rugosity. The heatmap indicates predicted habitat suitability with colors (and values) ranging from high suitability in red (one) to low predicted suitability (zero).

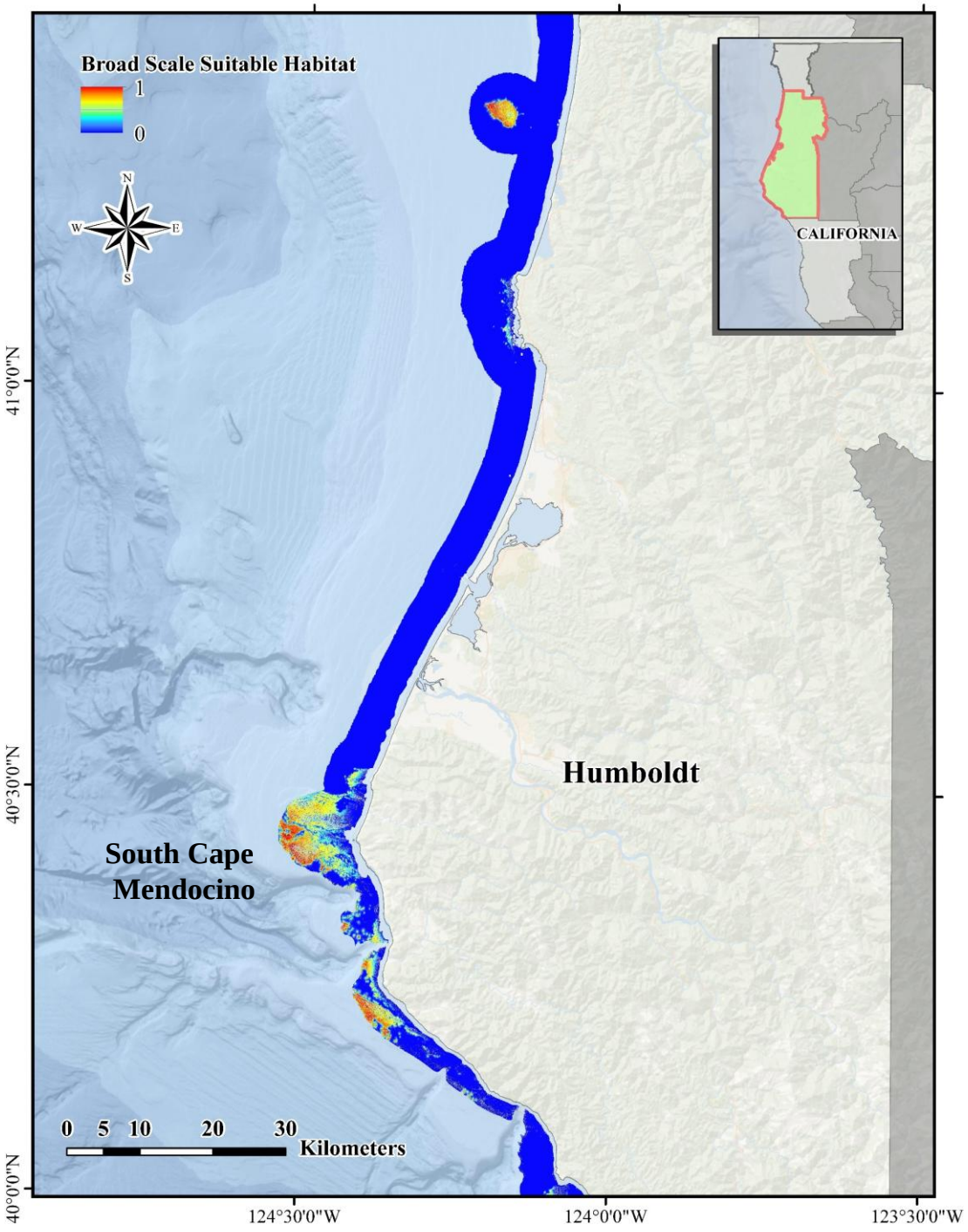

Figure 8. Map of the suitable habitat for Humboldt County based on the occurrence data for *S. pinniger* and the environmental variables of the most parsimonious model (model 16): cost distance, depth, VRM, and Rugosity. The heatmap indicates predicted habitat suitability with colors (and values) ranging from high suitability in red (one) to low predicted suitability (zero).

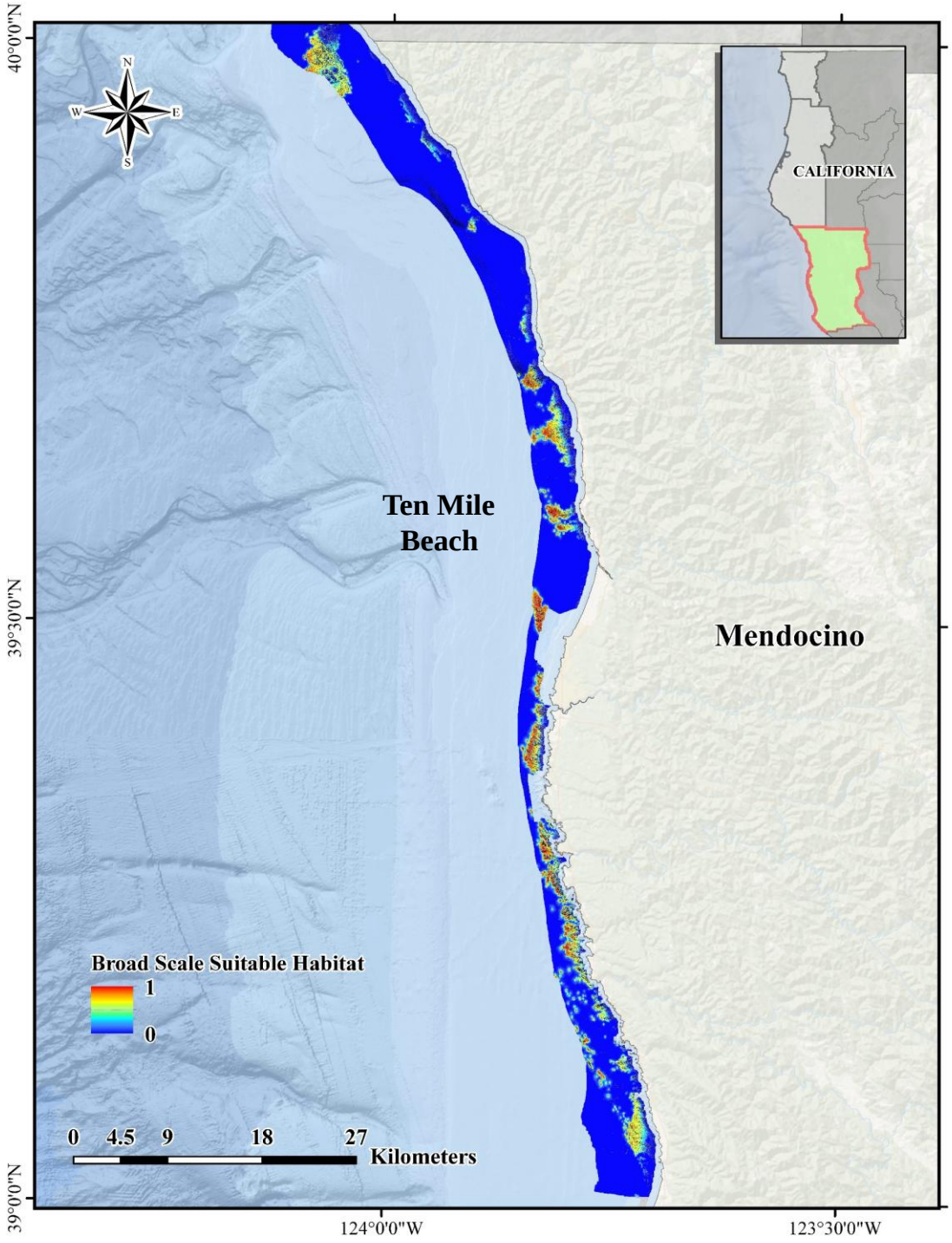

Figure 9. Map of the suitable habitat for Mendocino County region based on the occurrence data for *S. pinniger* and the environmental variables of the most parsimonious model (model 16): cost distance, depth, VRM, and Rugosity. The heatmap indicates predicted habitat suitability with colors (and values) ranging from high suitability in red (one) to low predicted suitability (zero).

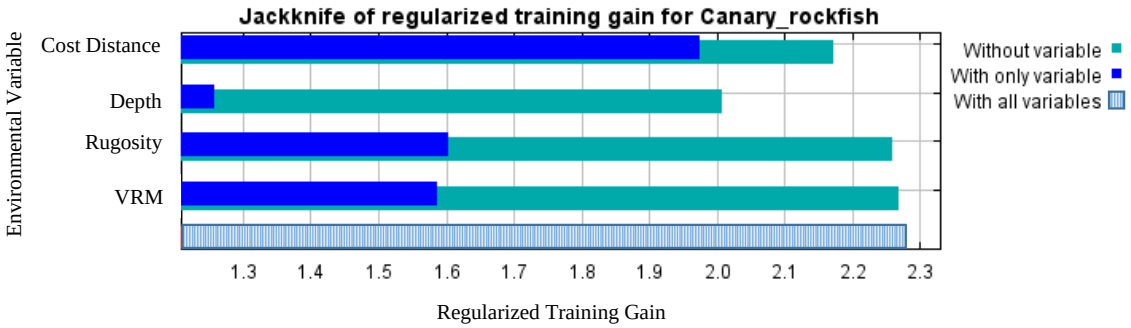

Figure 10. Jackknife test results performed on the training dataset for the broad-scale analysis for the most parsimonious model; model 16. The jackknife test indicates how much each predictive variable affects the model by creating a new model with the removal individual covariates (Burnham and Anderson 2002).

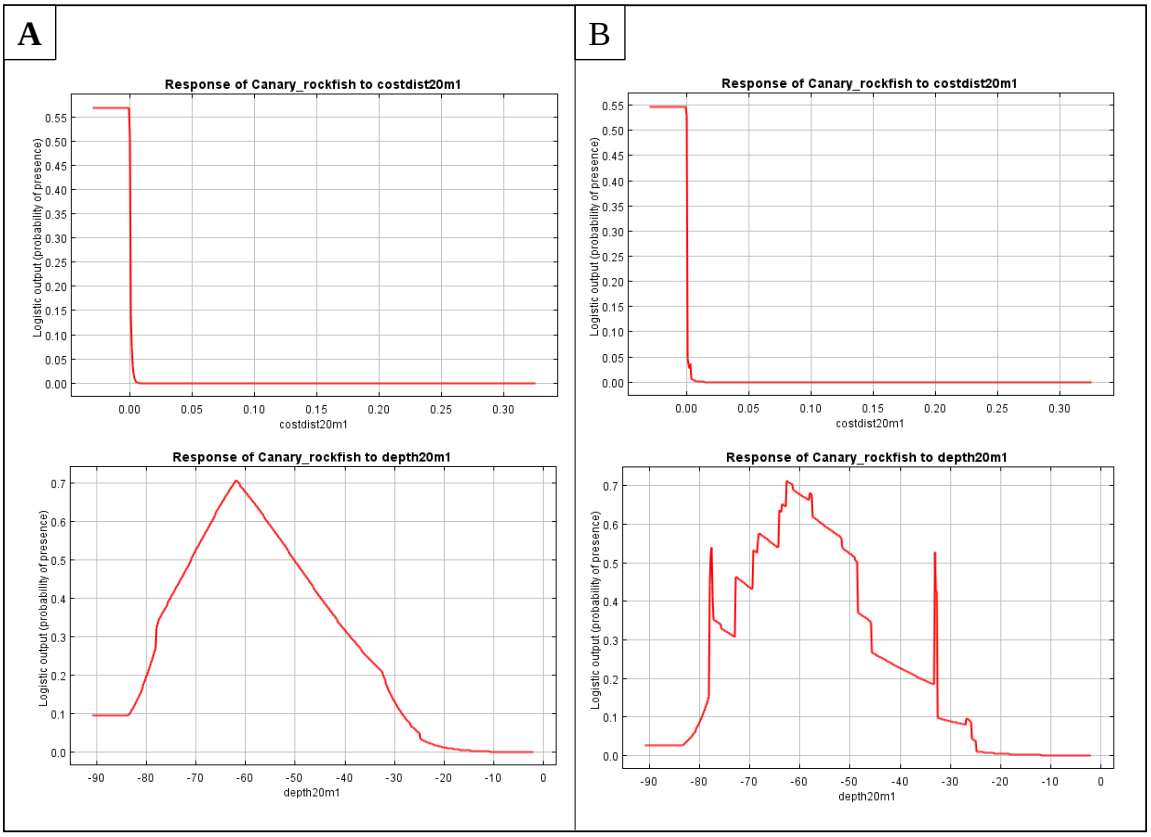

Figure 11. Response curves for covariates used in (A) model 16 (best model) and (B) model 25 (overfitted model) for the broad-scale study region. Environmental covariate acronyms are cost distance (costdist20m1), depth (depth20m1).

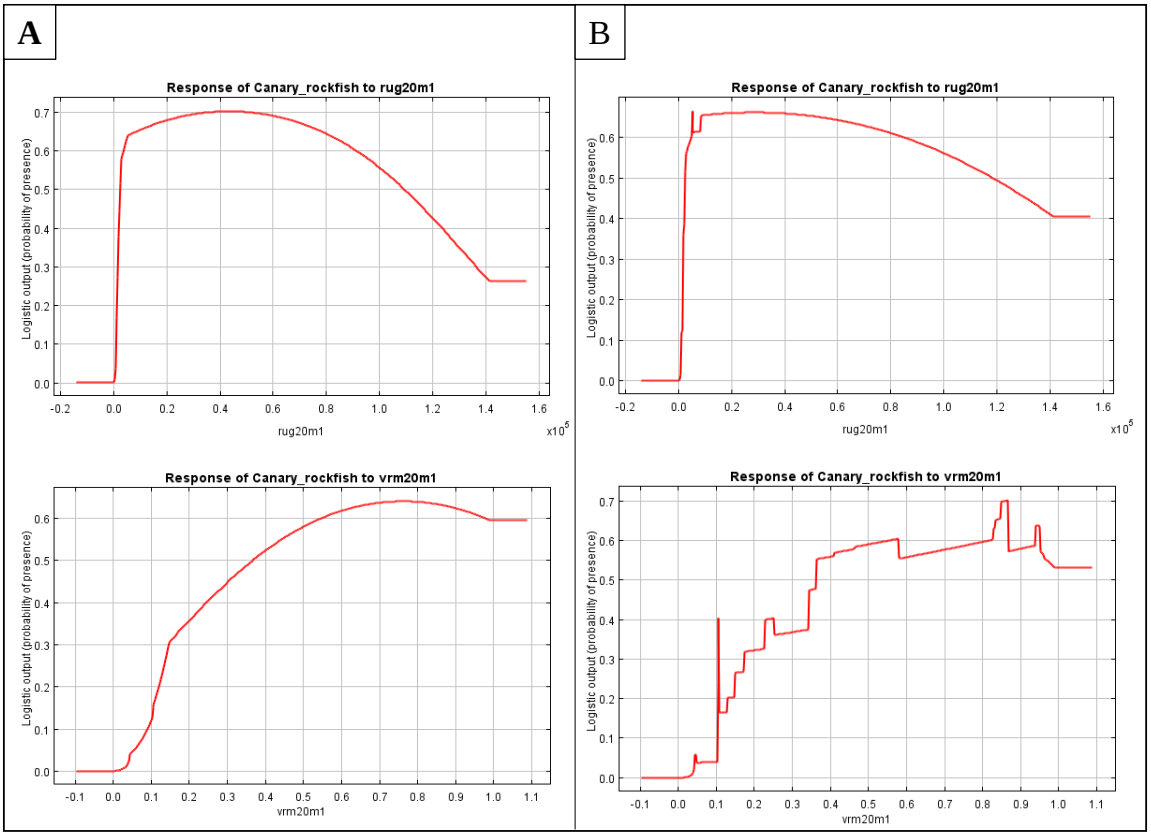

Figure 12. Response curves for covariates used in (A) model 16 (best model) and (B) model 25 (overfitted model) for the broad-scale study region. Environmental covariate acronyms are rugosity (rug20m1) and VRM (vrm20m1).

Fine-scale

After the broad-scale modeling efforts were completed, I conducted fine-scale studies focused on three areas within the broad-scale study region that displayed highly suitable habitat and where *S. pinniger* occurrence data were available. The Del Norte County study region, in the vicinity of Point Saint George, spanned approximately 128.2 km^2; the Humboldt County study region, in the vicinity of Cape Mendocino, approximately 132.4 km^2; the Mendocino County study region, in the vicinity of Ten Mile Beach, approximately 84.6 km^2.

I generated several predictive models and reported on the top performing models based on model contribution and permutation importance of each of the covariates. The top performing models for the fine-scale study regions include 11 predictive models for the Point Saint George area of the Del Norte County region, six predictive models for the South Cape Mendocino area of the Humboldt County region, and four predictive models for the Ten Mile Beach area of the Mendocino County region.

Del Norte

In the area I selected near Point Saint George off the Del Norte County coast (Figure 13), with data for 287 *S. pinniger* (Figure 14). The selected area included three sampling locations including and MPA. Though there were additional occurrences of *S.* pinniger in the reef south of the selected area (Figure 4), including them would have made this area substantially larger than the other fine-scale regions.

Results of the fine-scale predictive modeling effort for the Point Saint George area indicated that the highest performing model was model 7, which accounted for 99.99% of weight in the table, had a β value of 1, AUC of 0.987, and included four environmental covariates: cost distance, depth, VRM, and rugosity. The selected and most parsimonious model to predict *S. pinniger* for the broad-scale region was model 11, which accounted for 0.00% of weight in the table, used a β value of 5, reported AUC of 0.979, and included four environmental covariates: cost distance, depth, VRM, and rugosity (Table 5). The habitat suitability map produced from model 11 (Figure 15) predicted high suitability at the interface between hard and soft substrates and low suitability in areas where larger-bodied *S. pinniger* tend not to aggregate (i.e. sand flats) (Love et al. 2002). Results of the jackknife test for model 11 indicate the most influential environmental covariates were cost distance, depth, rugosity, VRM, respectively (Figure 16). Areas of high suitability occurred where cost distance was zero or close to zero and a depth range of approximately 62 to 67 m (Figures 17 and 18).

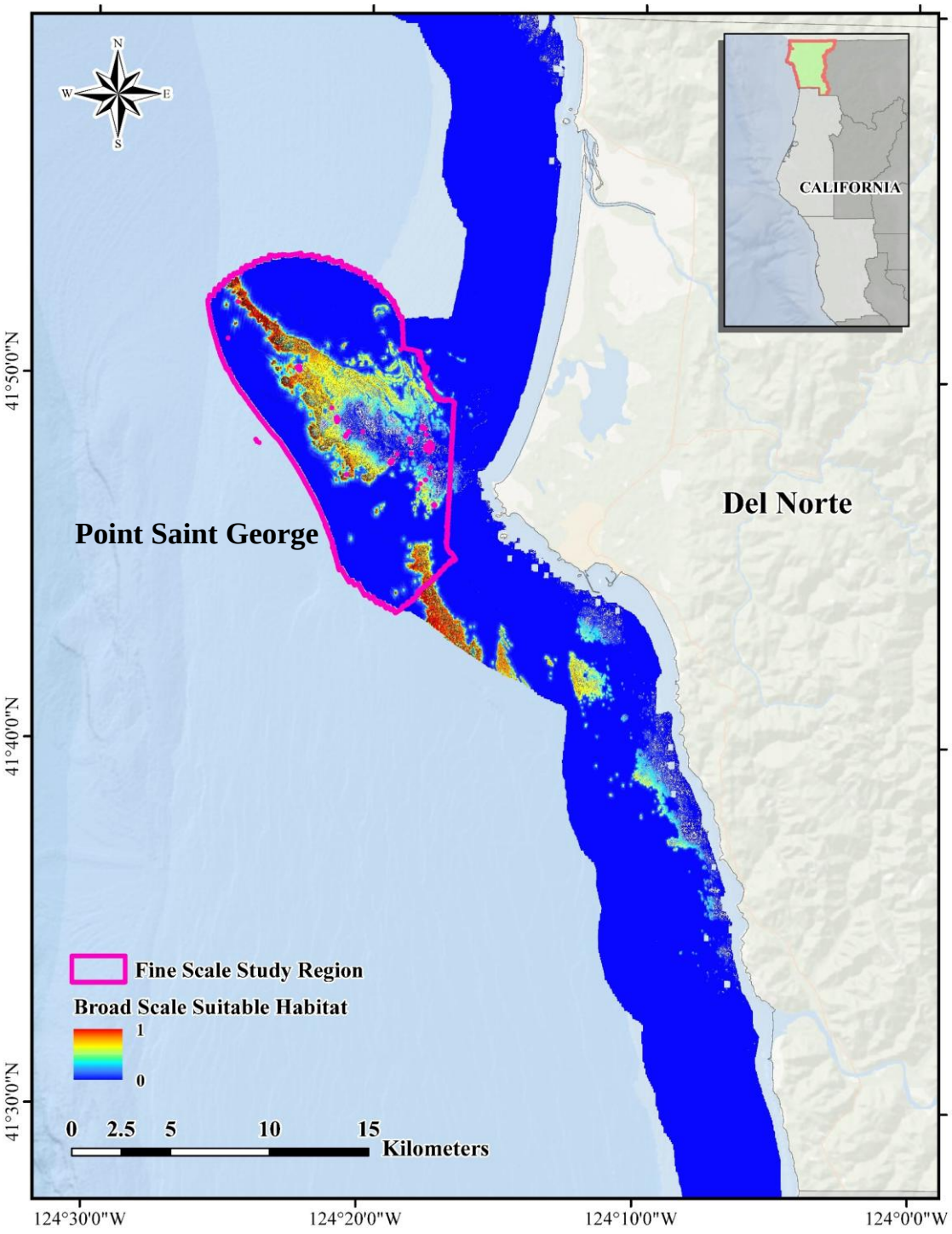

Figure 13. Selected Point Saint George area (outlined) for fine-scale modeling off the Del Norte County study region, California, USA.

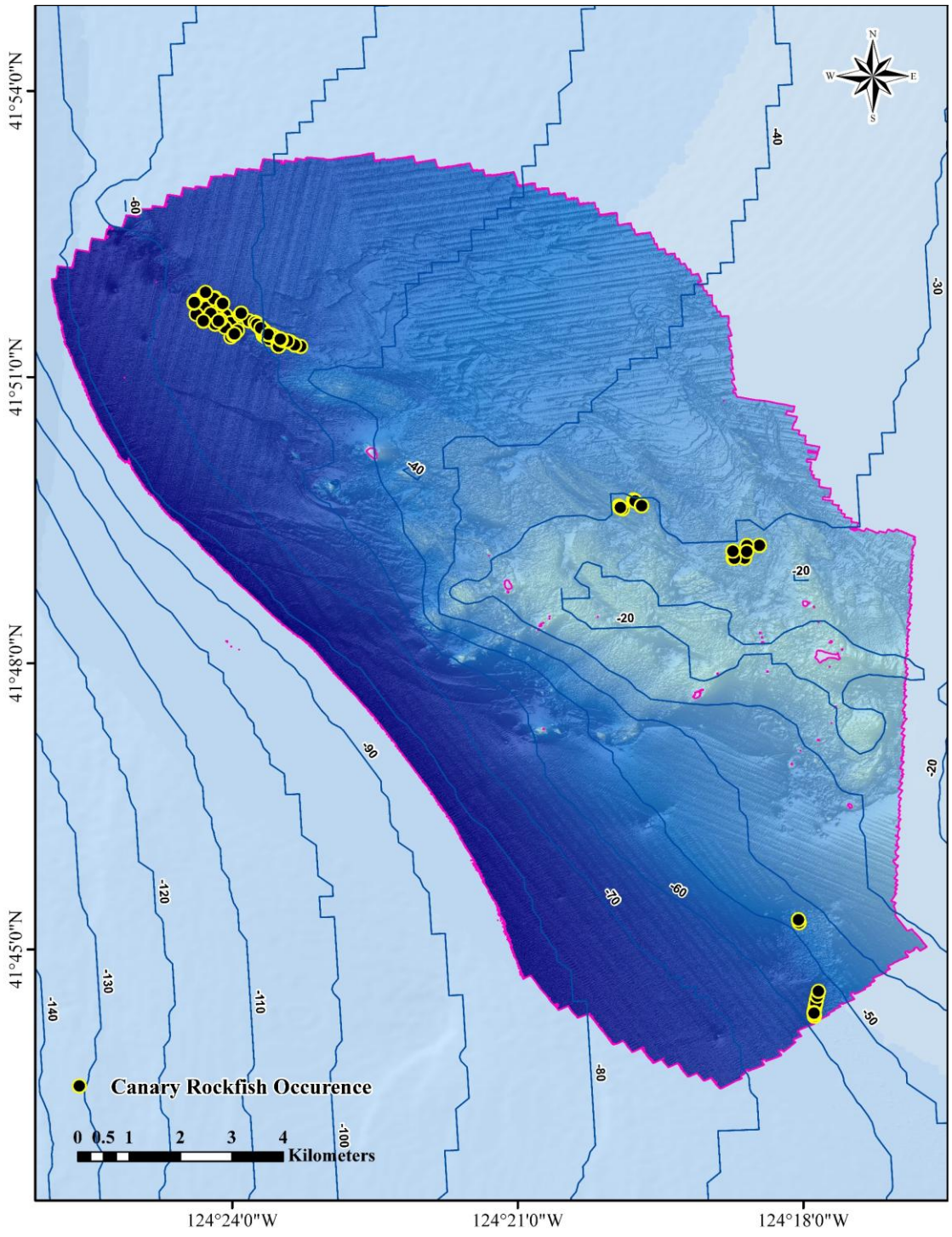

Figure 14. Map of the canary rockfish (*S. pinniger*) recorded occurrences within the Point Saint George area off the coast of Del Norte County, California, USA.

Table 5. Criterion used to select the highest performing models for the Point Saint George area of the Del Norte County region: relative contributions of the major environmental covariates, regularization parameter used, AUC, AIC, ΔAIC, and ω_i.

Model	*Covariates*	*β*	*AUC*	*AIC*	*ΔAIC*	ω_i
1	Cost Dist. (56.0%)	1	0.988	4168.703	21.249	< 0.001
	Depth (33.9%)					
	VRM (2.6%)					
	Rugosity (5.0%)					
	Slope (0.5%)					
	Aspect (0.7%)					
	Curvature (1.3%)					
2	Cost Dist. (56.4%)	1	0.988	4160.431	12.977	< 0.001
	Depth (34.3%)					
	VRM (2.7%)					
	Rugosity (5.2%)					
	Curvature (1.3%)					
3	Cost Dist. (60.3%)	2	0.984	4203.873	56.419	< 0.001
	Depth (31.8%)					
	VRM (2.6%)					
	Rugosity (4.9%)					
	Curvature (0.4%)					
4	Cost Dist. (62.7%)	3	0.980	4233.952	86.498	< 0.001
	Depth (30.5%)					
	VRM (2.2%)					
	Rugosity (4.3%)					
	Curvature (0.4%)					
5	Cost Dist. (62.8%)	4	0.980	4247.473	100.019	< 0.001
	Depth (30.3%)					
	VRM (1.8%)					
	Rugosity (4.7%)					
	Curvature (0.4%)					
6	Cost Dist. (64.4%)	5	0.979	4274.856	127.402	< 0.001
	Depth (29.6%)					
	VRM (2.0%)					
	Rugosity (3.5%)					
	Curvature (0.4%)					
7	Cost Dist. (57.0%)	1	0.987	4147.454	0	0.999
	Depth (34.7%)					
	VRM (3.0%)					
	Rugosity (5.4%)					
8	Cost Dist. (60.5%)	2	0.983	4208.842	61.388	< 0.001
	Depth (32.1%)					
	VRM (2.6%)					
	Rugosity (4.7%)					
9	Cost Dist. (63.0%)	3	0.980	4232.083	84.629	< 0.001
	Depth (30.6%)					
	VRM (2.2%)					
	Rugosity (4.2%)					
10	Cost Dist. (63.5%)	4	0.979	4254.880	107.426	< 0.001
	Depth (30.3%)					
	VRM (1.8%)					

Model	*Covariates*	*β*	*AUC*	*AIC*	*ΔAIC*	ω_i
	Rugosity (4.5%)					
11	Cost Dist. (64.2%)	5	0.979	4260.178	112.724	< 0.001
	Depth (30.0%)					
	Rugosity (3.4%)					
	VRM (2.3%)					

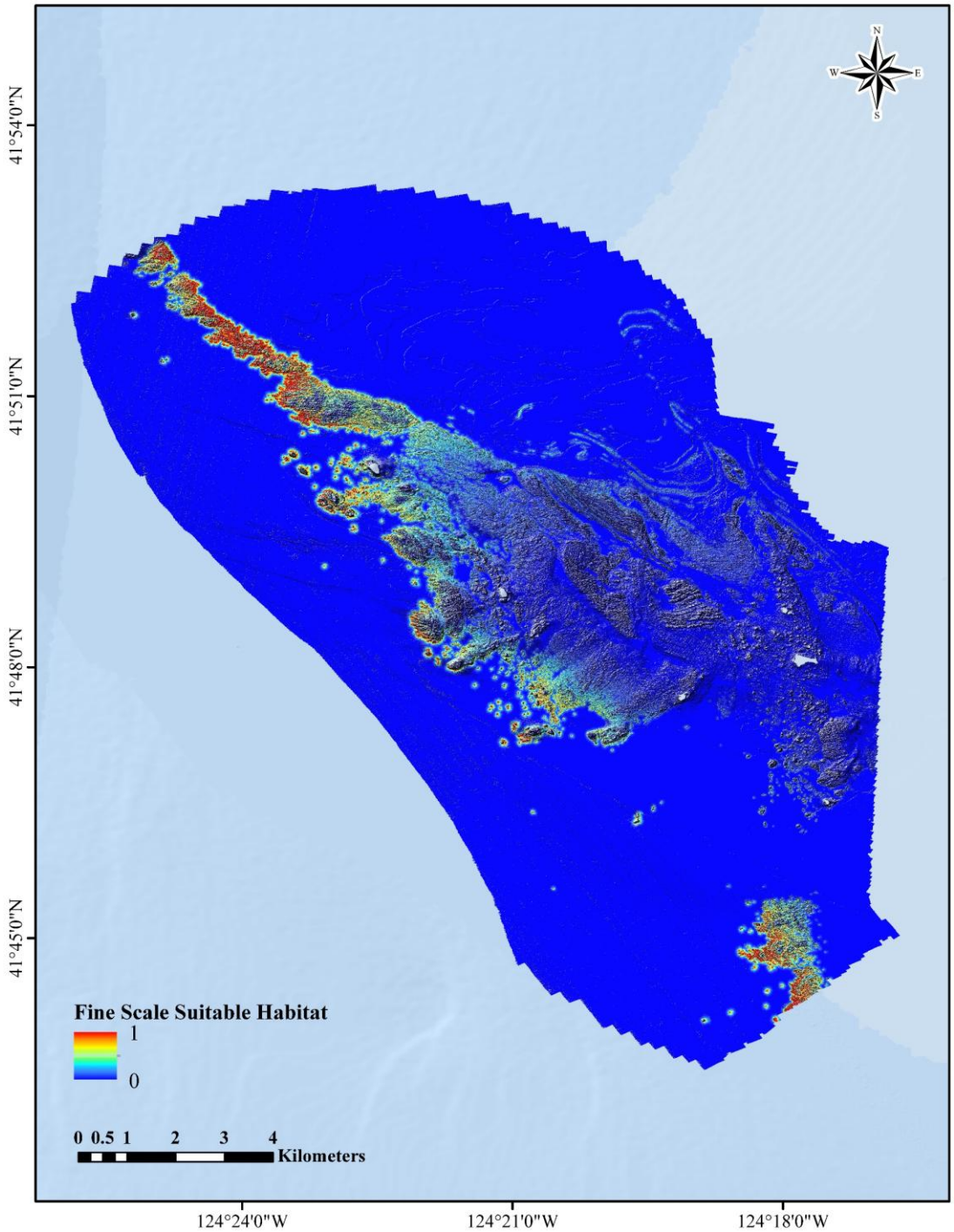

Figure 15. Fine-scale map of the suitable habitat based on the occurrence data for *S. pinniger* and the environmental variables of the most parsimonious model (model 11) of the Point Saint George area of Del Norte County study region, California, USA. The heatmap indicates predicted habitat suitability with colors (and values) ranging from high suitability in red (one) to low predicted suitability (zero).

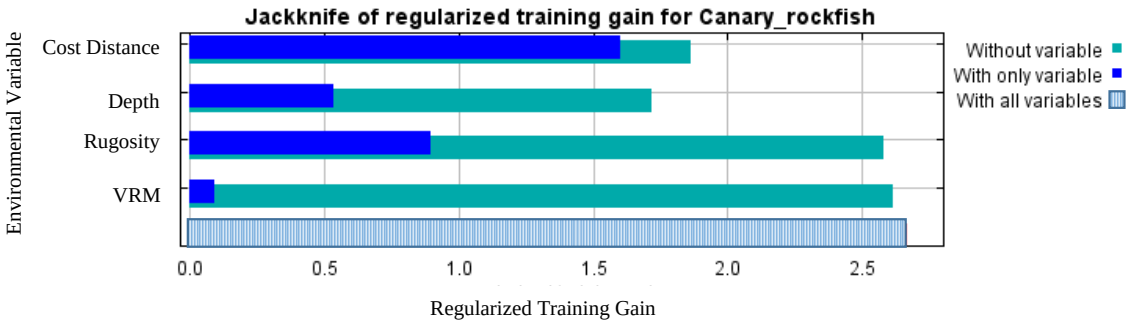

Figure 16. Jackknife test results performed on the training dataset for the Del Norte fine-scale analysis for the most parsimonious broad-scale model; model 11. The jackknife test indicates how much each predictive variable affects the model by creating a new model with the removal individual covariates (Burnham and Anderson 2002).

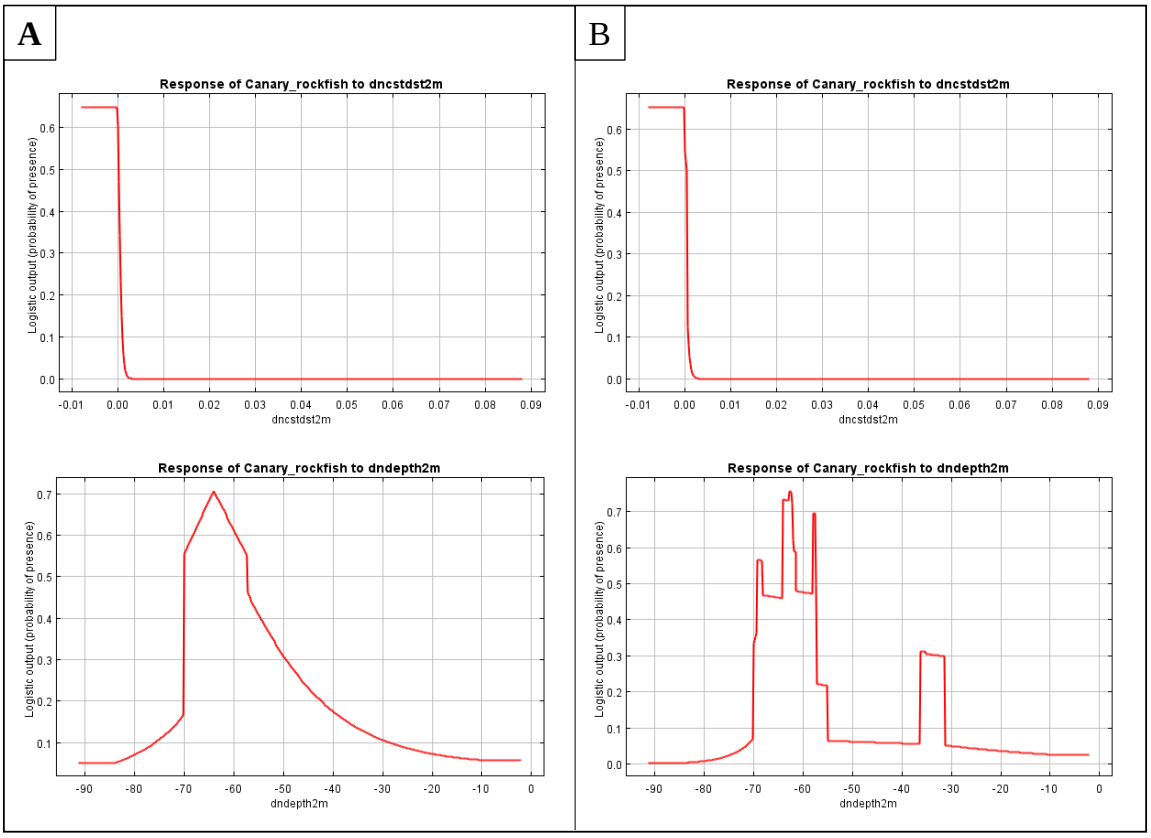

Figure 17. Response curves for covariates used in (A) model 11(best model) and (B) model 7 (overfitted model) for the Point Saint George area of the Del Norte County study region. Environmental covariate acronyms: cost distance (dncostdist2m), depth (dndepth2m).

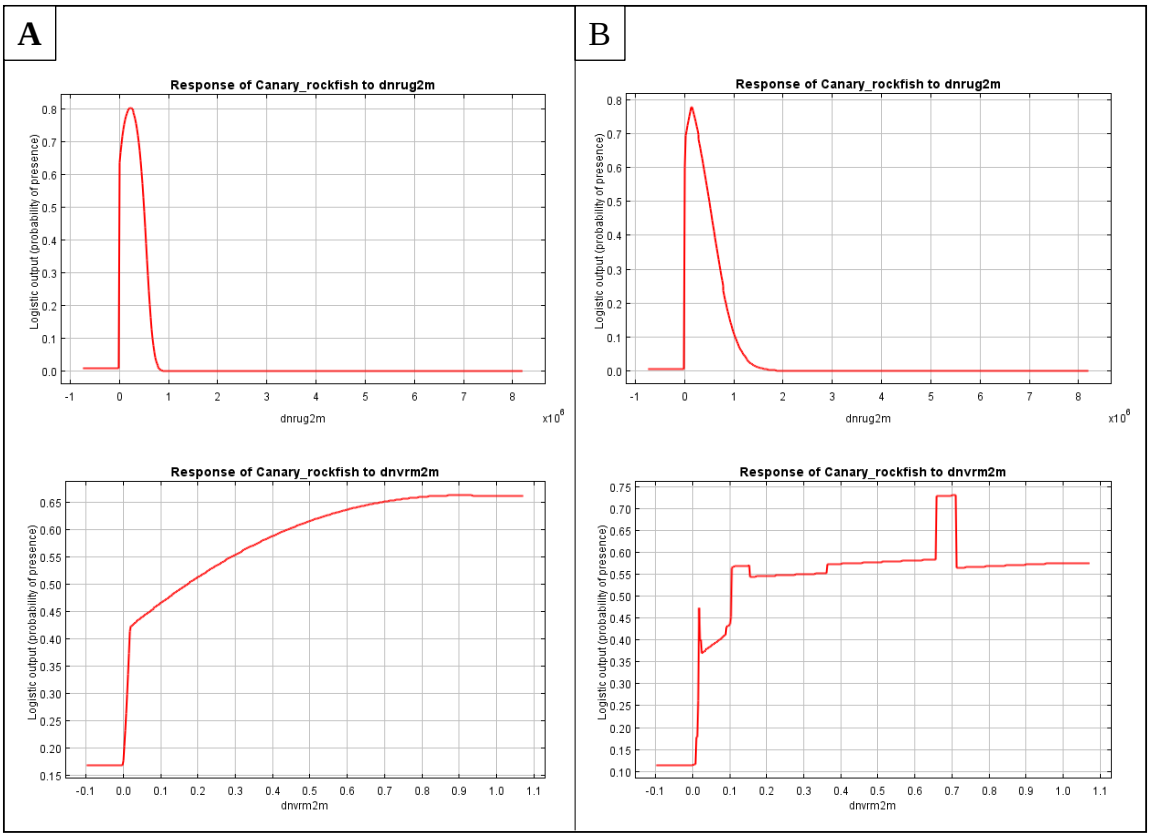

Figure 18. Response curves for covariates used in (A) model 11 (best model) and (B) model 7 (overfitted model) for the Point Saint George area of the Del Norte County study region. Environmental covariate acronyms: rugosity (dnrug2m), and VRM (dnvrm2m).

Humboldt

In the area I selected near South Cape Mendocino off the Humboldt County coast (Figure 19), 59 *S. pinniger* occurrences were used (Figure 20). Results of the fine-scale predictive modeling effort for the South Cape Mendocino area indicated that the highest performing models were model 3 and model 5, both of which accounted for 33.4% of weight in the table. Models 3 and 5 used β values of 1, and the AUC for model 3 was 0.952, whereas model 5 reported an AUC of 0.945. Six environmental covariates were used in model 3: cost distance, depth, rugosity, aspect, VRM, and slope. Model 5 used

five environmental covariates: cost distance, depth, rugosity, and VRM. The selected and most parsimonious model to predict *S. pinniger* for this area was model 3 (Table 6). The habitat suitability map produced from model 3 (Figure 21) predicted high suitability at the interface between hard and soft substrates and low suitability in areas where larger-bodied *S. pinniger* tend not to aggregate (i.e. sand flats) (Love et al. 2002). Results of the jackknife test for model 3 indicate the most influential environmental covariates were cost distance, depth, rugosity, aspect, VRM, and slope, respectively (Figure 22). Areas of high suitability occurred where cost distance was near or equal to zero and depth was approximately 56 to 67 m (Figures 23, 24, and 25).

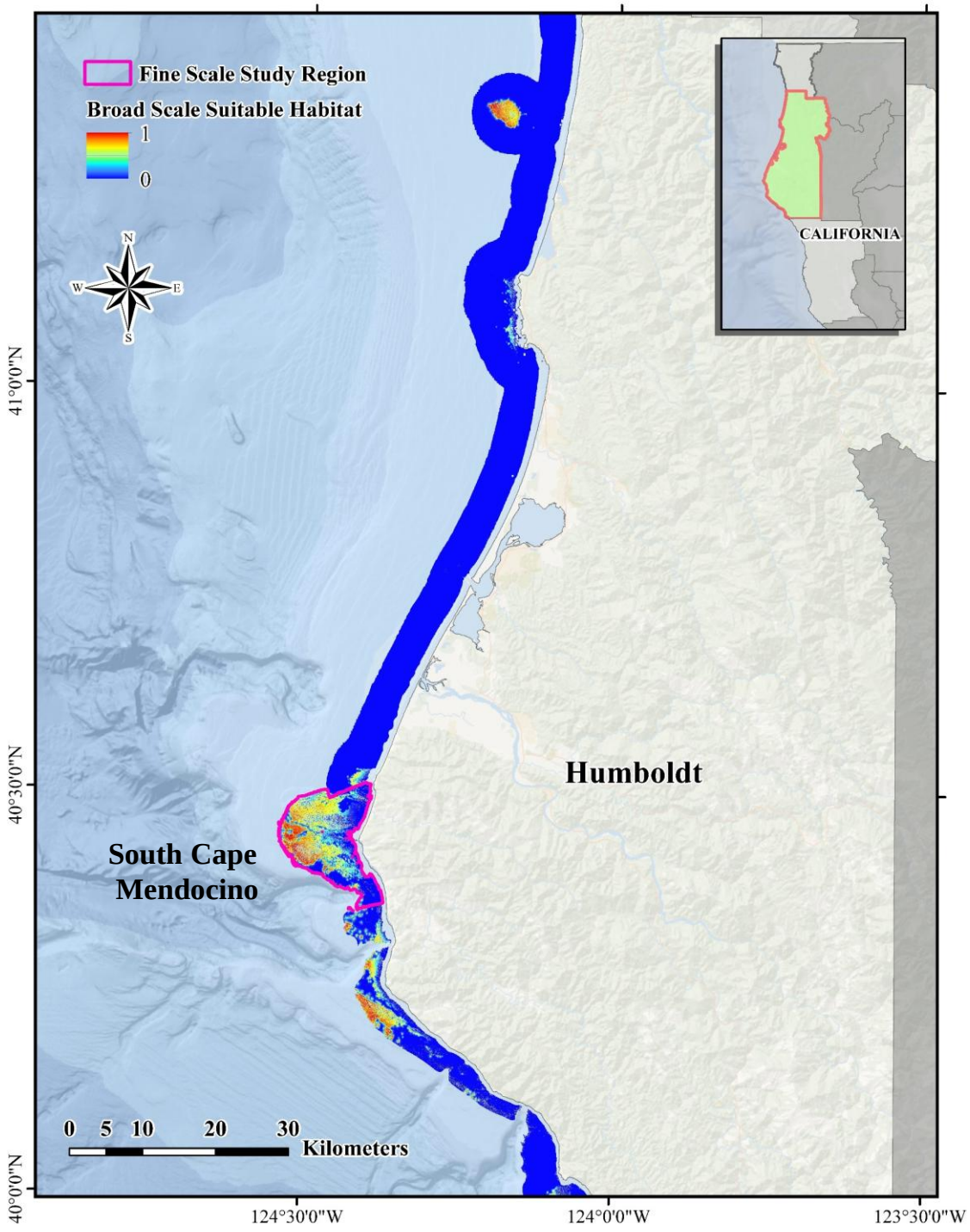

Figure 19. Selected South Cape Mendocino area (outlined) for fine-scale modeling off the Humboldt County study region, California, USA.

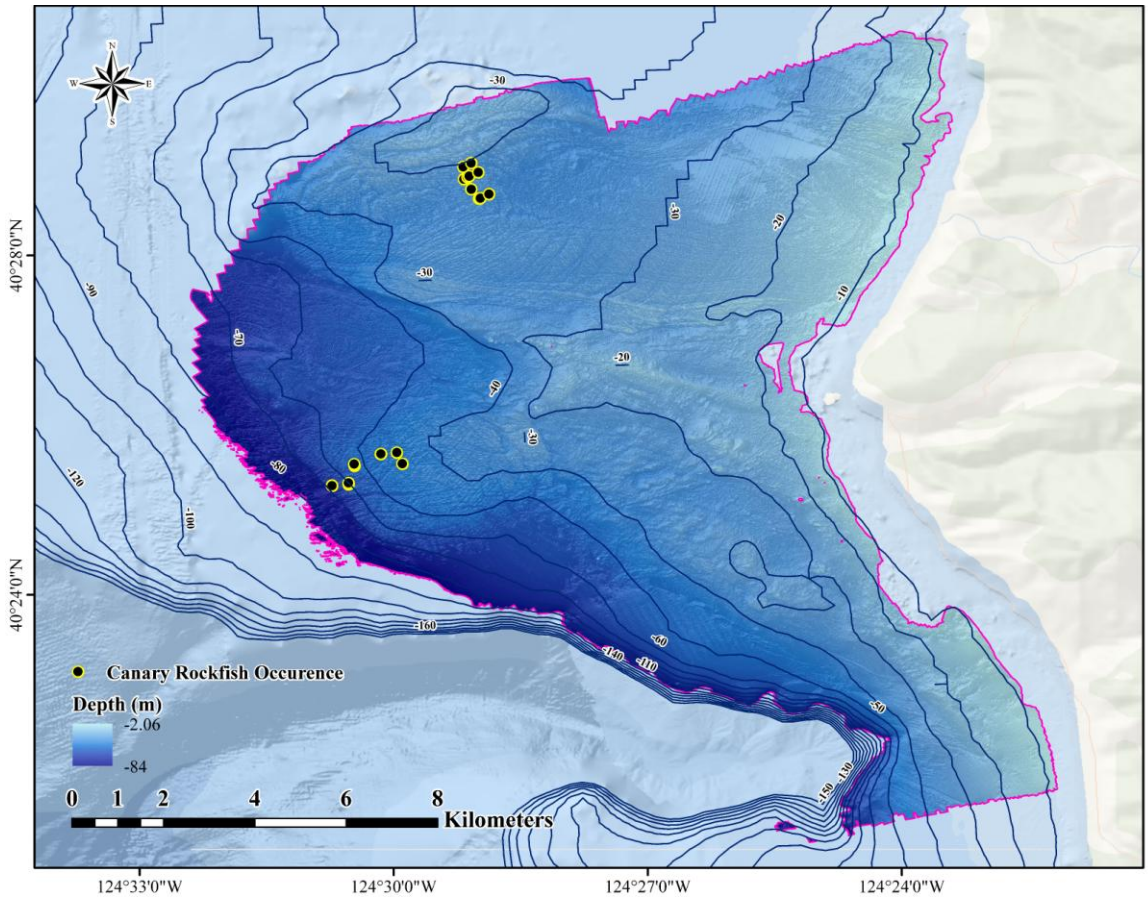

Figure 20. Map of the canary rockfish (*S. pinniger*) recorded occurrences within the South Cape Mendocino area off the coast of Humboldt County, California, USA.

Table 6. Criterion used to select the highest performing models for the fine-scale Humboldt County region: relative contributions of the major environmental covariates, regularization parameter used, AUC, AIC, ΔAIC, and ω_i.

Model	*Covariates*	*β*	*AUC*	*AIC*	*ΔAIC*	*ω_i*
1	Cost Dist. (47.1%)	1	0.955	419.610	2.242	0.109
	Depth (36.3%)					
	Rugosity (6.0%)					
	Aspect (6.0%)					
	VRM (2.4%)					
	Slope (1.8%)					
	Curvature (0.4%)					
2	Cost Dist. (51.5%)	2	0.938	420.605	3.237	0.066
	Depth (38.5%)					
	Slope (3.6%)					
	VRM (3.2%)					
	Aspect (2.8%)					
	Rugosity (0.3%)					
	Curvature (0.3%)					
3	Cost Dist. (47.4%)	1	0.952	417.368	0	0.334
	Depth (36.7%)					
	Rugosity (6.0%)					
	Aspect (6.0%)					
	VRM (2.4%)					
	Slope (1.5%)					
4	Cost Dist. (51.6%)	2	0.937	418.883	1.515	0.157
	Depth (38.4%)					
	Slope (3.6%)					
	VRM (3.3%)					
	Aspect (2.9%)					
	Rugosity (0.3%)					
5	Cost Dist. (48.6%)	1	0.945	417.368	0	0.334
	Depth (37.6%)					
	Aspect (6.2%)					
	Rugosity (5.1%)					
	VRM (2.4%)					
6	Cost Dist. (43.3%)	1	0.933	431.886	14.518	< 0.001
	Depth (42.3%)					
	Aspect (9.7%)					
	Slope (3.1%)					
	VRM (1.6%)					

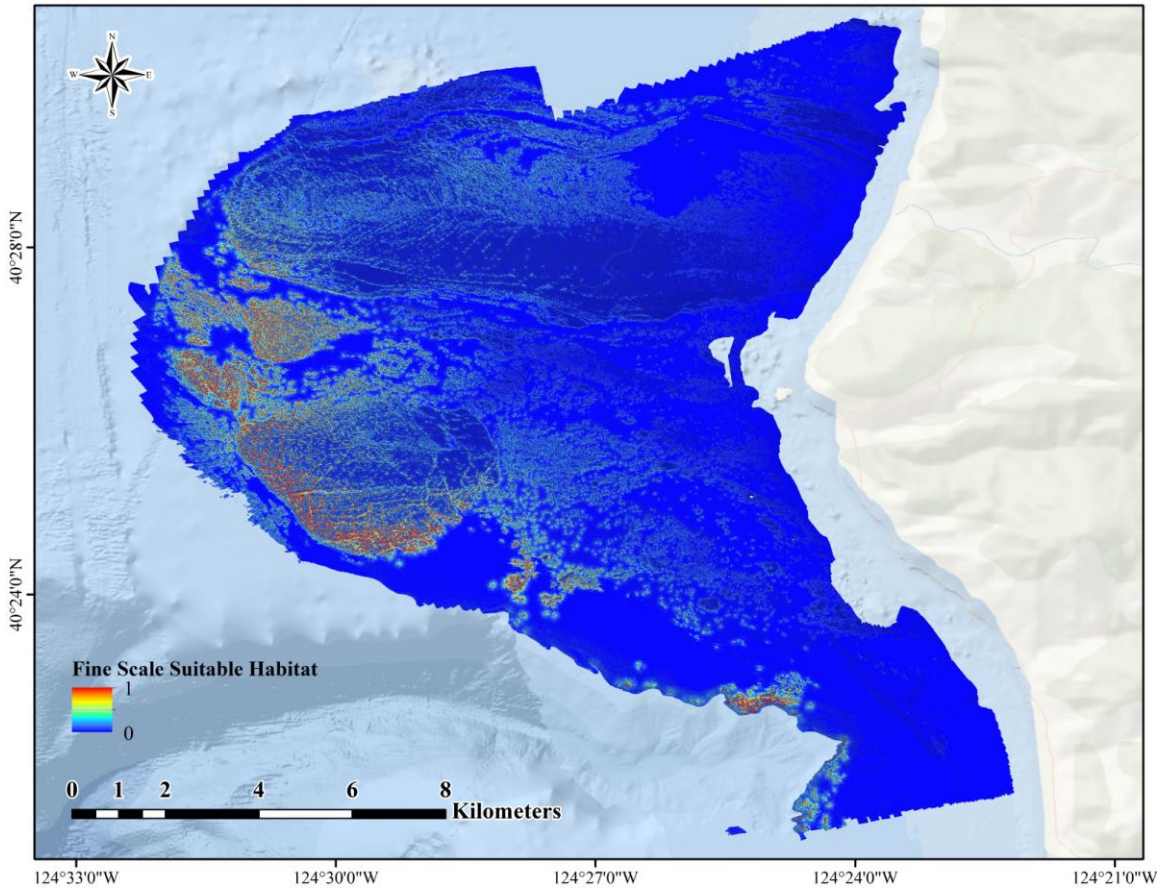

Figure 21. Fine-scale map of the suitable habitat based on the occurrence data for *S. pinniger* and the environmental variables of the most parsimonious model (model 3) of the South Cape Mendocino area of Humboldt County study region, California, USA. The heatmap indicates predicted habitat suitability with colors (and values) ranging from high suitability in red (one) to low predicted suitability (zero).

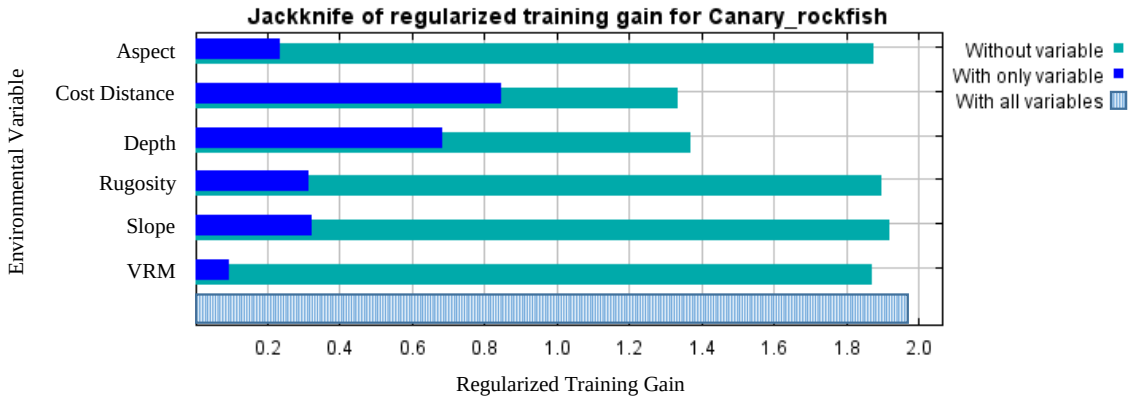

Figure 22. Jackknife test results performed on the training dataset for the South Cape Mendocino area of Humboldt County for the most parsimonious model, model 3. The jackknife test indicates how much each predictive variable affects the model by creating a new model with the removal of individual covariates (Burnham and Anderson 2002).

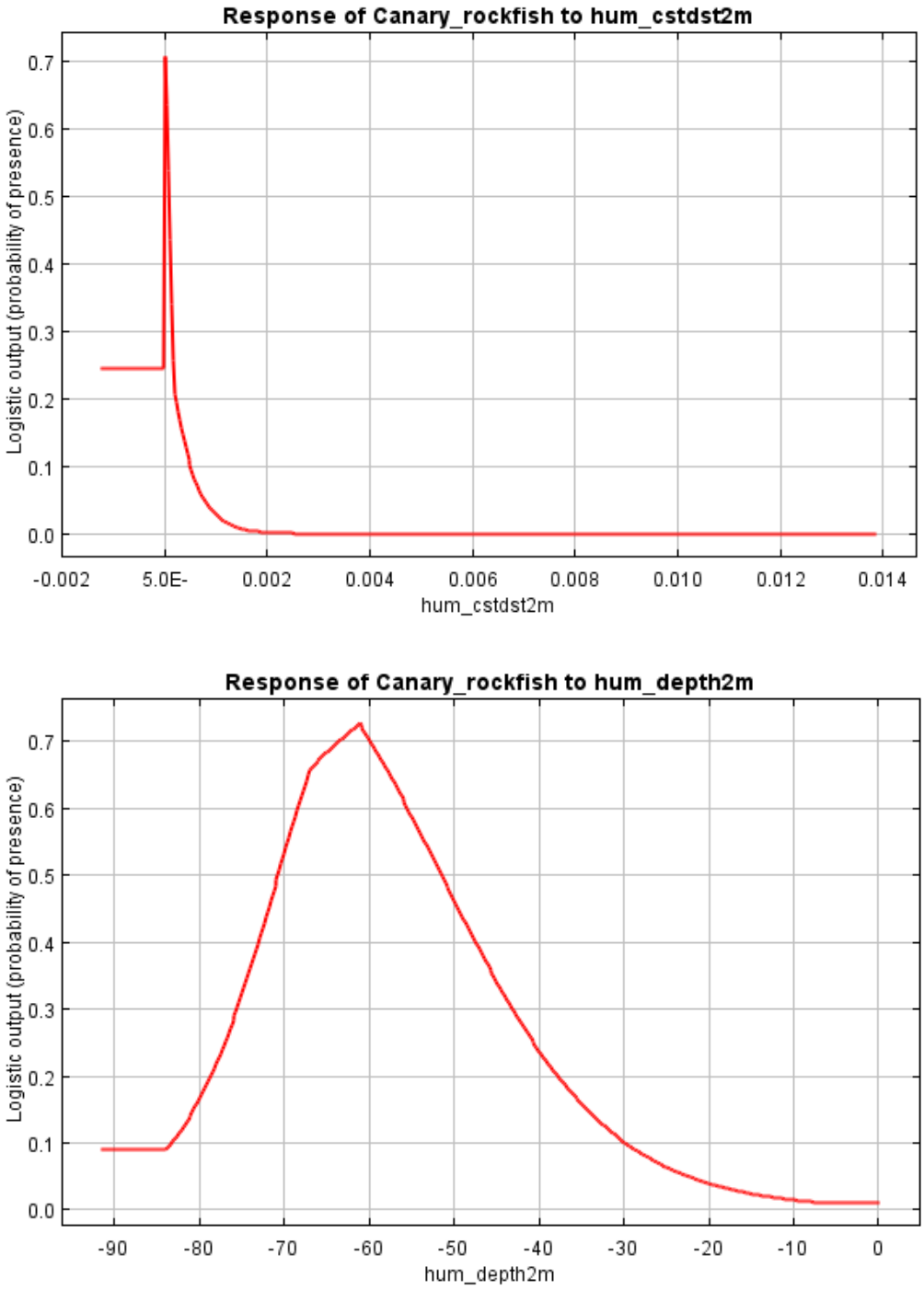

Figure 23. Response curves for environmental covariates used in the best model (model 3) for the South Cape Mendocino area of the Humboldt County region. Environmental covariate acronyms: cost distance (hum_cstdst2m) and depth (hum_depth2m). Note the peaks in the probability at aspects of roughly 180° (south-facing) and 335° (north-northwest-facing).

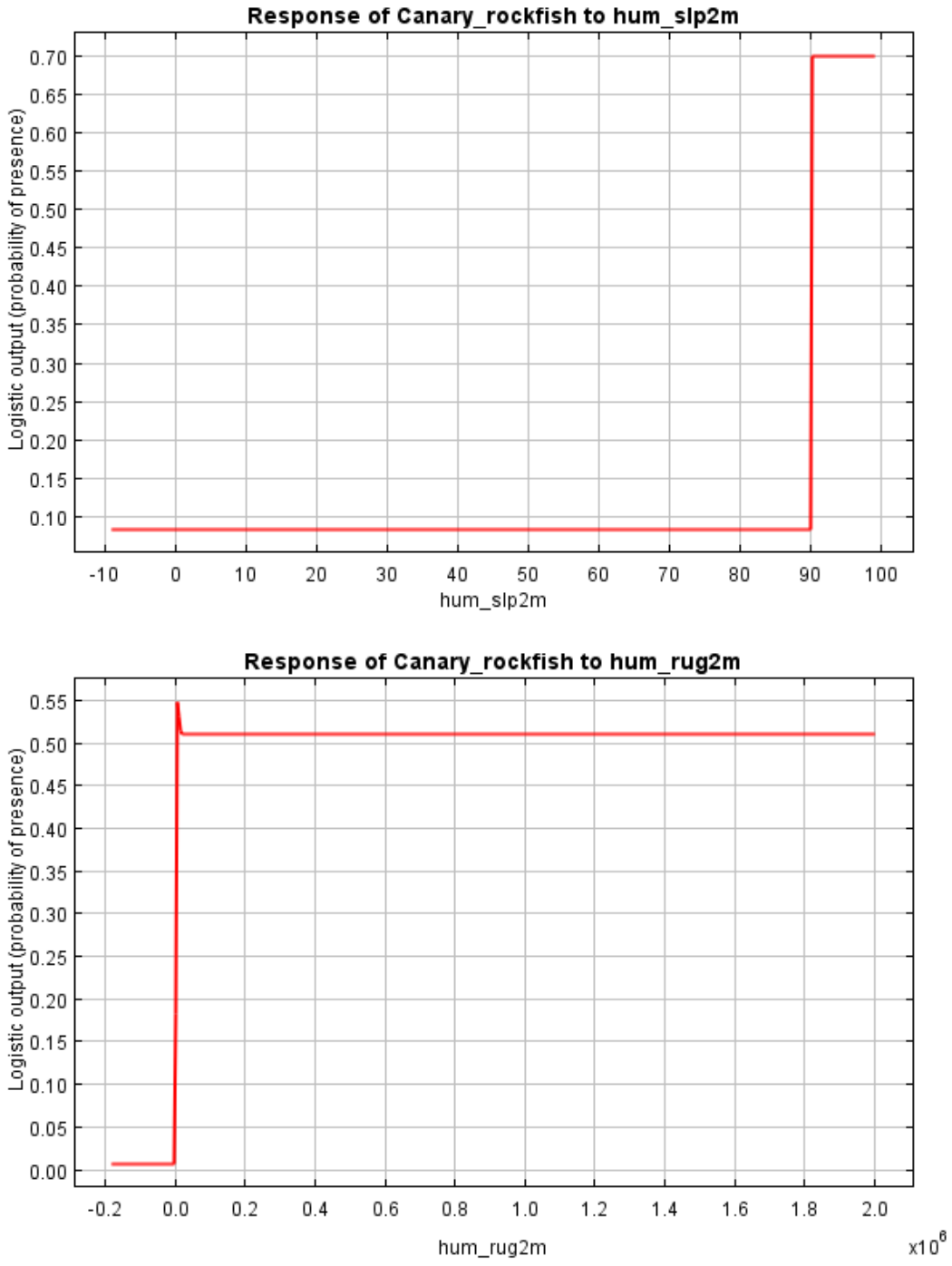

Figure 24. Response curves for environmental covariates used in the best model (model 3) for the South Cape Mendocino area of the Humboldt County region. Environmental covariate acronyms: slope (hum_slp2m) and rugosity (dnrug2m).

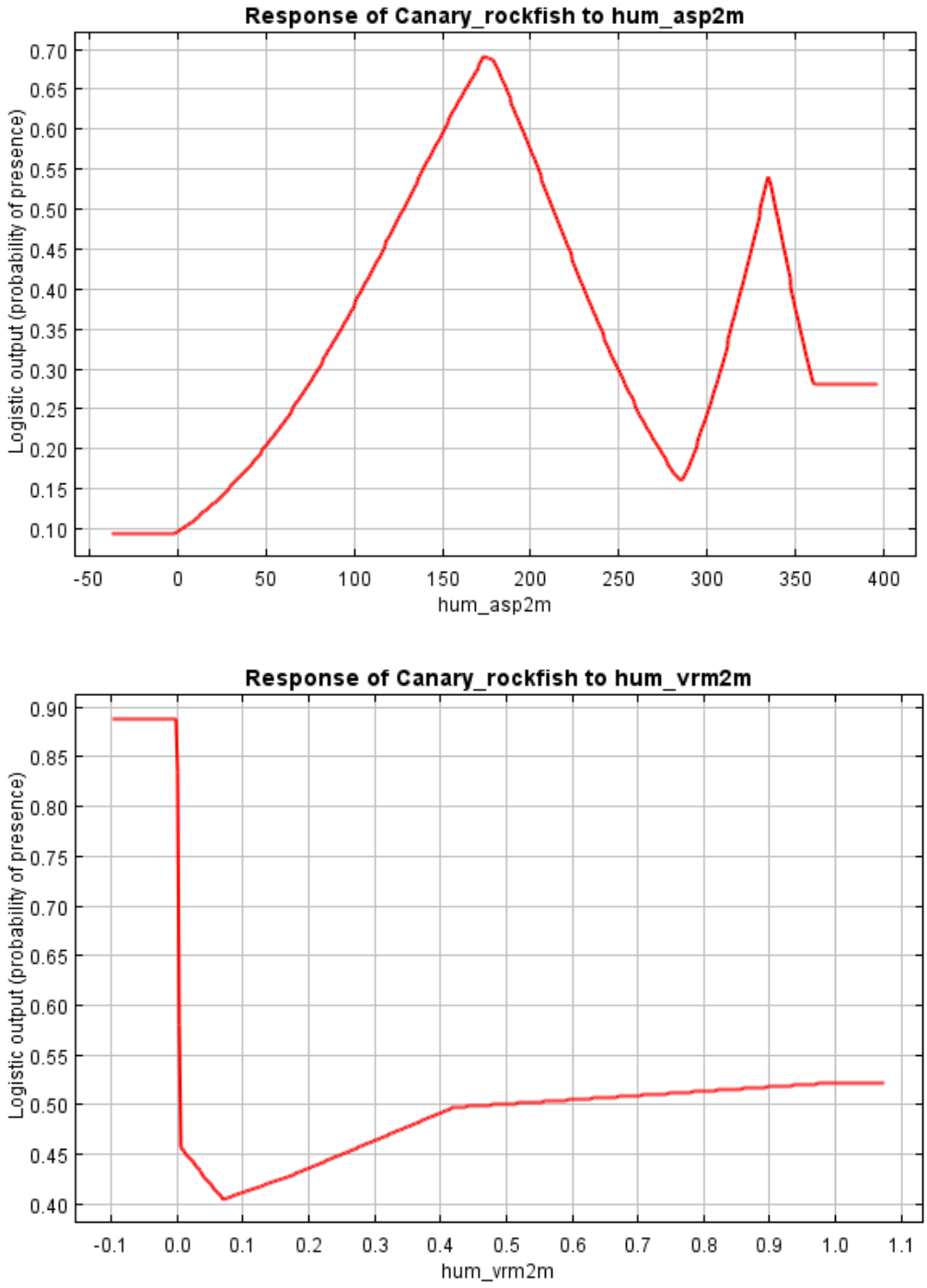

Figure 25. Response curves for environmental covariates used in the best model (model 3) for the South Cape Mendocino area of the Humboldt County region. Environmental covariate acronyms: aspect (hum_asp2m) and VRM (hum_vrm2m).

Mendocino

In the area I selected near Ten Mile Beach off the Mendocino County coast (Figure 26), 111 canary rockfish occurrences were used (Figure 27). Results of the fine-scale predictive modeling effort for the Mendocino County region indicated that the highest performing model was model 4, which accounted for 94.5% of weight in the table, had a β value of 1, AUC of 0.983, and included four environmental covariates: cost distance, depth, VRM, and rugosity (Table 7). Model 4 was the most parsimonious model for predicting *S. pinniger* for the Mendocino fine-scale. The habitat suitability map produced from model 4 (Figure 28) predicted high suitability at the interface between hard and soft substrates and low suitability in areas where larger-bodied *S. pinniger* tend not to aggregate (i.e. sand flats) (Love et al. 2002). Results of the jackknife test for model 4 indicate the most influential environmental covariates were cost distance, depth, rugosity, and VRM, respectively (Figure 29). Areas of high suitability occurred where cost distance was near or equal to zero and depth was approximately 52 to 61 m (Figures 30 and 31).

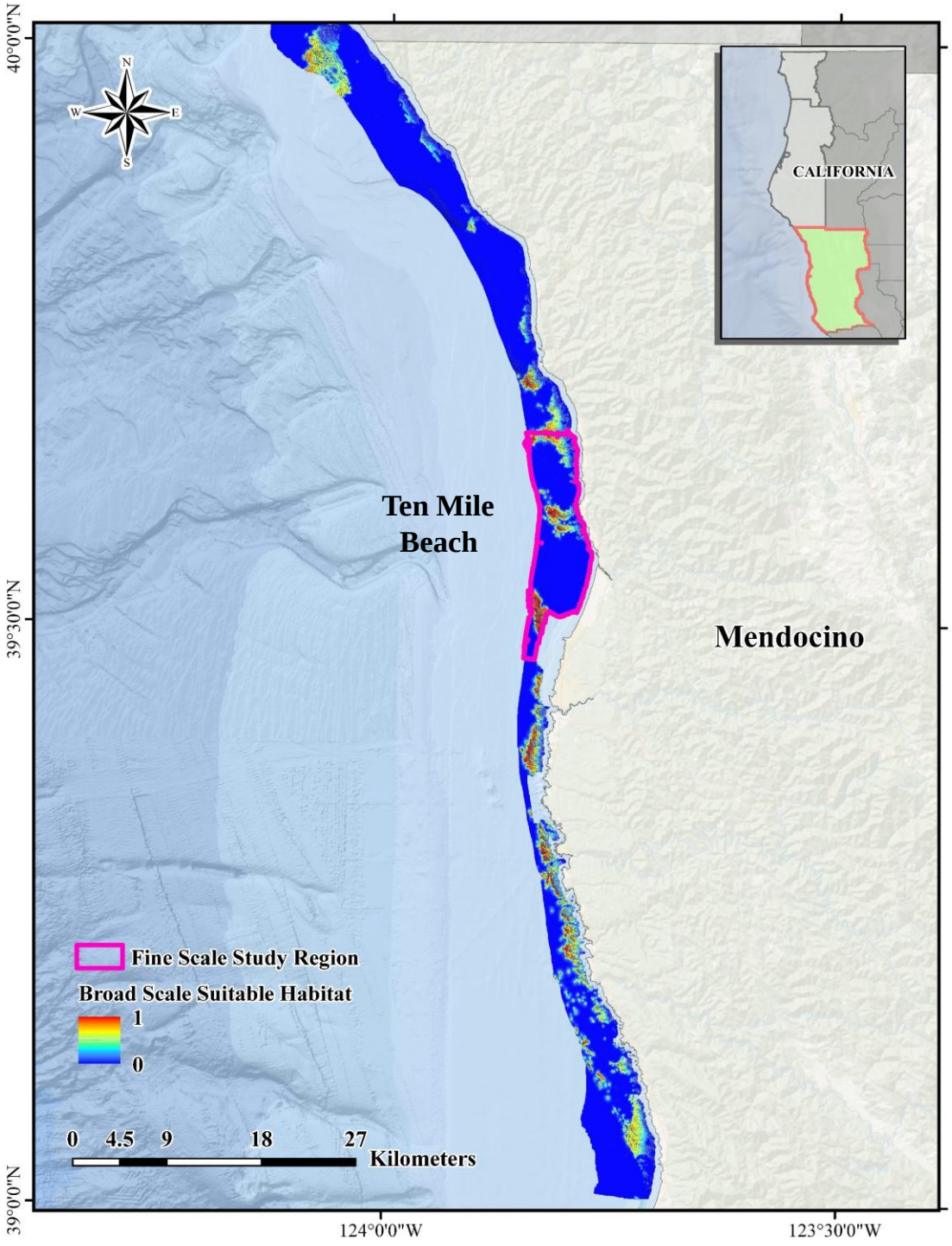

Figure 26. Selected Ten Mile Beach area (outlined) for fine-scale modeling off the Mendocino County study region, California, USA.

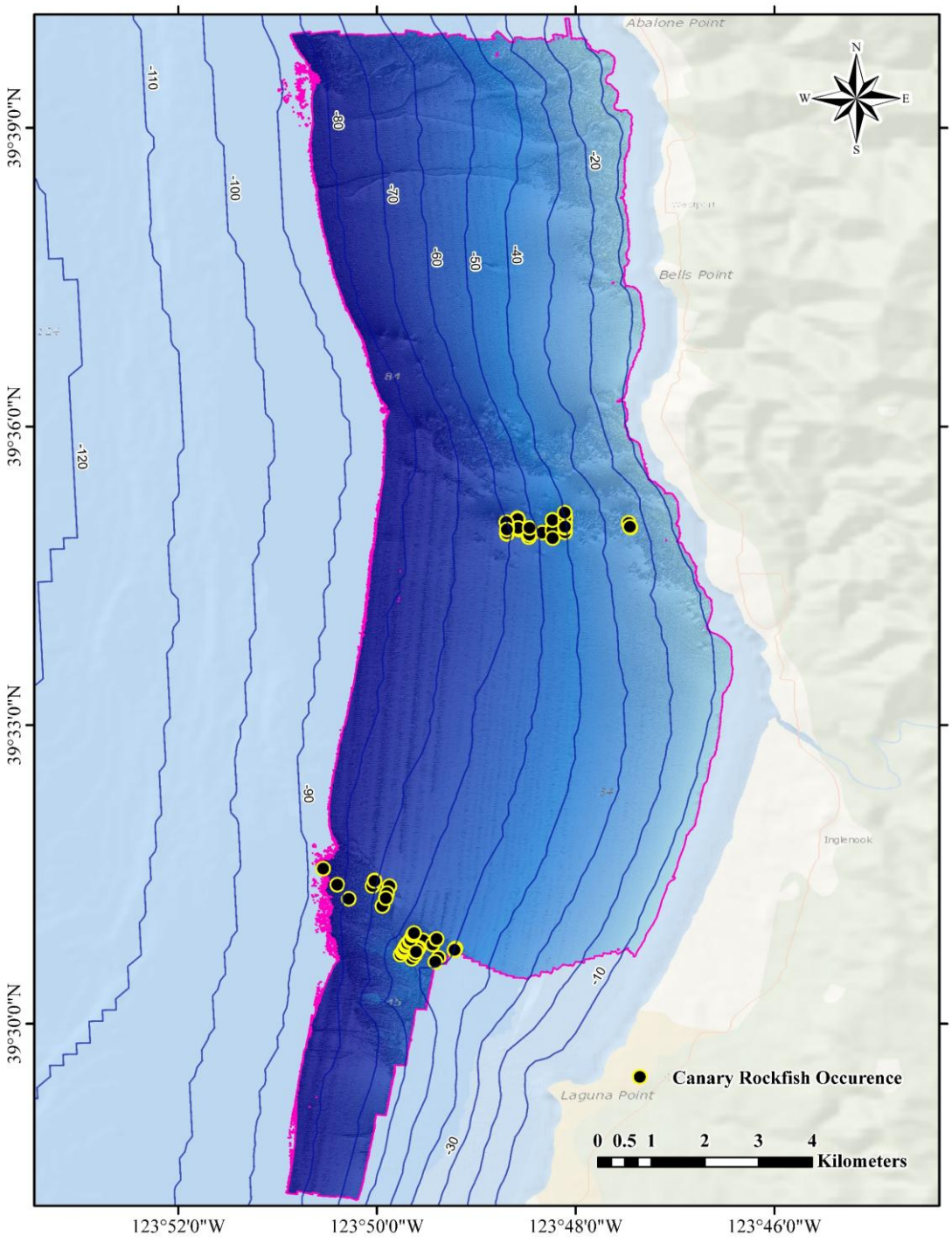

Figure 27. Map of the canary rockfish (*S. pinniger*) recorded occurrences within the Ten Mile Beach area off the coast of Mendocino County, California, USA.

Table 7. Criterion used to select the best models for the Ten Mile Beach area of the Mendocino County region: relative contributions of the major environmental variables, regularization parameter, AUC, AIC, ΔAIC, and ω_i.

Model	*Covariates*	*β*	*AUC*	*AIC*	*ΔAIC*	*ω_i*
1	Cost Dist. (69.6%)	1	0.986	1620.206	11.474	0.003
	Depth (20.3%)					
	Rugosity (5.2%)					
	VRM (3.2%)					
	Curvature (0.7%)					
	Slope (0.5%)					
	Aspect (0.4%)					
2	Cost Dist. (70.0%)	1	0.985	1614.530	5.798	0.052
	Depth (20.5%)					
	Rugosity (5.3%)					
	VRM (3.3%)					
	Curvature (0.5%)					
	Slope (0.4%)					
3	Cost Dist. (70.1%)	1	0.985	1626.582	17.850	< 0.001
	Depth (20.4%)					
	Rugosity (5.3%)					
	VRM (3.3%)					
	Aspect (0.4%)					
	Curvature (0.3%)					
4	Cost Dist. (70.7%)	1	0.983	1608.732	0	0.945
	Depth (20.6%)					
	Rugosity (5.4%)					
	VRM (3.3%)					

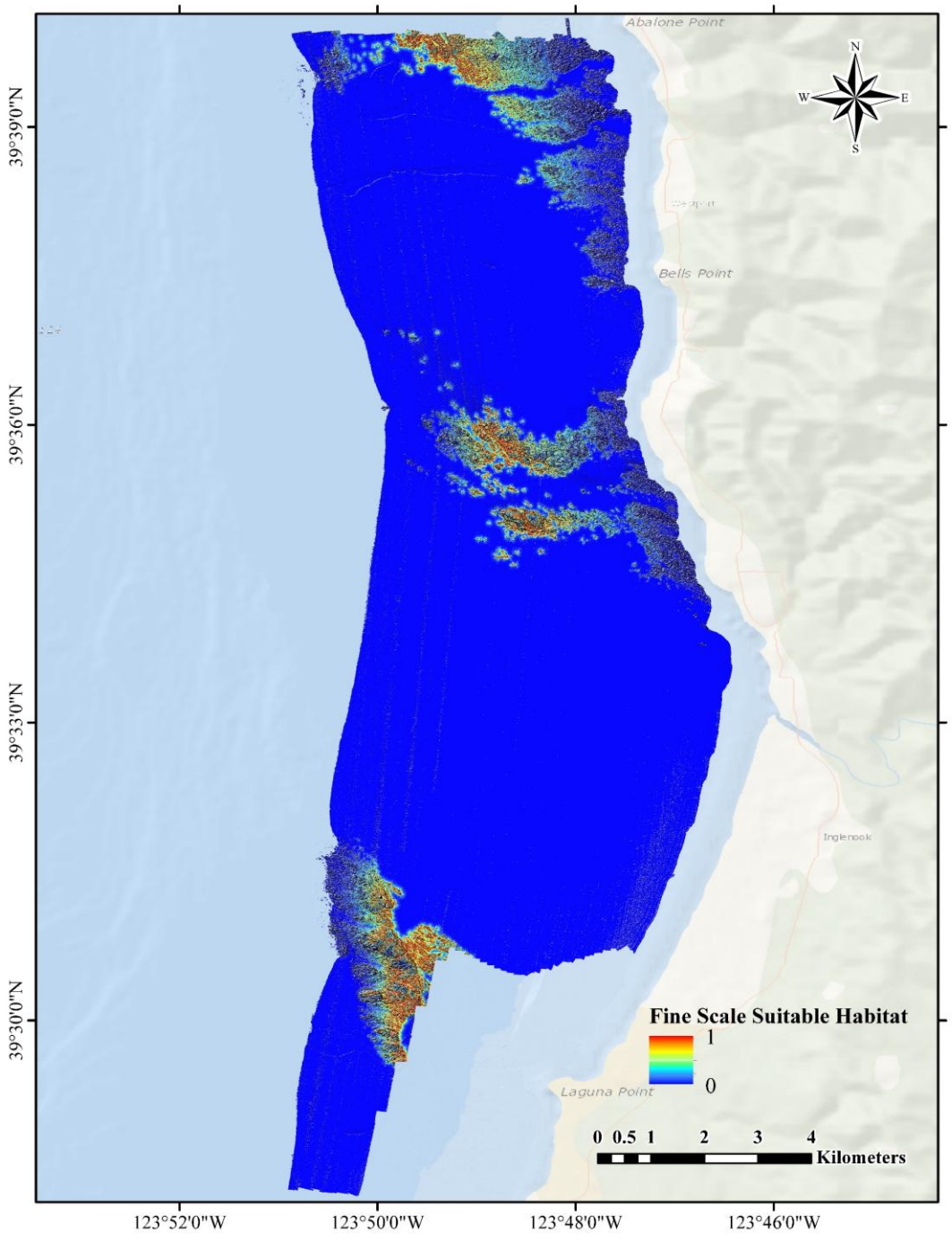

Figure 28. Fine-scale map of the suitable habitat based on the occurrence data for *S. pinniger* and the environmental variables of the most parsimonious model (model 4) of the Ten Mile Beach area of Mendocino County study region, California, USA. The heatmap indicates predicted habitat suitability with colors (and values) ranging from high suitability in red (one) to low predicted suitability (zero).

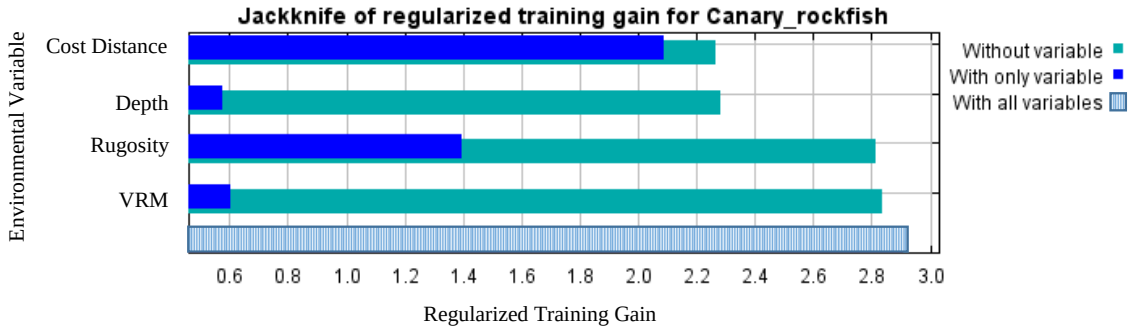

Figure 29. Jackknife test results performed on the training dataset for the Ten Mile Beach area of Mendocino County analysis for the most parsimonious model; model 4. The jackknife test indicates how much each predictive variable affects the model by creating a new model with the removal of individual covariates (Burnham and Anderson 2002).

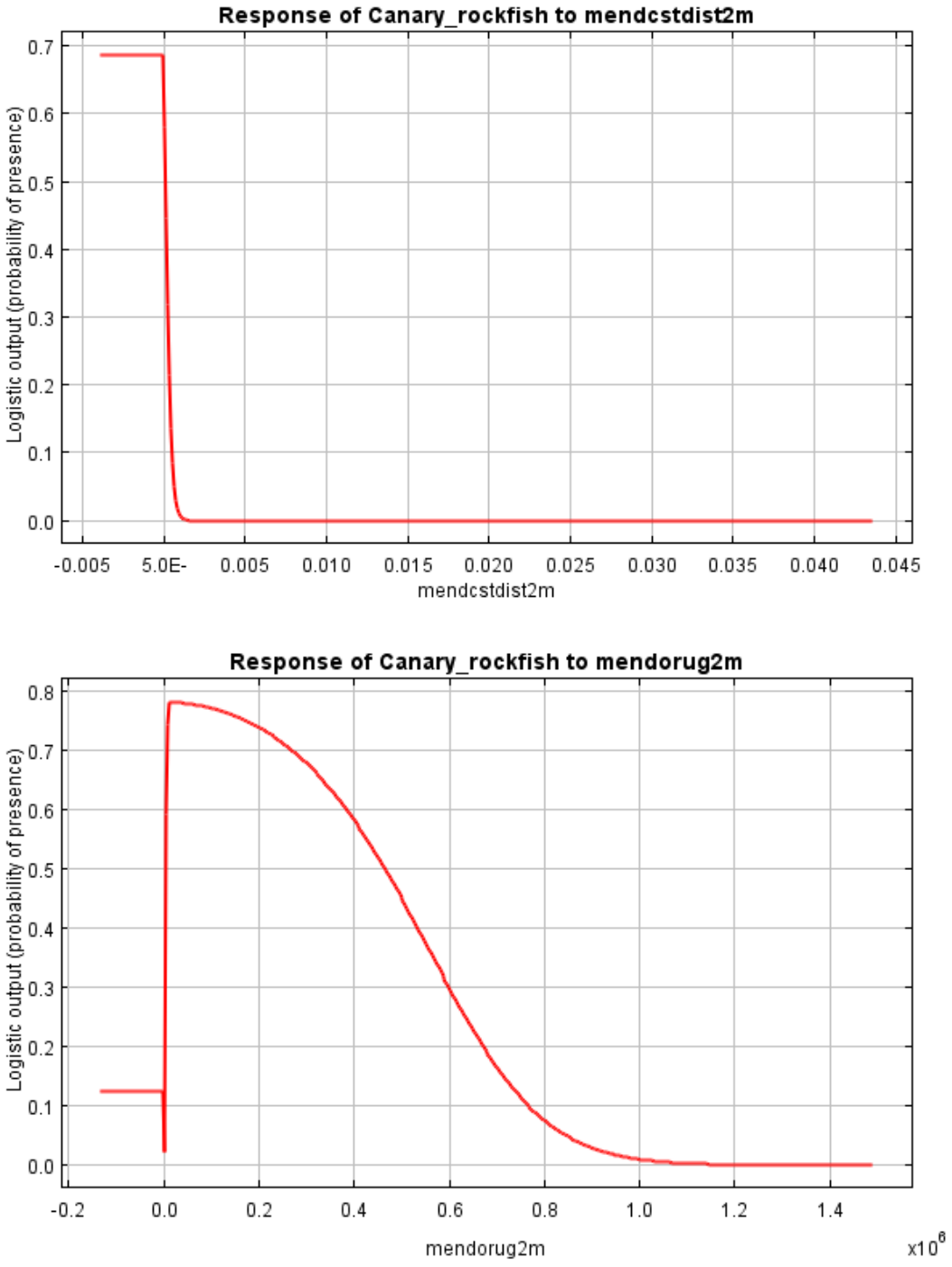

Figure 30. Response curves for environmental covariates used in the best model (model 4) for the Ten Mile Beach area of the Mendocino County study region. Environmental covariate acronyms: cost distance (mendcstdst2m) and rugosity (mendorug2m).

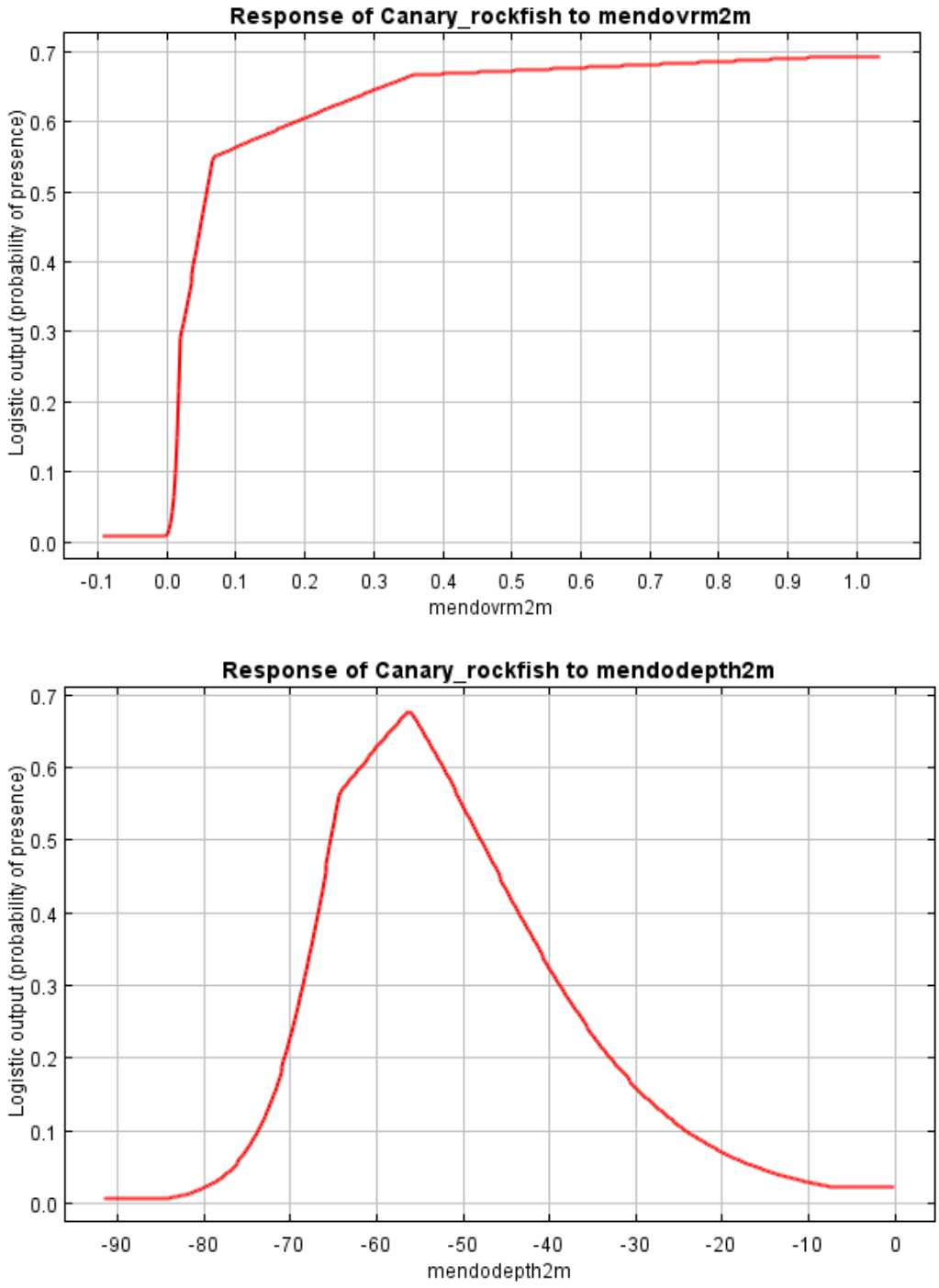

Figure 31. Response curves for environmental covariates used in the best model (model 4) for the Ten Mile Beach area of the Mendocino County study region. Environmental covariate acronyms: VRM (mendovrm2m) and depth (mendodepth2m).

Predicted probability of presence

The MaxEnt algorithm assumes a baseline species presence of 0.5 by default (Phillips and Dudík 2008). I examined the model output value for each *S. pinniger* occurrence for each of the best models. The probability values assigned to the broad-scale predictive map was on average 0.59, while the fine-scale predictive maps were assigned slightly higher probability values with the highest probability values assigned in the South Cape Mendocino area of the Humboldt County region (0.86) followed by the Point Saint George area of the Del Norte County region (0.69) and the Ten Mile Beach area of the Mendocino County region (0.62), respectively (Figure 32).

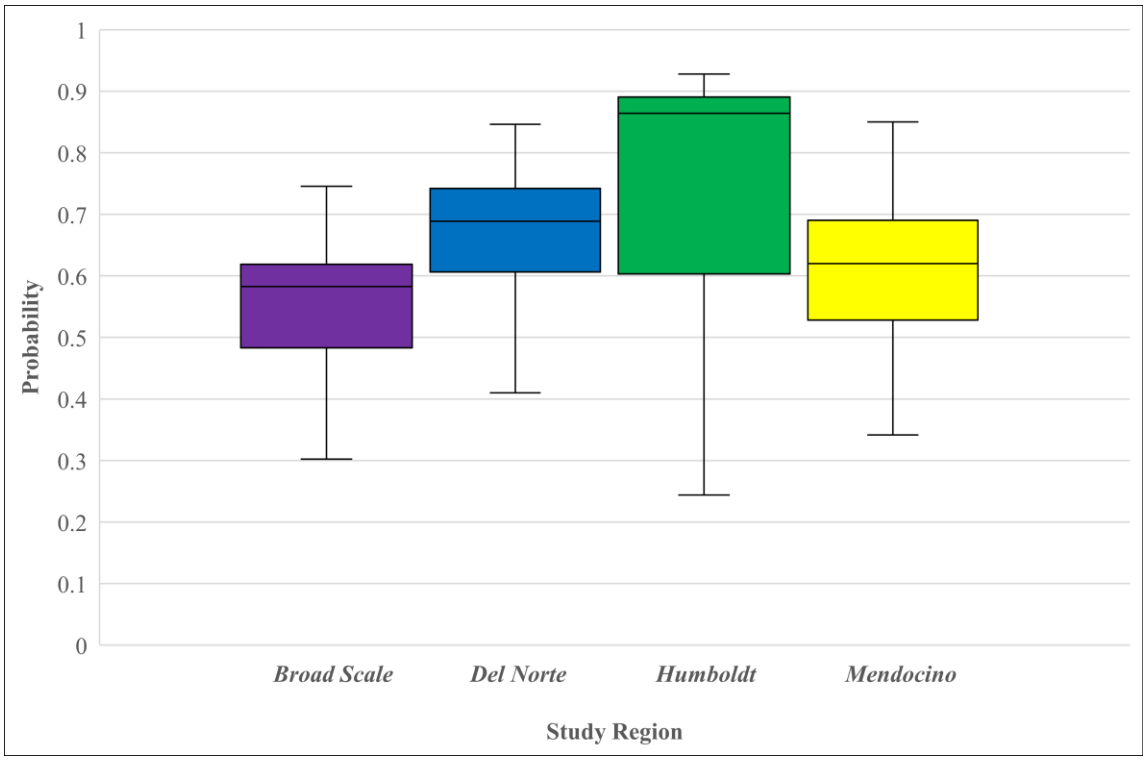

Figure 32. Box plot displaying the 25th and 75th percentiles around the median predicted probability of presence for *S. pinniger* occurrence locations. Average overall average of the predicted probability of presence for the broad-scale (Del Norte, Humboldt, and Mendocino County region) habitat suitability model was 0.59; the Point Saint George area of Del Norte County model was 0.69; the South Cape Mendocino area of Humboldt County model was 0.86; and the Ten Mile Beach area of the Mendocino County model was 0.62.

Uncertainty

Broad-scale

The top model selected was model 16 (Table 4) for the broad-scale study region. To create a map of spatial uncertainty for the occurrence data for the broad-scale region, 100 iterations of MaxEnt were batch processed in BlueSpray. I used the Monte Carlo feature within BlueSpray and specified the maximum amount of cumulative "noise" or uncertainty in the occurrence location data ranging from -15 m to 15 m. I plotted the standard deviation of the running mean for AIC and AUC for the model runs of the broad-scale study region, and interpreted the leveling off of the Monte Carlo iterations as an indication that I had accurately represented the impact of the noise injection. The AUC standard deviation required substantially fewer iterations to reach equilibrium than did the standard deviation of AIC values (Figure 33). The ranges of values in the ROC curves were close to the mean (Figure 34) and the histograms of the performance metrics approached a normal distribution (Figure 35).

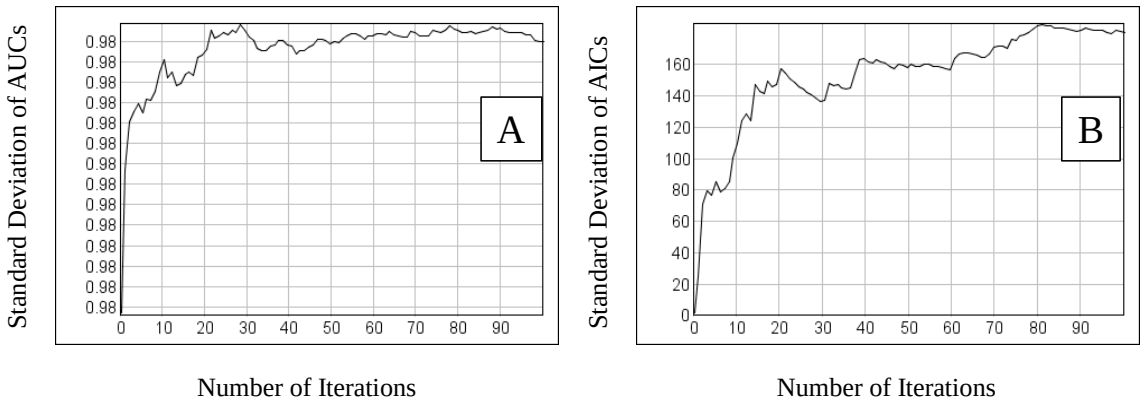

Figure 33. Plots of the standard deviation of the mean among the 100 iterations for AUC (A) and AIC (B) for the broad-scale study region.

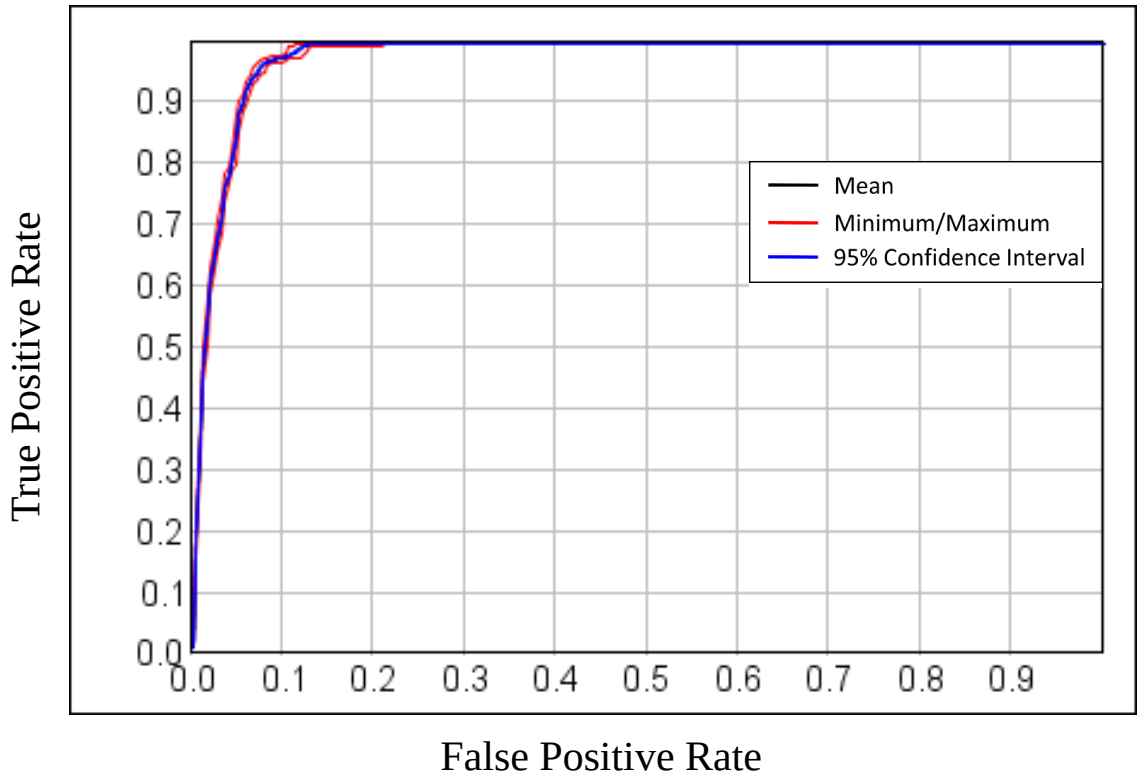

Figure 34. Overall ROC with a 95% confidence interval shown in blue, minimum and maximum values in red, and the mean value in black for the broad-scale study region.

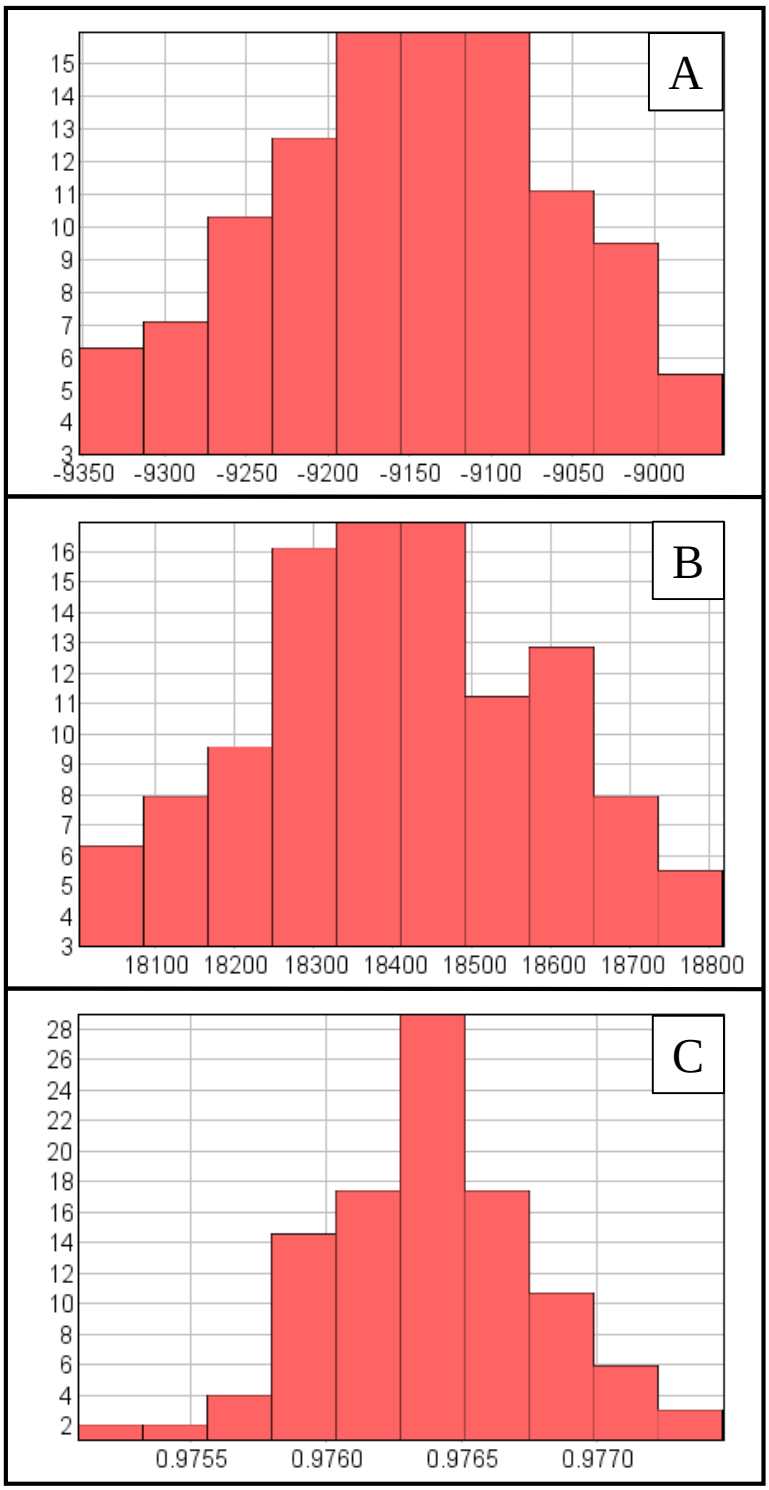

Figure 35. Log Likelihood value histogram (A), cumulative histogram of AIC values for the broad-scale region (B), and cumulative histogram of AUC values for the broad-scale region (C).

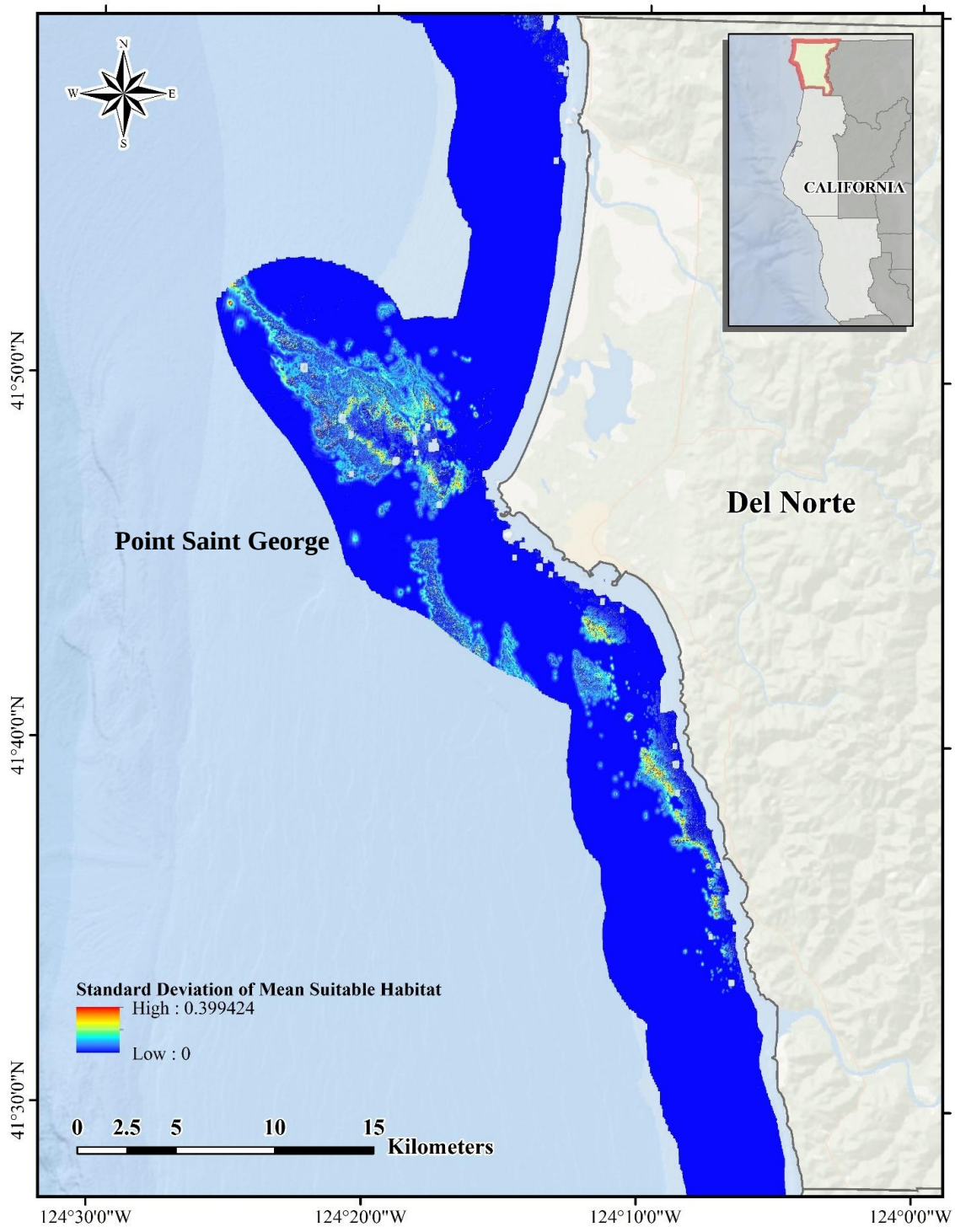

Figure 36. Broad-scale map of the spatial uncertainty for *S. pinniger* along the Del Norte County coast.

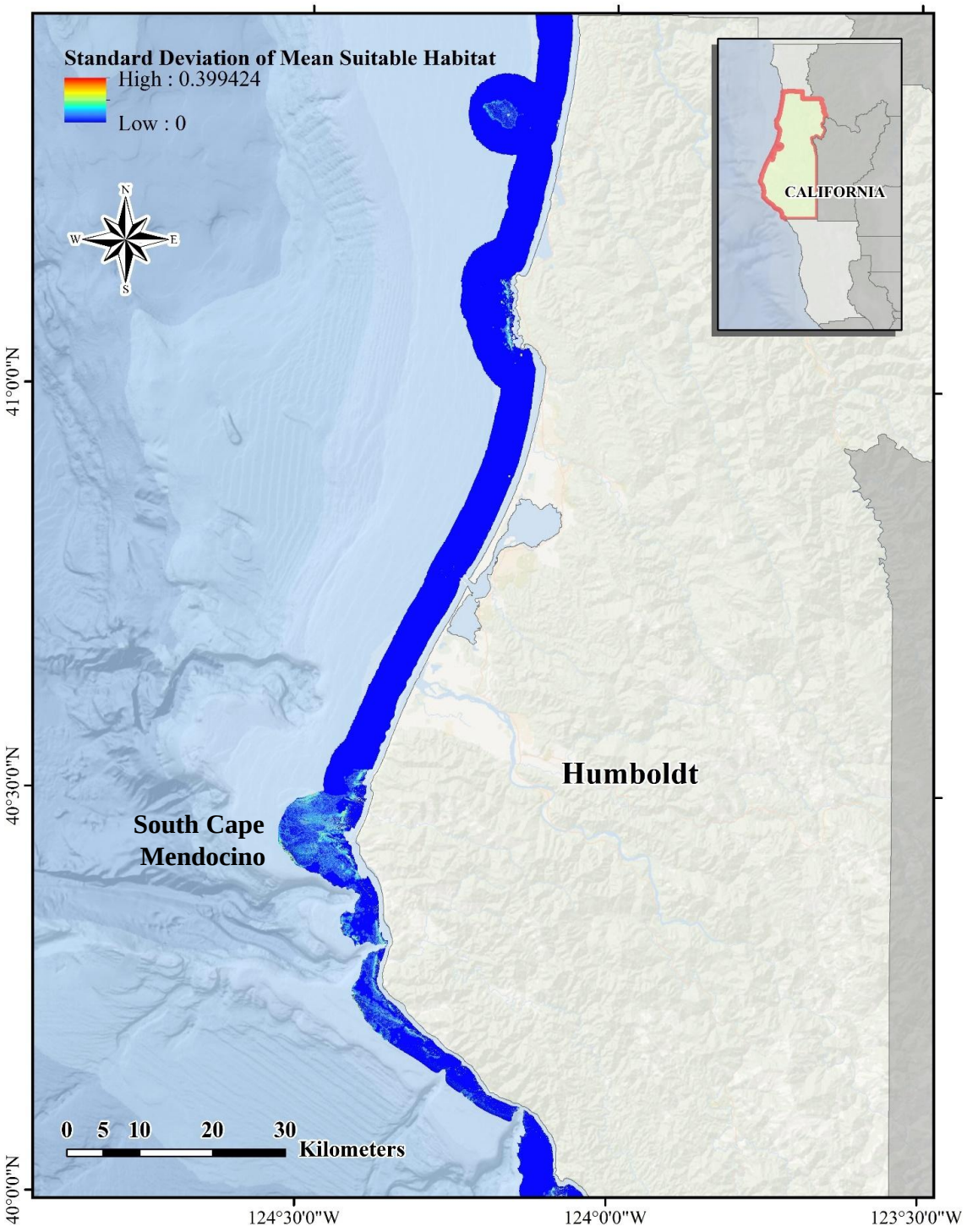

Figure 37. Broad-scale map of the spatial uncertainty for *S. pinniger* along the Humboldt County coast.

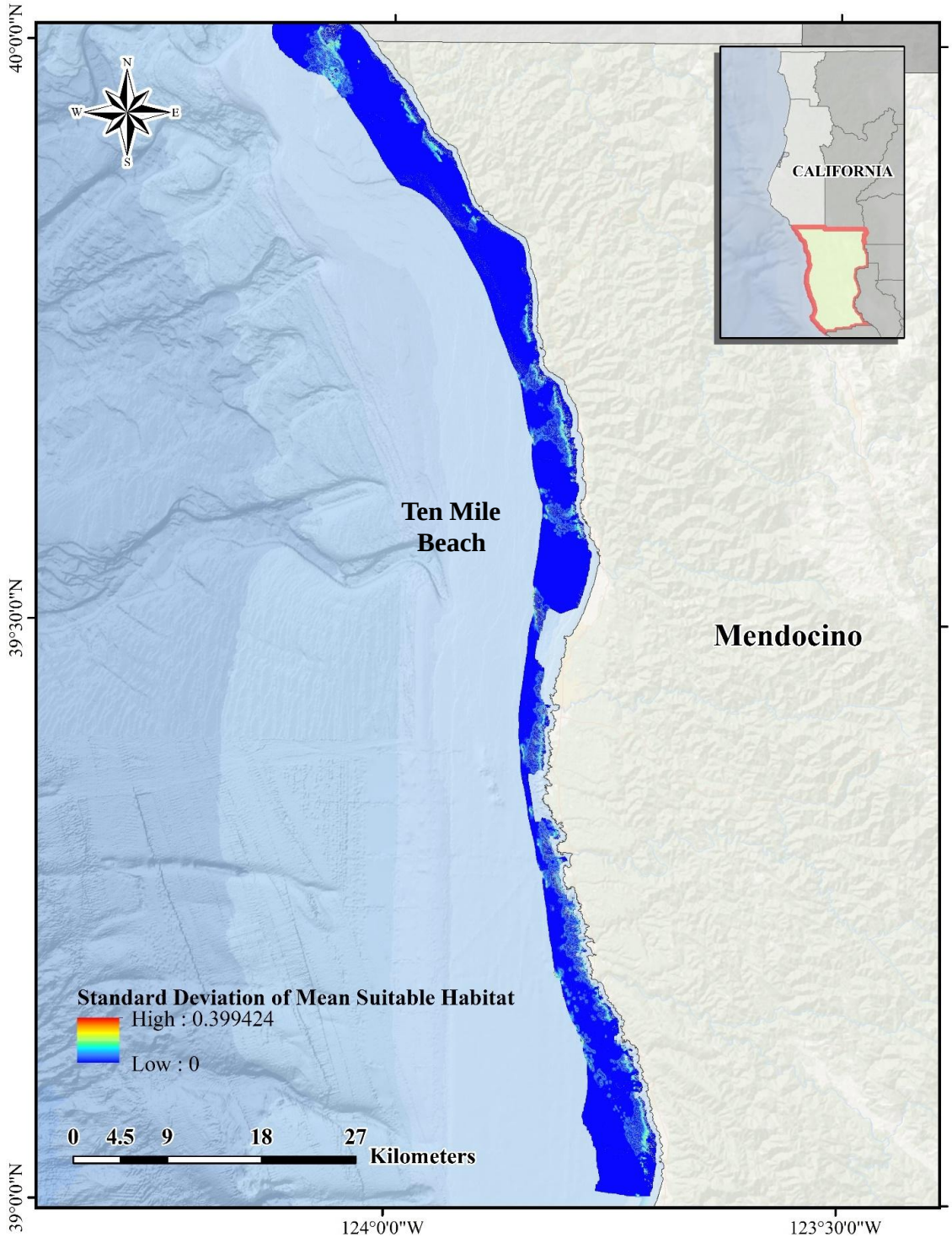

Figure 38. Broad-scale map of the spatial uncertainty for *S. pinniger* along the Mendocino County coast.

Fine-scale

Del Norte

The top model selected was model 11 (Table 5) for the Point Saint George area of the Del Norte County study region. To create a map of spatial uncertainty for the occurrence data for this area, 100 iterations of MaxEnt were batch processed in BlueSpray. I used the Monte Carlo feature within BlueSpray and specified the maximum amount of cumulative "noise" or uncertainty in the occurrence data ranging from -15 m to 15 m. I plotted the standard deviation of the running mean for AIC and AUC for the model runs of this region and interpreted the leveling-off of the Monte Carlo iterations as an indication that I had accurately represented the impact of the noise injection. The standard deviation of the AUC and AIC plateaued at approximately 30 iterations (Figure 39). The ranges of values in the ROC curves were close to the mean (Figure 40) and the histograms of the performance metrics approached a normal distribution (Figure 41).

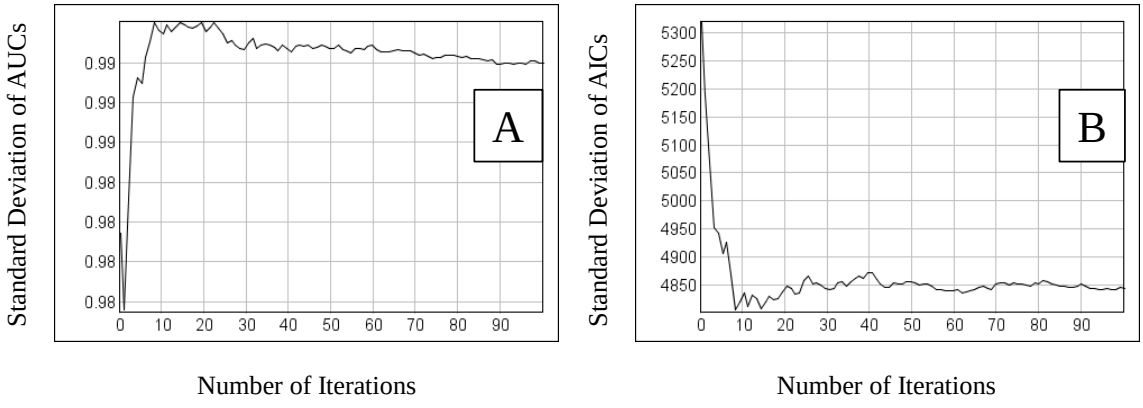

Figure 39. Plots of the standard deviation of the mean among the 100 iterations for AUC (A) and AIC (B) for the Point Saint George area of the Del Norte County study region.

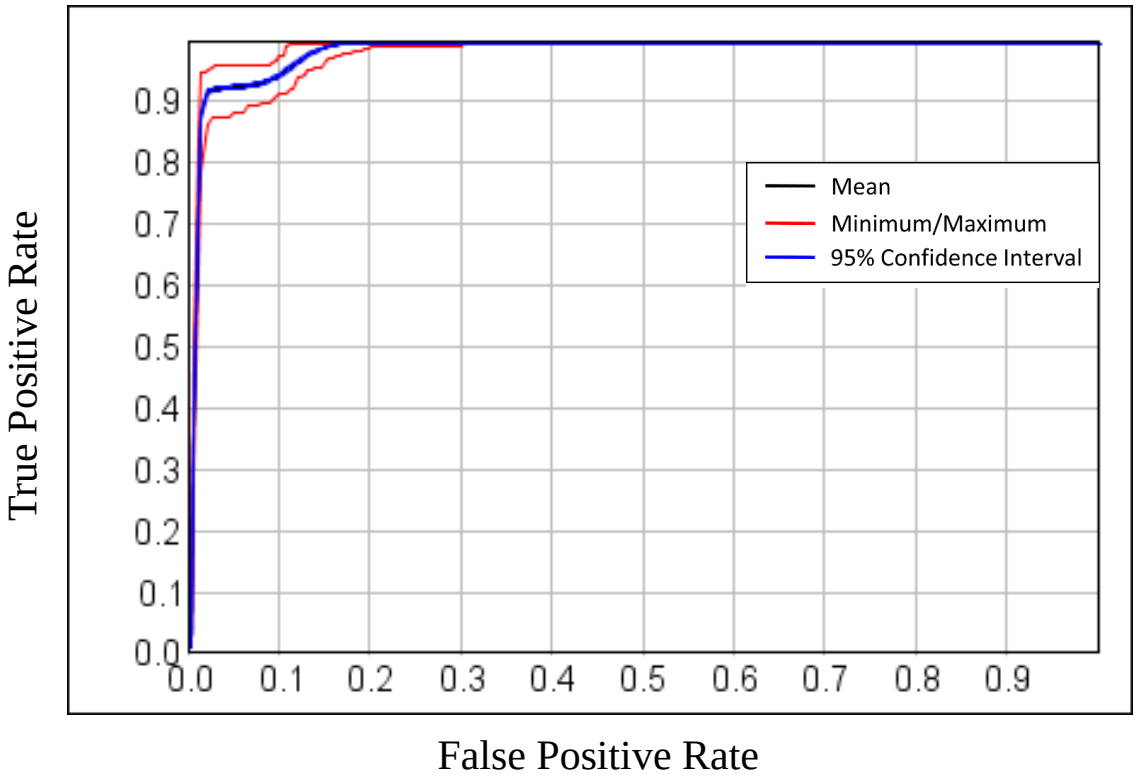

Figure 40. Overall ROC with a 95% confidence interval shown in blue, minimum and maximum values in red, and the mean value in black for the Point Saint George area of the Del Norte County study region.

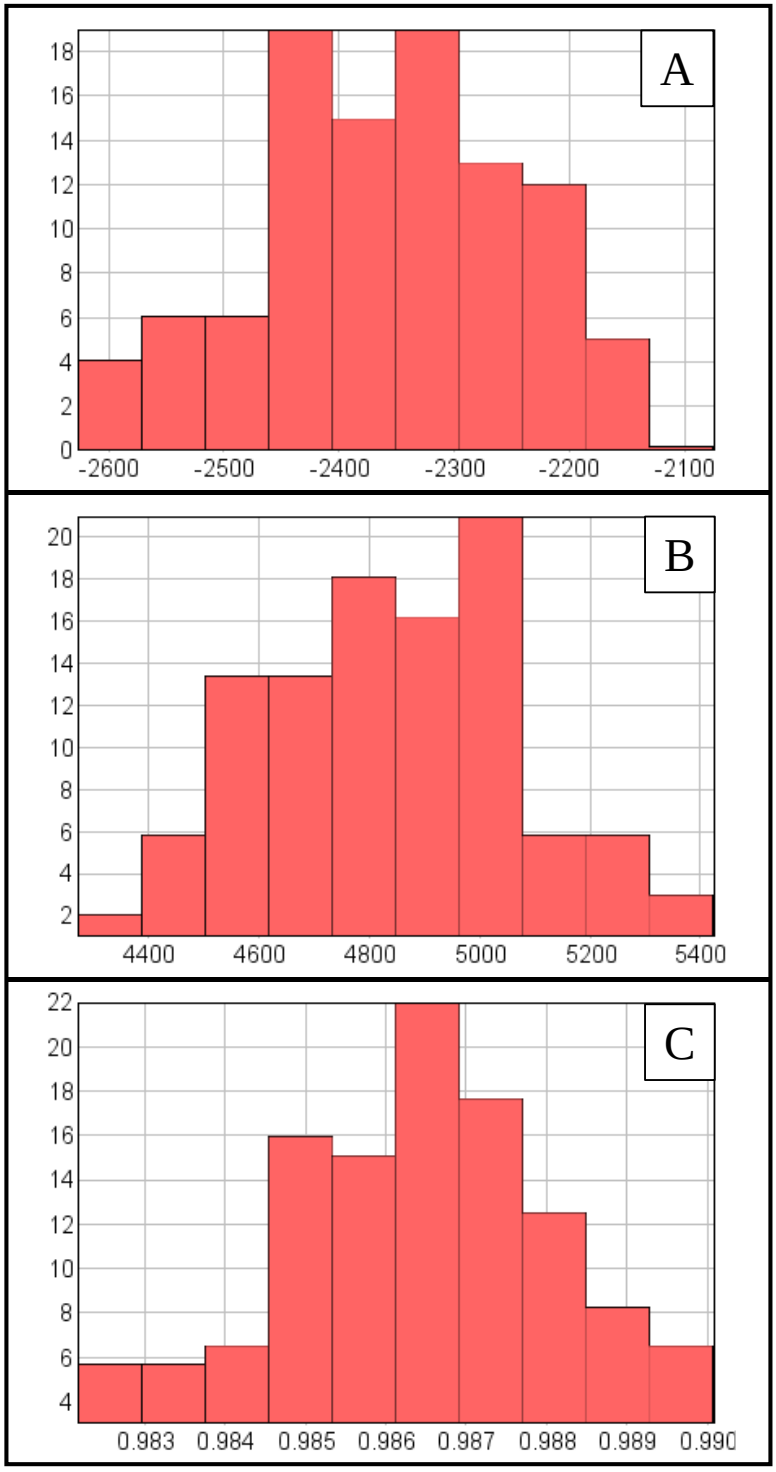

Figure 41. Log Likelihood value histogram (A), cumulative histogram of AIC (B), and Cumulative histogram of AUC values for the Point Saint George area in the Del Norte County study region (C).

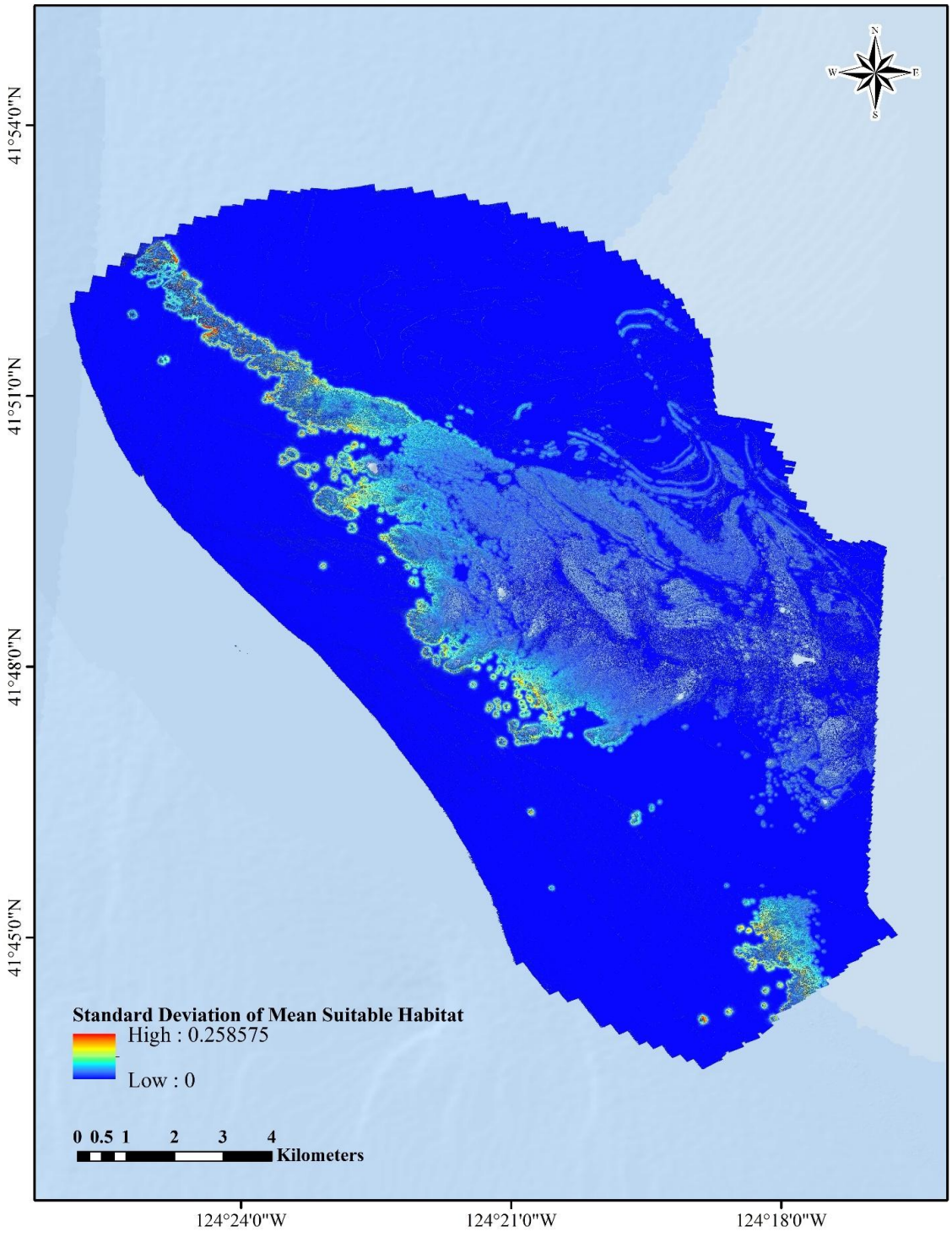

Figure 42. Map of the spatial uncertainty for *S. pinniger* in the area of Point Saint George in the Del Norte County study region.

Humboldt

The top model selected was model 3 (Table 6) of the South Cape Mendocino area of the Humboldt County study region models. To create a map of spatial uncertainty for the occurrence data for this region, 100 iterations of MaxEnt were batch processed in BlueSpray. I used the Monte Carlo feature within BlueSpray and specified the maximum amount of cumulative "noise" or uncertainty in the occurrence data ranging from -15 m to 15 m. I plotted the standard deviation of the running mean for AIC and AUC for the model runs of this region; I interpreted the leveling-off of the Monte Carlo iterations as an indication that I had accurately represented the impact of the noise injection. The AUC standard deviation required substantially fewer iterations to reach equilibrium than did the standard deviation of AIC (Figure 43). However, the ranges of values in the ROC curves were much higher (Figure 44) and the histograms of the performance metrics did not approach a normal distribution (Figure 45).

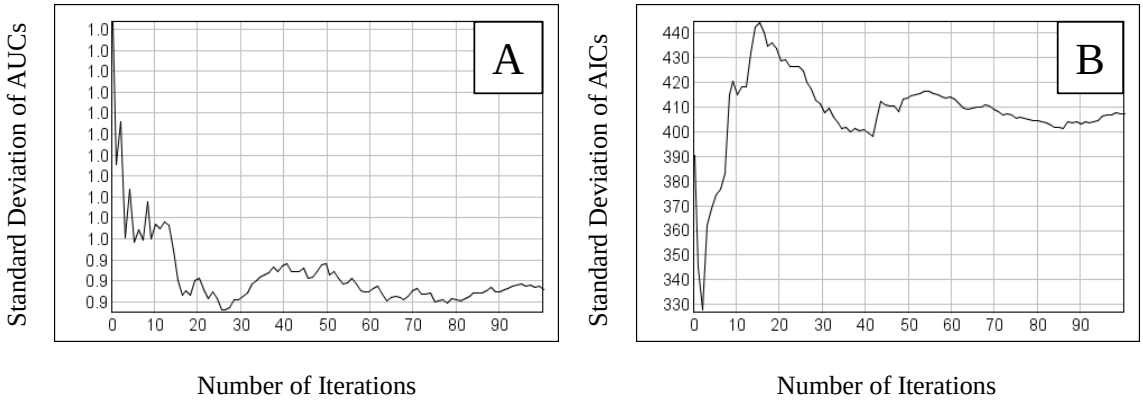

Figure 43. Plots of the standard deviation of the mean among the 100 iterations for AUC (A) and AIC (B) for South Cape Mendocino area in the Humboldt County study region.

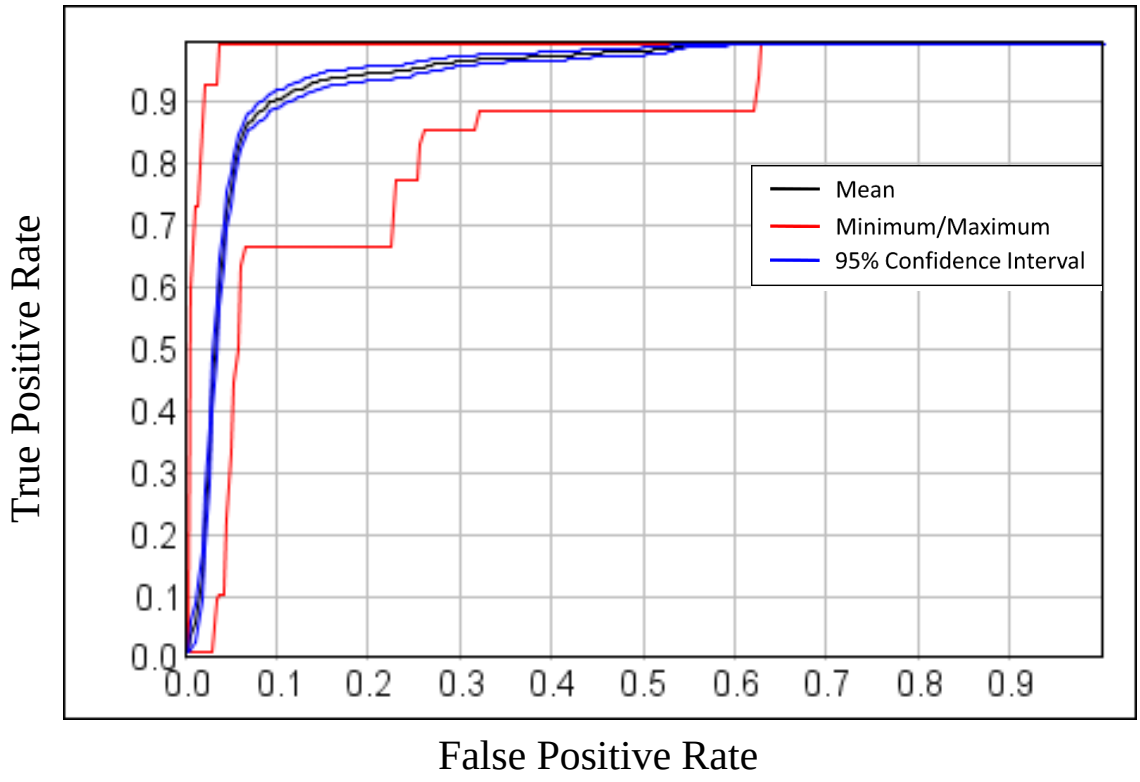

Figure 44. Overall ROC with a 95% confidence interval shown in blue, minimum and maximum values in red, and the mean value in black for South Cape Mendocino area in the Humboldt County study region.

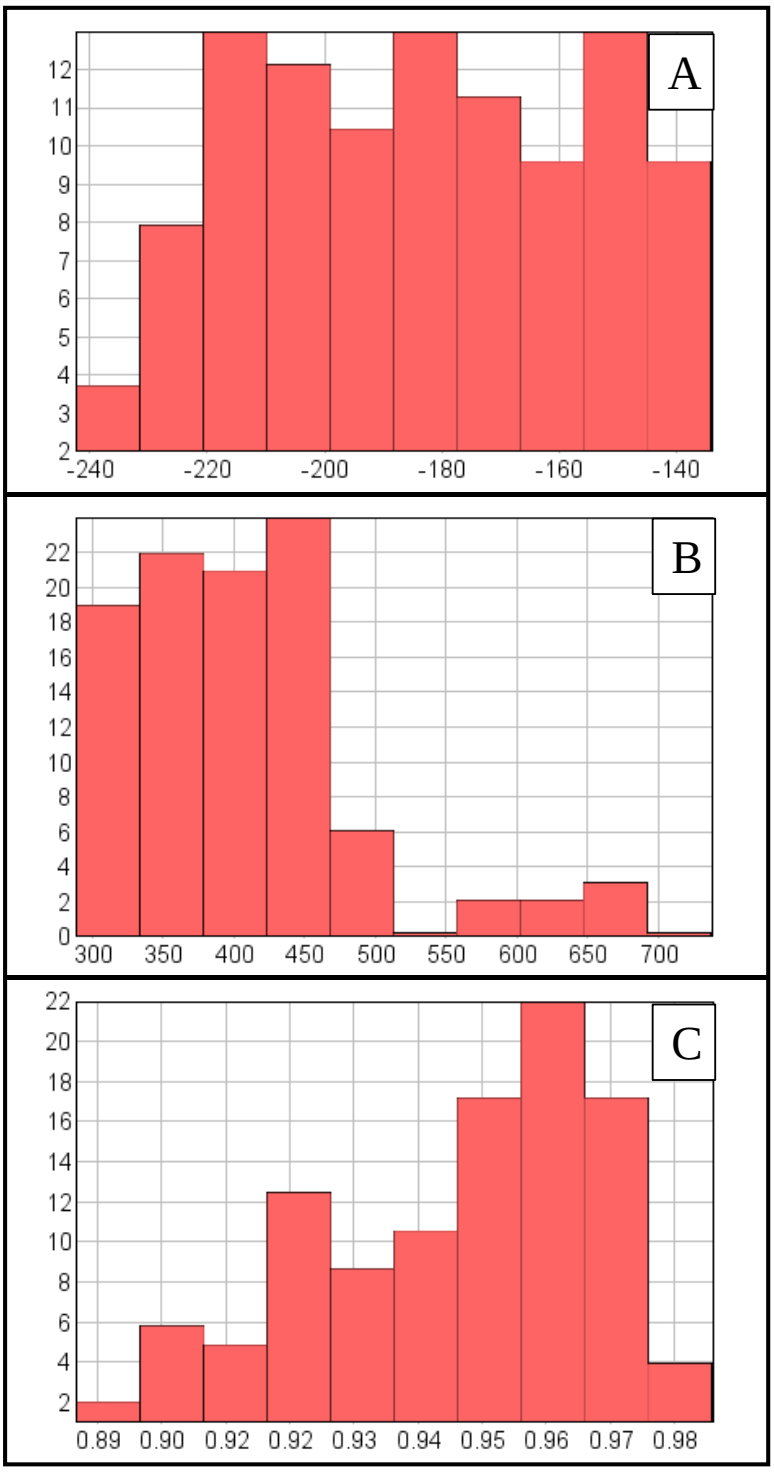

Figure 45. Log Likelihood value histogram (A), cumulative histogram of AIC values (B), and Cumulative histogram of AUC values (C) for South Cape Mendocino area in the Humboldt County study region.

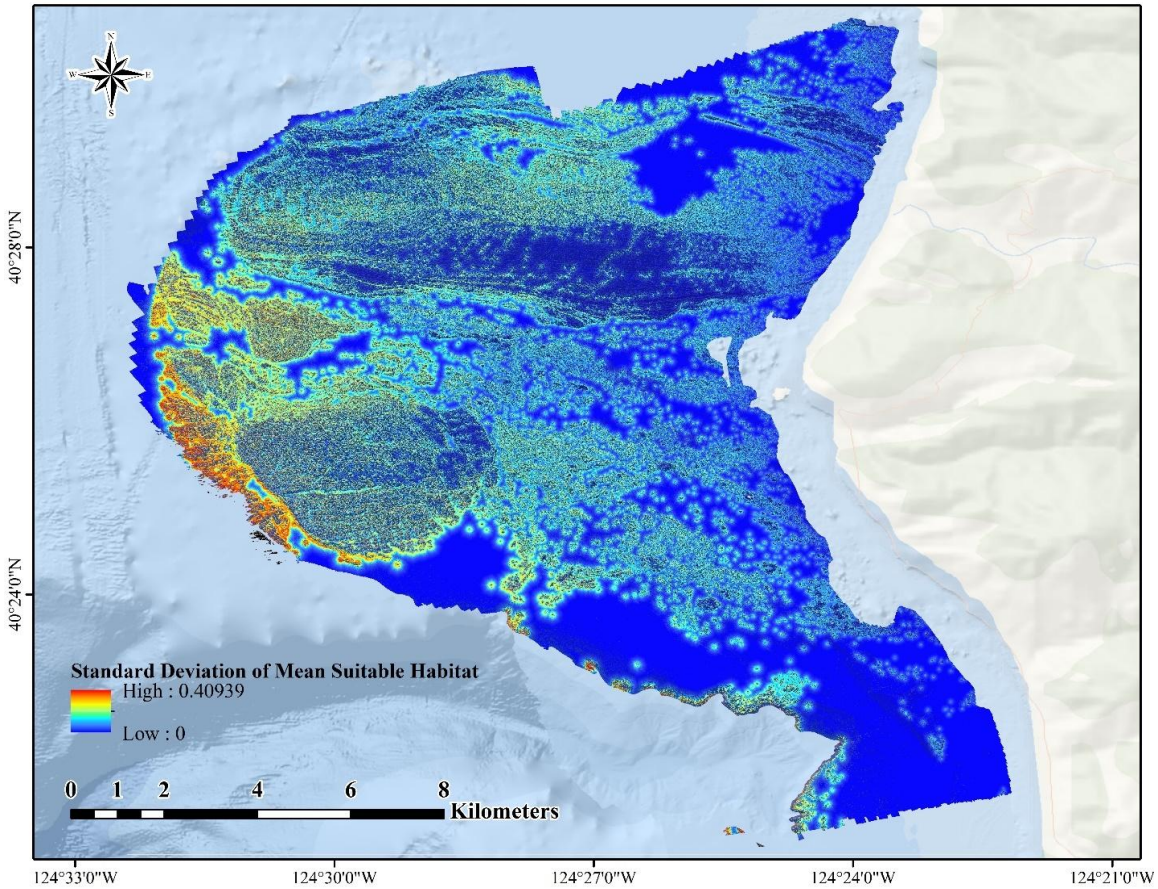

Figure 46. Fine-scale map of the spatial uncertainty for *S. pinniger* for the South Cape Mendocino area of the Humboldt County study region.

Mendocino

The top model selected was model 4 (Table 7) of the fine-scale Mendocino County Region models. To create a map of spatial uncertainty for the occurrence data for this region, 100 iterations of MaxEnt were batch processed in BlueSpray. I used the Monte Carlo feature within BlueSpray and specified the maximum amount of cumulative "noise" or uncertainty in the occurrence data ranging from -15 m to 15 m. As with the plots of standard deviation of the running mean AIC and AUC for the other regions, I interpreted the leveling off of the Monte Carlo iterations as an indication that I had

accurately represented the impact of the noise injection. The AUC standard deviation required substantially fewer iterations to reach equilibrium than did the standard deviation of AIC equilibrium (Figure 47). The ranges of values in the ROC curves were close to the mean (Figure 48) and the histograms of the performance metrics approached a normal distribution as expected (Figure 49).

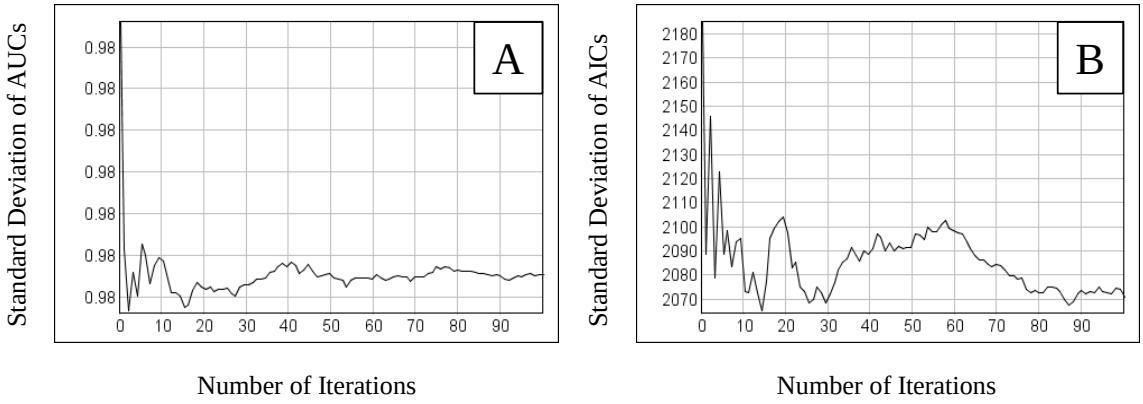

Figure 47. Plots of the standard deviation of the mean among the 100 iterations for AUC (A) and AIC (B) for the Ten Mile Beach area in the Mendocino County study region.

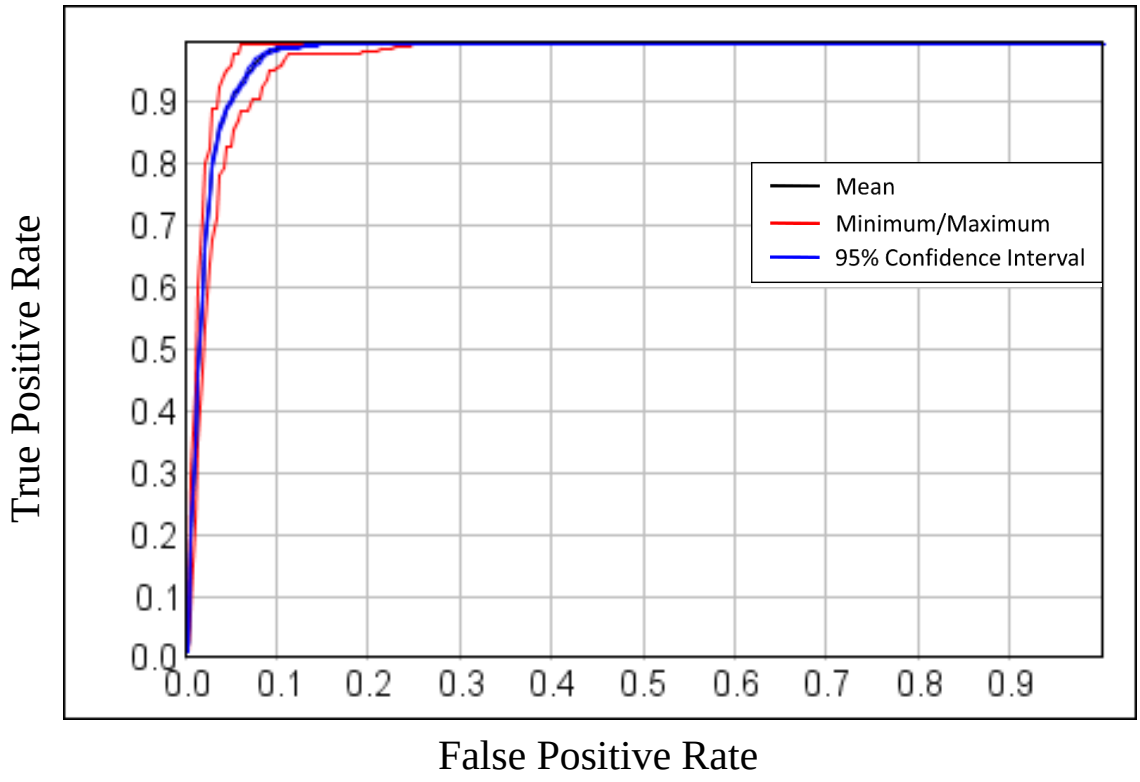

Figure 48. Overall ROC with a 95% confidence interval shown in blue, minimum and maximum values in red, and the mean value in black for the Ten Mile Beach area in the Mendocino County study region.

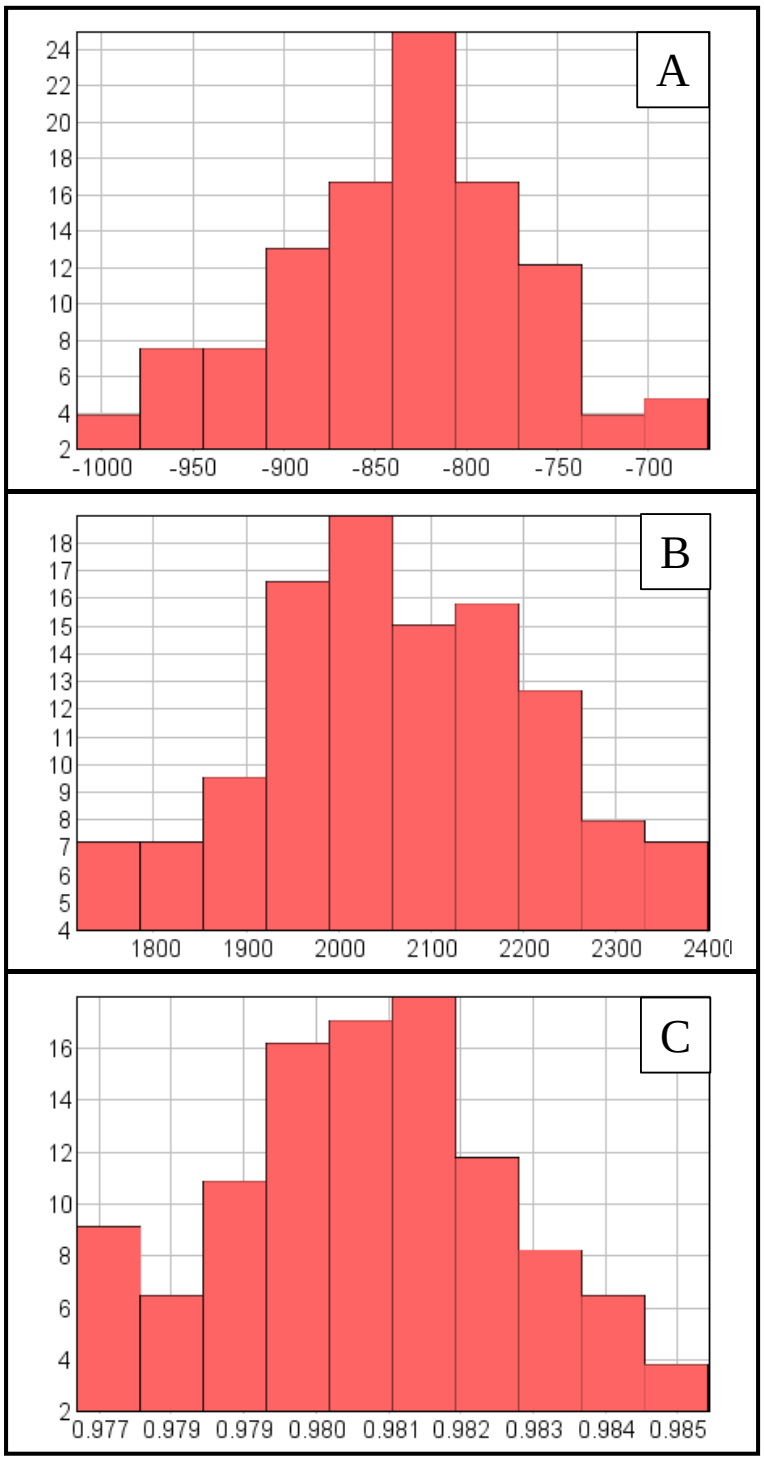

Figure 49. Log Likelihood value histogram (A), cumulative histogram of AIC values (B), and Cumulative histogram of AUC values for the Ten Mile Beach area in the Mendocino County study region (C).

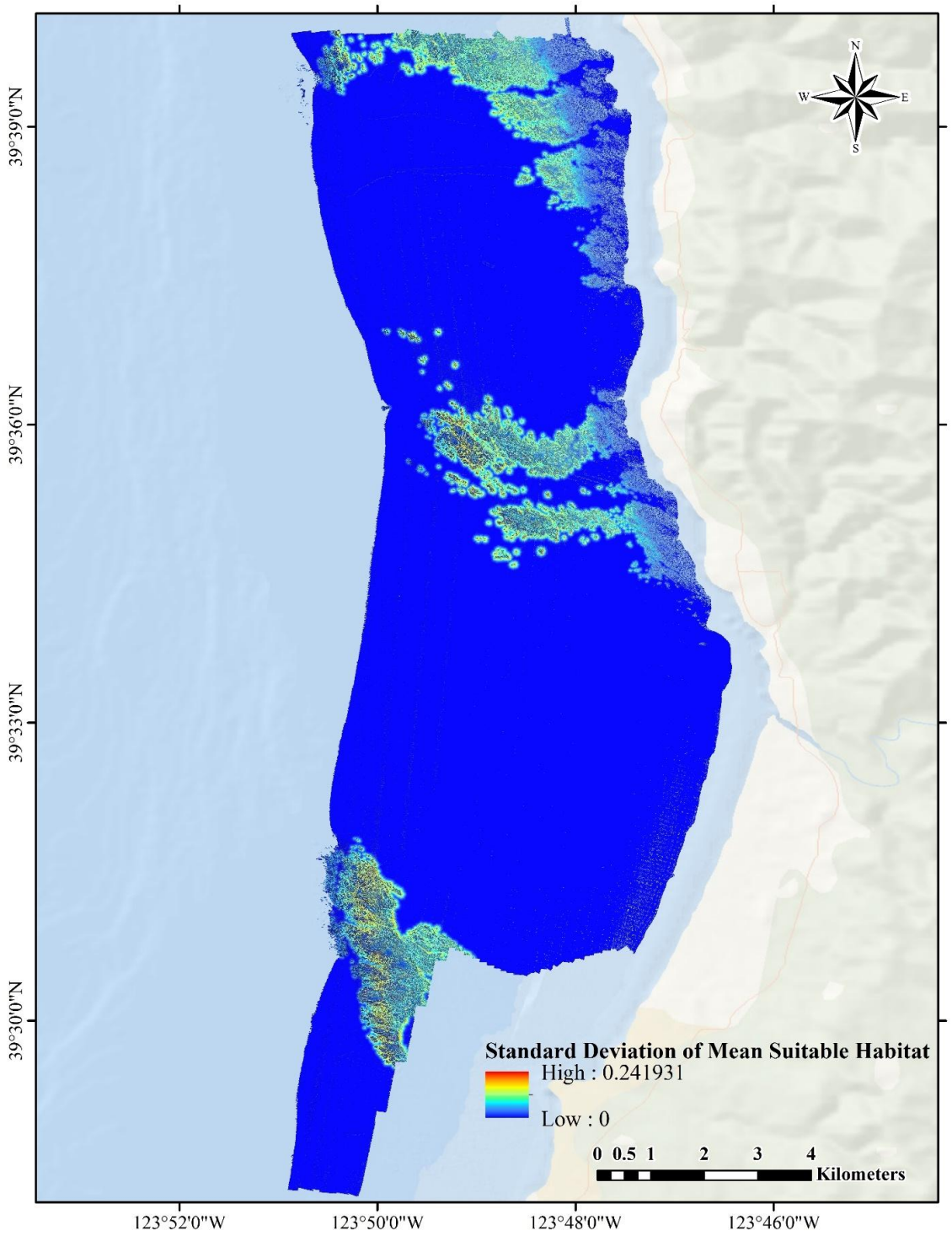

Figure 50. Fine-scale map of the spatial uncertainty for *S. pinniger* for the Ten Mile Beach area of the Mendocino County study region.

.

DISCUSSION

This study demonstrates that by integrating occurrence data, predictive habitat covariates and techniques, geographical information science, and advanced machine-learning algorithms, it is possible develop predictive maps in a temperate marine ecosystem for a single species. My results are consistent with what other studies have found in that they show suitable habitat for *S. pinniger* along the bathymetrically complex temperate marine ecosystem off the coast of northern California is in areas where *S. pinniger* is known to occur (Yoklavich et al. 2000 and 2002; Young et al. 2010). Satisfying consistency was observed in the identity and order of importance of environmental covariates for the best model across the broad- and fine-scale analyses; all models included the same four covariates: cost distance, depth, rugosity, and VRM (Table 8). The most influential environmental covariate at all scales was proximity to the hard/soft substrate interface (cost distance) (Young et al. 2010); depth was the second most important (Table 8).

Table 8. Environmental covariates included the best model for broad- and fine-scale analyses in order of importance.

	Environmental covariates (in order of importance)					
Broad-scale (20 m)	Cost distance	Depth	VRM	Rugosity	-	-
Del Norte (2 m)	Cost distance	Depth	Rugosity	VRM	-	-
Humboldt (2 m)	Cost distance	Depth	Rugosity	Aspect	VRM	Slope
Mendocino (2 m)	Cost distance	Depth	Rugosity	VRM	-	-

Multi-scale modeling approaches like the one used in this study have been shown to be appropriate when there is insufficient information on habitat use patterns, individual movements, and when it is likely that species respond hierarchically to spatial structure within different scales (Pittman et al. 2004; Valavanis et al. 2008).

Habitats are defined by a multitude of variables that can influence the distribution and abundance of species and, when available, it is best practice to include pertinent variables specific to the species of interest. I included metrics derived from the seafloor, but other metrics such as currents, water temperature, nutrient availability, and macroinvertebrate habitat structures, and kelp forest cover are also likely to influence *S. pinniger* distribution in this region. I was unable to determine specific habitat types where *S. pinniger* occurred in this study. Although I did use values associated with the complexity of the substrate, I was unable to resolved whether *S. pinniger* exhibits a preference for specific habitat types such as boulder/cobble fields (Stein et al. 1992), or if they are generalists as described by Tissot et al. (2007), etc. One aspect of my results that agrees with Yoklavich et al. (2000 and 2002) is that *S. pinniger* is associated with benthic habitat that transition from areas of low (mud/sand) to high relief. Further, edge effects have been studied extensively in terrestrial ecology (Reis et al. 2004); potential drivers of the edge effect observed in my study include a variety of factors such as predator/prey interactions, water flow, and migratory/spawning fishes (Friedlander and Parrish 1998).

My focus on larger body fish may have contributed to the high model performance, as Costa et al. (2014) previously found in studies of fish in the U.S. Virgin Islands. The total length of each *S. pinniger* observed was an approximation based on

laser width and may have been confounded by error in both fish mobility and measurements estimated without laser contact on fish bodies (Rochet et al. 2006). Further, the size class that I targeted may have captured the commercially important size classes (Hixon et al. 2014) for this species that is believed to reach 50% maturity at approximately 40 cm (NMFS 2014).

Broad-scale

At the broad-scale, my results indicate *S. pinniger* select areas close to the interface of hard and soft substrates, at moderate depths, in areas with moderate rugosity, and areas with high terrain variation (VRM). Several recent studies conducted at similar resolutions have produced very informative outcomes (Pittman and Brown 2011, Razgour et al. 2011, Bellamy et al. 2013). The uncertainty analysis revealed that at the broad-scale to which I down-sampled resulted in lower uncertainty than in the fine-scale models. One area I thought would have had higher suitability reported by the model outputs was off the coast of Trinidad, California in the Humboldt County region. The lack of occurrence data in the area near Trinidad likely contributed to this (Figure 51).

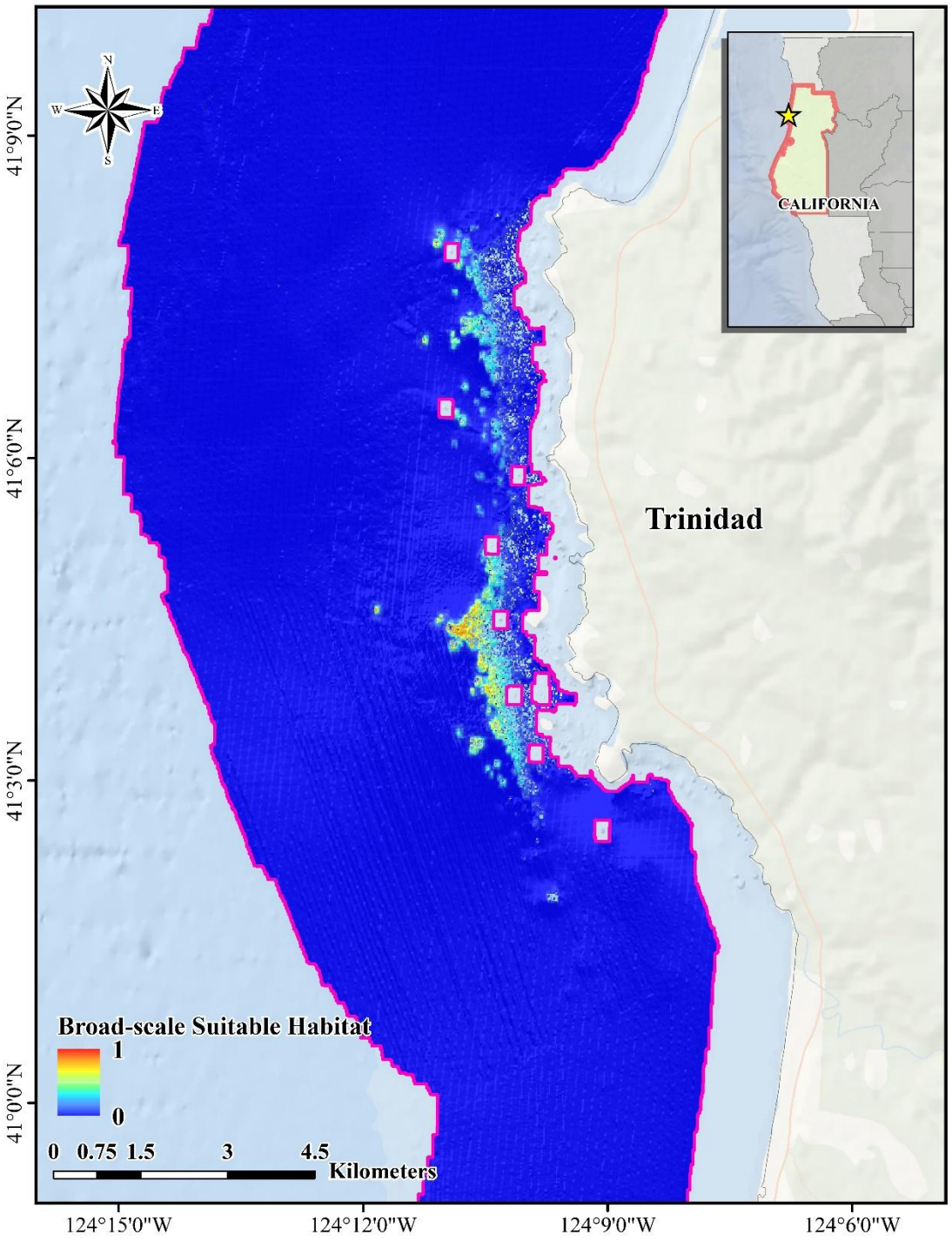

Figure 51. Map of the suitable habitat near Trinidad, California in the Humboldt County broad-scale study region. The heatmap indicates predicted habitat suitability with colors (and values) ranging from high suitability in red (one) to low suitability in blue (zero).

Fine-scale

At the fine-scale, cost distance to the hard/soft substrate interface and depth were the most significant and consistent covariates in all models. There was, however, a slight variation in the contributions of less influential covariates for the Humboldt County South Cape Mendocino region.

Within the Del Norte County Point Saint George region, the less influential covariates were depth, rugosity, and VRM, respectfully. In this region, highly suitable habitat for *S. pinniger* occurred at moderate depths (57 to 70 m), and where rugosity was near zero (flat). Habitat suitability increased with terrain complexity (VRM). This region had the highest sample size of the three fine-scale regions and the second to largest area.

Within the Humboldt County South Cape Mendocino region, the less influential covariates were depth, rugosity, aspect, VRM, and slope, respectively. In this region, highly suitable habitat for *S. pinniger* occurred at a broader range of depths (40 to 77 m), where rugosity was near zero (flat), on southeast and northwest facing slopes (aspect), where terrain complexity (VRM) ranged from no to moderate complexity, and at steep slope angles. The substrate in this region is largely covered by hard substrate and may have been more complex than that of the other two fine scale regions assessed. This complexity may account for the variability in the predicted results. The inconsistent rugosity values may have been a result of overfitting. This region also had the lowest sample size of the three fine-scale regions and largest area. The combination of low sample size and large study area resulted in a model with poor performance compared to

the broad-scale and other fine-scale analyses. Additionally, the probability of presence result was artificially elevated, the uncertainty analyses showed a high range of ROC curves, and the performance metrics did not approach a normal distribution. Interestingly, in contrast to the broad-scale and other fine-scale analyses, only the model for the South Cape Mendocino Humboldt County region included aspects and slope as environmental covariates (Table 8).

Within the Mendocino County Ten Mile Beach region, the less influential covariates that indicated highly suitable habitats for *S. pinniger* were depth, rugosity, and VRM, respectively. In this region, highly suitable habitat for *S. pinniger* was in areas of moderate depth (44 to 67 m), with low rugosity (flat), and areas with high terrain variation (VRM). This region was similar to the bathymetric features that exist at Point Saint George area in the Del Norte County region: large outcroppings of hard substrate within large areas of soft substrate.

Recently, many studies have created categorical predictive layers using high backscatter coupled with *in situ* sampling (Brown et al. 2011). The acoustic survey datasets used in this study were dissimilar in that only one was processed to indicate the primary and secondary substrate types along each transect (Greene et al. 1995), thus this additional habitat classification data could not be used in the modeling efforts. I attempted to classify substrate using backscatter data (Whitmire et al. 2004), but was unable to distinguish between sandy and muddy substrates, which appeared to be an important factor to consider in all three fine-scale regions examined. During video

processing, *S. pinniger* was most often observed at the interface of mud and contiguous rock.

CONCLUSIONS

In this study, I successfully created predictive models at multiple scales to elucidate *S. pinniger* habitat use. *S. pinniger* habitat use at the interface between hard and soft substrates was consistent in all study regions at both scales. This finding is consistent with previous research in which *S. pinniger* was found to occur near the interface of soft and hard substrata (Carr 1991). The other covariates I used in both the broad- and fine-scale modeling efforts only slightly varied in their importance, with the exception of the Humboldt County South Cape Mendocino region (Table 8).

Future research could be incorporate not only metrics derived from seafloor bathymetry data, but also data pertaining to macroinvertebrate habitat structures, oceanic currents, seawater water temperature, seawater pH, nutrient availability, kelp forest cover, and most importantly classification of primary and secondary substrate types for all transects within the study region (Greene et al. 1995; Whitmire et al. 2007). Future studies could also benefit from more accurate estimation of fish length, potentially by using software like EventMeasure (SeaGIS Pty Ltd, Bacchas Marsh, Victoria, Australia), recently employed by Dunlop et al. (2015) to measure mobile epibenthic megafauna.

Habitat suitability maps like these have numerous useful applications including prioritization of habitat conservation and the evaluation of anthropogenic impacts at both broad- and fine-scales. Model selection should include comprehensive evaluation of the spatial distribution of predicted habitat, response curves, and AUC and AIC values. Uncertainty estimation is valuable when using an approach like habitat suitability

modeling to inform decision-making despite limitations in the available data (Johnson and Gillingham 2004).

Distribution and abundance information along the northern California coast for this species will be valuable to state and federal fishery managers. These results provide a method for studying the distributions of other Pacific coast rockfish species across a multitude of coastal habitats and a technique for integrating uncertainty analyses as well. The results of this study will be useful to state and federal fishery managers by providing insight into: the distribution and abundance of fish and suitable habitat; ways that MPA design and monitoring efforts might be improved; and identification of important areas that could benefit from restoration.

LITERATURE CITED

Able, K. W., D. C. Twitchell, C. G. Grimes, and R. S. Jones. (1987). Sidescan sonar as a tool for detecting demersal fish habitats. Fish. Bull. 85:725–744.

Anderson, R.P. and I. Gonzalez, Jr. (2011). Species-specific tuning increases robustness to sampling bias in models of species distributions: an implementation with MaxEnt. Ecological Modelling, 222:2796–2811.

Auster, P.J., J. Lindholm, and P.C. Valentine. (2003). Variation in habitat use by juvenile Acadian redfish, *Sebastes fasciatus*. Environmental Biology of Fishes 68:381-189.

Auster, P.J. (2005). Are deep-water corals important habitats for fishes? In: A. Freiwald and J.M. Roberts, editor. Cold-water corals and ecosystems. Berlin: Springer-Verlag; p. 747–760.

Baldwin, R.A. (2009). Use of maximum entropy modeling in wildlife research. Entropy 11:854-866.

Barve, N., V. Barve, A. Jimenez-Valverde, A. Lira-Noriega, S.P. Maher, A.T. Peterson, J. Soberon, and F. Villalobos. (2011). The crucial role of accessible area in ecological niche modeling and species distribution modeling. Ecological Modelling 222:1810-1819.

Beck, M.W. (2000). Separating the elements of habitat structure: independent effects of habitat complexity and structural components on rocky intertidal gastropods. Journal of Experimental Marine Biology and Ecology, 249(1):29-49.

Bellamy, C., C. Scott, and J. Altringham. (2013). Multiscale, presence-only habitat suitability models: fine-resolution maps for eight bat species. Journal of Applied Ecology 50:892-901.

Bloeser, J. A. (1999). Diminishing returns: the status of west coast rockfish. Pacific Marine Conservation Council, P.O. Box 59, Astoria, OR 97103

BlueSpray GIS Software. (2013). SchoonerTurtles, Inc. <*http://www.schoonerturtles.com*>, 2013.

Bohrer do Amaral, K., D.J. Alvares, L. Heinzelmann, M. Borges-Martins, S. Siciliano, and I.B. Moreno. (2015). Ecological nice modeling of stenella dolphins

(Cetartiodactyla: Delphinidae) in the southeastern Atlantic Ocean. Journal of Experimental Marine Biology and Ecology 472:166-179.

Bolstad, P. (2012). *GIS Fundamental: A First Text on Geographic Information System* (4th ed.) Eider Press, USA.

Brown, C.J., S.J. Smith, P. Lawton, and J.T. Anderson. (2011) Benthic habitat mapping: a review of progress towards improved understanding of the spatial ecology of the seafloor using acoustic techniques. Estuarine, Coastal and Shelf Science. 92: 502-520.

Burnham, K. and D. Anderson. (2002). Model Selection and Multimodel Inference: A Practical Information-Theoretic Approach. Springer. New York, NY.

Busby, M.S., K.L. Mier, and R.D. Brodeur. (2005). Habitat associations of demersal fishes and crabs in the Pribilof Islands region of the Bering Sea. Fisheries Research 75: 15-28.

Caley, M. J., and J. St John. (1996). Refuge availability structures assemblages of tropical reef fishes. The Journal of Animal Ecology, 65, 414−428. Ecological Modeling.

Carr, M. (1991). Habitat selection and recruitment of an assemblage of temperate zone reef fishes. Journal of Experimental Marine Biological Ecology. 146:113-137.

Convertino, M., P. Welle, R. Munoz-Carpena, G.A. Kiker, M. Chu-Agor, R.A. Fischer, and I. Linkov. (2012). Epistemic uncertainty in predicting shorebird biogeography affected by sea-level rise. Ecological Modeling. 240:1-15.

Costa, B., J.C.Taylor, L. Kracker, T. Battista, and S. Pittman. (2014). Mapping reef fish and the seascape: using acoustics and spatial modeling to guide coastal management. PLoS ONE 9: e85555

Dormann, C. F., J. Elith, S. Bacher, C. Buchmann, G. Carl, G. Carré, G., and T. Münkemüller. (2013). Collinearity: a review of methods to deal with it and a simulation study evaluating their performance. Ecography, 36(1), 27-46.

Dorenbosch, M., M.G.G. Grol, I. Nagelkerken, and G. van der Velde. (2005). Distribution of coral reef fishes along a coral reef−seagrass gradient: edge effects and habitat segregation. Marine Ecology Progress Series 299:277−288.

Dudík, M., R.E. Schapire, and S.J. Phillips. (2005). Correcting sample selection bias in maximum entropy density estimation. Appearing in Advances in Neural Information Processing Systems. Vol. 18.

Dunlop, K.M., L.A. Kuhnz, H. A. Ruhl, C. L. Huffard, D. W. Caress, R. G. Henthorn, B. W. Hobson, P. McGill, and K. L. Smith. (2015). An evaluation of deep-sea benthic megafauna length measurements obtained with laser and stereo camera methods. Deep-Sea Research. Part I, 96, pp. 38–48

Eastman, JR. (1999). Guide to GIS and Image Processing. vol. 2. Clark University; Worcester, MA: Idrisi32.

Elith, J., C.H. Graham, R.P. Anderson, M. Dudík, S. Ferrier, A. Guisan, R.J. Hijmans, F. Huettmann, J.R Leathwick, A. Lehmann, J. Li, L.G. Lohmann, B.A. Loiselle, F. Manion, C. Moritz, M. Nakamura, Y. Nakazawa, J.M.M. Overton, A.T. Peterson, S.J. Phillips, K. Richardson, R. Scachetti-Pereira, R.E. Scharire, J. Soverón, S. Williams, M.S. Wisz, and N.E. Zimmermann. (2006). Novel methods improve prediction of species' distributions from occurrence data. Ecography 29: 129–151.

Elith, J., M. Kearney, and S.J. Phillips. (2010). The art of modelling range-shifting species. Methods Ecol Evol 1: 330–342.

Fielding, A.H., and J.F. Bell. (1997). A review of methods for the assessment of prediction errors in conservation presence/absence models. Environmental Conservation 24:38–49.

Fielding, A.H., and P.F. Haworth. (1995). Testing the generality of bird-habitat models. Conservation Biology. 9:1466–1481.

Fitzpatrick, M.C., N.J. Gotelli, and A.M. Ellison. (2013). MaxEnt vs. Maxlike: Empirical comparisons with and species distributions. Ecosphere 4:1-15.

Franklin, J. (2009). Mapping species distributions. *Cambridge University Press* pp 278.

Friedlander, A. M., and F. Parrish. (1998). Habitat characteristics affecting fish assemblages on a Hawaiian coral reef. Journal of Experimental Marine Biology and Ecology, 224,1−30.

Fox, D., M. Amend, and A. Merems. (1999). Nearshore rocky reef assessment. Coastal Management Section 309 Grant. Contract No. 99-072. Oregon Department of Fish and Wildlife, 2040 SE Marine Science Drive, Newport, OR 97365

Garcia-Alegre, A., F. Sánchez, M. Gómez-Ballesteros, H. Hinz, A. Serrano, and S. Parra. (2014). Modelling and mapping the local distribution of representative species on

the Le Danois Bank, El Cachucho Marine Protected Area (Cantabrian Sea) Deep Sea Res. Part II, 106 (2014), pp. 151–164

Gratwicke, B., and M.R. Speight. (2005). The relationship between fish species richness abundance and habitat complexity in a range of shallow tropical marine habitats. Journal of Fish Biology, 66, 650−667.

Greene, H. G., M. M. Yoklavich, D. Sullivan, and G. Cailliet. (1995). A geophysical approach to classifying marine benthic habitats: Monterey Bay as a model. Alaska Dep. Fish and Game Special Publ. 9:15–30.

Gu, W., and R.K. Swihart. (2004). Absent or undetected? Effects of non-detection of species occurrence on wildlife-habitat models. *Biological Conservation*. 116:195–203. Guinotte, J.M. and A.J. Davies. (2012) Predicted deep-sea coral habitat suitability for the U.S. West Coast. Report to NOAA-NMFS. 85 pp.

Guisan A, and W. Thuiller. (2005) Predicting species distribution: offering more than simple habitat models. Ecology Letters 8(9):993-1009.

Guisan, A., and N.E. Zimmermann. (2000). Predictive habitat distribution models in ecology. *Ecological Modelling*, 135:147–186.

Handley, J.A. and B.J. McNeil. (1982). The meaning and use of the area under the receiver operating characteristic curve. Radiology 143:29-36.

Hermosilla, C., F. Rocha, and V.D. Valavanis. (2011). Assessing *Octopus vulgaris* distribution using presence-only model methods. Hydrobiologia, 670 (2011), pp. 35–47

Hixon, M.A., D.W. Johnson, and S.M. Sogard. (2014). BOFFFFs: on the importance of conserving old-growth age structure in fishery populations. Journal of Marine Science. 71(8):2171-2185.

Hughes Clarke, J. E., L. A. Mayer, and D. E. Wells. (1996). Shallow-water imaging multibeam sonars: a new tool for investigating seafl oor processes in the coastal zone and on the continental shelf. Mar. Geophys. Res. 18:607–629.

Hyde, J.R., C.A. Kimbrell, J.E. Budrick, E.A. Lynn, and R.D. Vetter. (2008). Cryptic speciation in the vermilion rockfish (Sebastes miniatus) and the role of bathymetry in the speciation process. Mol. Ecol. 17:1122-1136.

Idrisi 32.11, 2000. Guide to GIS and Image Processing, vols, 1-2. Clark Labs, Worcester, MA.

Iampietro, P. J., and R. G. Kvitek. (2002). Quantitative Seafloor Habitat Classification using GIS Terrain Analysis: Effects of Data Density, Resolution and Scale (Poster), Symposium on Effects of Fishing Activities on Benthic Habitats: Linking Geology, Biology, Socioeconomics, and Management, Tampa, FL.

Iampietro, P.J., E. Summers-Morris, and R.G. Kvitek. (2004). Species-Specific Marine HabitatMaps from High-Resolution, Digital Hydrographic Data, 24th Annual ESRI User Conference. San Diego, CA: ESRI.

Jaynes, E.T. (1957). Information theory and statistical mechanics. Physical Review. 106, 620-630.

Jenness, J., 2003. *Grid Surface Areas: Surface Area and Ratios from Elevation Grids* [Electronic manual]. Jenness Enterprises: ArcView Extensions, http://www.jennessent.com/arcview/arcview_extensions.htm

Jenness, J. (2004). Calculating Landscape Surface Area from Digital Elevation Models. *Wildlife Society Bulletin (1973-2006),* 32(3), 829-839. Retrieved from http://www.jstor.org/stable/3784807

Johnson, C., & Gillingham, M. (2004). Mapping uncertainty: Sensitivity of wildlife habitat ratings to expert opinion. Journal of Applied Ecology, 41(6), 1032-1041.

Johnson, S.W., M.L. Murphy, and D.J. Csepp (2003). Distribution, Habitat, and Behavior of Rockfishes, *Sebastes* spp., in Nearshore Waters of Southeastern Alaska: Observations From a Remotely Operated Vehicle. *Environmental Biology of Fishes* 66(3), 259.

Jones, M.C., S.R. Dye, J.K. Pinnegar, R. Warren, and W.W.L. Cheung. (2013). Modelling commercial fish distributions: prediction and assessment using different approaches. Ecological Modelling, 225, pp. 133–145.

Jordan, A., M. Lawler, V. Halley, and N. Barrett. (2005). Seabed habitat mapping in the Kent Group of islands and its role in marine protected area planning. Aquatic Conservation: *Marine and Freshwater Ecosystems* 15:51–70.

Karpov, K.A., A. Lauermann, M. Bergen, and M. Prall. (2006). Accuracy and precision of measurements of transect length and width made with a remotely operated vehicle. Marine Technology Society Journal 40(3):79-85.

Lamb, A. and P. Edgell (1986). *Coastal Fishes of the Pacific Northwest*. BC, Canada: Harbour Publishing.

Lauermann, A.R. (2015) September/October 2014 ROV Survey Interim Report: North Coast Marine Protected Area Study Region Remotely Operation Vehicle Deployment 3, Contract #P1370005. Marine Applied Research and Exploration. (unpublished manuscript)

Lauermann, A.R., D. Rosen, K. Martin-Harbick, H.M. Lovig, D. Kline, and R. Starr. (2017) North Coast Baseline Program Final Report: Mid-depth and Deep Subtidal Ecosystems. California Sea Grant, San Diego, CA. (in press)

Leathwick, J.R., J. Elith, M.P. Francis, T. Hastie, and P. Taylor. (2006). Variation in demersal fish species richness in the oceans surrounding New Zealand: an analysis using boosted regression trees. *Mar Ecol Prog Ser* 321, 267–281.

Lobo, J. M., A. Jiménez-Valverde, and R. Real. (2008). AUC: a misleading measure of the performance of predictive distribution models. Global Ecology and Biogeography 17: 145 –151.

Love, M.S., M. Yoklavich and L. Thorsteinson. (2002). The rockfishes of the Northeast Pacific. University of California Press. 404 p.
DOI: http://dx.doi.org/

Love, M.S., D.M. Schroeder, B. Lenarz, and G.R. Cochrane (2006). Gimme shelter: The importance of crevices to some fish species inhabiting a deeper-water rocky outcrop in southern California. California Cooperative Ocean Fishing Investigation Report 47:119-126.

Love, M.S. and M. Yoklavich (2006). Deep Rock Habitats. In: Allen LG, Pondella DJ, Horn MH, editors. The Ecology of Marine Fishes, California and Adjacent Waters. Berkeley and Los Angeles: University of California Press; p. 253-266.

Lucieer, V.L. (2008). Object-oriented classification of sidescan sonar data for mapping benthic marine habitats. International Journal of Remote Sensing 29, 905–921.

Luckhurst, B. E. and K. Luckhurst (1978). Analysis of the influence of substrate variables on coral reef communities. Marine Biology, 49, 317−323.

Lundblad, E.R., D.J. Wright, J. Miller, E.M. Larkin, R. Rinehart, D.F. Naar, B.T. Donahue, S.M. Anderson, and T. Battista. (2006). A benthic terrain classification scheme for American samoa. Marine Geodesy 29, 89–111.

Maravelias, C.D., J. Haralabous and C. Papaconstantino. (2003). Predicting demersal fish species distributions in the Mediterranean Sea using artificial neural networks. *Marine Ecology Progress Series*, 255:249–258.

MAXENT (2012) MaxEnt software for species habitat modeling. Available at: ⟨http:// www.cs.princeton.edu/_schapire/MaxEnt/⟩ (accessed 06.05.16).

Miller, D. J. and R.N. Lea. (1972). Guide to the coastal marine fishes of California. Calif. Dep. Fish Game, Fish Bull. 157,235 p.

Mohn, C. and A. Beckmann. (2002). Numerical studies on flow amplification at an idolated shelfbreak, with application to Porcupine Bank. Continental Shelf Research 22(9):1325-1338.

Moore, I. D., R. B. Grayson, and A. R. Landson. (1991). Digital Terrain Modelling: A Review of Hydrological, Geomorphological, and Biological Applications. Hydrological Processes 5: 3–30.

Nasby-Lucas, N., B. Embley, M.A. Hixon, S.G. Merle, B.N. Tissot, and D.J. Wright. (2002). Integration of submersible transect data and high-resolution multibeam sonar imagery for a habitat-based groundfish assessment of Heceta Bank, Oregon. Fishery Bulletin 100:739-751.

[NMFS] National Marine Fisheries Service. (2014). Designation of Critical Habitat for the Distinct Population Segments of Yelloweye Rockfish, Canary Rockfish, and Bocaccio. Biological Report. http://www.westcoast.fisheries.noaa.gov/publications/protected_species/other/rockfish/rockfish_ch_biological_report.pdf

[NOAA] National Oceanic and Atmospheric Administration. (2017) Fisheries, Protected Resources, Species, Canary Rockfish (*Sebastes pinniger*) Status. Accessed February 2017, http://www.fisheries.noaa.gov/pr/species/fish/canary-rockfish.html

O'Brien, L., and P. Rago. (1996). An application of the generalized additive model to groundfish survey data with Atlantic cod off the Northeast coast of the United States as an example., NAFO Sci. Coun. Studies, 28:79-95.

Olden, J. D. and D. A. Jackson. (2002). A comparison of statistical approaches for modeling fish species distributions. *Freshwater Biology*, 47: 1976–1995.

Orr, J. W., M. A. Brown, and D. C. Baker. (2000). Guide to rockfishes (Scorpaenidae) of the genera Sebastes, Sebastolobus, and Adelosebastes of the Northeast Pacific

Ocean, second edition. U.S. Dep. Commer., NOAA Tech. Memo. NMFS-AFSC-117, 47 p.

Peterson, A. T., M. Papes, and J. Soberón. (2008). Rethinking receiver operating characteristic analysis applications in ecological nichemodeling. Ecological Modelling 213:63–72.

Parolo, G., G. Rossi, and A. Ferrarini. (2008). Toward improved species niche modelling: *Arnica montana* in the Alps as a case study. J. Appl. Ecol. 45, 1410–1418.

PFMC (Pacific Fishery Management Council). (2003). Status of the Pacific Coast Groundfish Fishery Through 2003: Stock Assessment and Fishery Evaluation. Pacific Fishery Management Council, Portland, OR.

Phillips, S.J., M. Dudík, and R.E. Schapire. (2004). A maximum entropy approach to species distribution modeling. Proceedings of the twenty-first international conference on Machine learning. New York, New York, USA: ACM. p. 83.

Phillips, S.J. and J. Elith. (2010). POC plots: calibrating species distribution models with presence-only data. Ecology, 91:2476–84.

Pittman, S.J., C.A. McAlpine, and K.M. Pittman. (2004). Linking fish and prawns to their environment: a hierarchial landscape approach. Marine Ecology Progress Series 283:233-254.

Pittman, S.J., and K.A. Brown. (2011). Multi-Scale approach for predicting fish species distributions across coral reef seascapes. PLoSONE 6(5):1-12.

Pittman, S.J., B.M. Costa, and T.A. Battista. (2009). Using Lidar Bathymetry and Boosted Regression Trees to Predict the Diversity and Abundance of Fish and Corals. Journal of Coastal Research. 25:27–38.

Pittman, S.J., J.D. Christensen, C. Caldow, C. Menza, and M.E. Monaco. (2007). Predictive mapping of fish species richness across shallow-water seascapes in the Caribbean. Ecological Modelling 204:9−21.

Plant, R. E. (2012). Spatial data analysis in ecology and agriculture using R. Boca Raton: CRC Press.

R Core Team. (2014). R: A language and environment for statistical computing. R Foundation for Statistical Computing, Vienna, Austria. URL http://www.R-project.org/

Radosavljevic, A., and R.P. Anderson. (2014). Making better MaxEnt models of species distributions: complexity, overfitting, and evalution. Journal of Biogeography 41:629-643.

Ready, J., K. Kaschner, A.B. South, P.D. Eastwood, T. Rees, J. Rius, E. Agbayani, S. Kullander, and R. Froese. (2010). Predicting the distributions of marine organisms at the global scale. *Ecological Modelling*, vol. 221, p. 467-478.

Richards, L. (1986). Depth and habitat distributions of three species of rockfish (*Sebastes*) in British Columbia: observations from the submersible PISCES IV. Environmental Biology of Fishes 17(1):13-21.

Ries, L., R.J. Fletcher Jr., J. Battin, and T.D. Sisk. (2004). Ecological responses to habitat edges: mechanisms, models, and variability explained. Annual Review of Ecological and Evolutionary Systems 35:491-522.

Roberts, J.M., C.J. Brown, D. Long, and C.R. Bates. (2005). Acoustic mapping using a multibeam echosounder reveals cold-water coral reefs and surrounding habitats. Coral Reefs 24(4):654-669.

Roberts, C. M., and R.F.G. Ormond. (1987). Habitat complexity and coral reef fish diversity and abundance on Red Sea fringing reefs. Marine Ecology Progress Series, 41, 1−8.

Rochet, M. J., J. F. Cadiou, and V. M. Trenkel. (2006). Precision and accuracy of fish length measurements obtained with two visual underwater methods. Fish. Bull. 104:1–9.

Stein, D. L., B. N. Tissot, M. A. Hixon, and W. Barss. (1992). Fish-habitat associations on a deep reef at the edge of the Oregon continental shelf. Fish. Bull. 90:540–551.

Thorson, J.T. and C. Wetzel. (2015). The status of the canary rockfish (*Sebastes pinniger*) in the California Current in 2015, 682 p. Northwest Fisheries Science Center, US Department of Commerce, National Oceanic and Atmospheric Administration, National Marine Fisheries Service, 2725 Montlake Boulevard East, Seattle, WA 98112-2097.

Tittensor, D.P., A.R. Baco, P.E. Brewin, M.R. Clark, M. Consalvey, J. Hall-Spencer, A.A. Rowden, T. Schlacher, K.I. Stocks, and A.D. Rogers. (2009). Predicting global habitat suitability for stony corals on seamounts. Journal of Biogeography 36:1111–1128.

Tissot, BN, M.M. Yoklavich, M.S. Love, K. York, and M. Amend. (2006). Benthic invertebrates that form habitat on deep banks off southern California, with special reference to deep sea coral. Fishery Bulletin 104:167-181.

Valavanis, V. D., G. J. Pierce, A. F. Zuur, A. Palialexis, A. Saveliev, I. Katara and J. Wang. (2008). Modelling of essential fish habitat based on remote sensing, spatial analysis and GIS. *Hydrobiologia* 612:5–20.

Valentine, P.C., S.J. Fuller, and L.A. Scully. (2004). Terrain Ruggedness Analysis and Distribution of Boulder Ridges in the Stellwagen Bank National Marine Sanctuary Region (poster). Galway, Ireland: 5th International Symposium on Marine Geological and Biological Habitat Mapping (GeoHAB), May 2004.

VanDerWal, J., L.P. Shoo, C. Graham, and S.E. Williams. (2009). Selecting pseudo-absence data for presence-only distribution modeling: How far should you stray from what you know? Ecological Modelling 220:589-594.

Wakefield, W.W., C.E. Whitmiren, J.E.R. Clemons, and B.N. Tissot. (2005). Fish habitat studies: combining high-resolution geological and biological data. American Fisheries Society Symposium 41:119-138.

Warren, D.L., and S.N. Seifert. (2011). Environmental niche modeling in MaxEnt: the importance of model complexity and the performance of model selection criteria. Ecological Applications 21:335-342. (doi: 10.1890/10-1171.1)

Wedding, L. and M.M. Yoklavich. (2015). Habitat-based perdicgtive mapping or rockfish density and biomass off the central California coast. Marine Ecology Progress Series 540: 235-250.

Weiss, A. D. (2001). Topographic Positions and Landforms Analysis (poster), ESRI International User Conference, July 2001. San Diego, CA: ESRI.

Whitmire, CE, and E. Clarke. (2007). State of deep coral ecosystems of the U.S. Pacific Coast: California to Washington. Pp. 109-154. In: SE Lumsden, Hourigan TF, Bruckner AW and Dorr G (eds.) The State of Deep Coral Ecosystems of the United States. NOAA Technical Memorandum CRCP-3. Silver Spring MD 365 pp.

Whitmire, CE, W.W. Wakefield, R.W. Embly, S.G. Merle, B.N. Tissot, and N. Puniwai. (2004). Quantitative benthic habitat characterization at Heceta Bank, Oregon. The Journal of the Acoustical Society of America 116(4):2486.

Wilson, M.F.J., B. O'Connell, C. Brown, J.C. Guinan, and A.J. Grehan. (2007). Multiscale terrain analysis of multibeam bathymetry data for habitat mapping on the continental slope. Marine Geodesy 30, 3–35.

Worm, B., E.B. Barbier, N. Baeumont, J.E. Duffy, C. Folke, B.S. Halpern, J.B.C. Jackson, H.K. Lotze, F. Micheli, S.R. Palumbi, E. Sala, K.A. Selkoe, J.J. Stachowicz, and R. Watson. (2006). Impacts of biodiversity loss on ocean ecosystem services. Science. 314: 787-790.

Yoklavich, M.M., G.M. Cailliet, D.E. Sullivan, R.N. Lea, H.G. Greene, R. Starr, J. DeMarignac, and J. Field. (2002). Deepwater habitat and fish resources associated with the Big Creek Marine Ecological Reserve. CCOFI Rep 43:120-140

Yoklavich, M.M., G. M. Cailliet, G. Greene, and D. Sullivan. (1995). Interpretation of sidescan sonar records for rockfish habitat analysis: examples from Monterey Bay. Alaska Dep. Fish and Game Special Publ. 9:11–14.

Yoklavich, M.M., G.H. Greene, G.M. Cailliet, D.E. Sullivan, R.N. Lea, and M.S. Love. (2000). Habitat associations of deep-water rockfishes in a submarine canyon: an example of a natural refuge. Fishery Bulletin 98:625-641.

Young, M.A., P.J.Iampietro, R.G. Kvitek, and C.D. Garza. (2010). Multivariate bathymetry-derived generalized linear model accuracy predicts rockfish distribution on Cordell Bank, California, USA. Marine Ecology Progress Series 415:247-261

Zweig, M.H. and G. Campbell. (1993). Receiver-operating characteristic (ROC) plots – a fundamental evaluation tool in clinical medicine. Clinical Chemistry 39:561–577.

APPENDIX A

Appendix A. All Environmental covariates used in the broad-scale habitat suitability models for the Del Norte County coastline: (A) depth, (B) cost distance, (C) rugosity, (D) aspect, (E) slope, (F) fine-scale BPI, (G) broad-scale BPI, and (H) VRM.

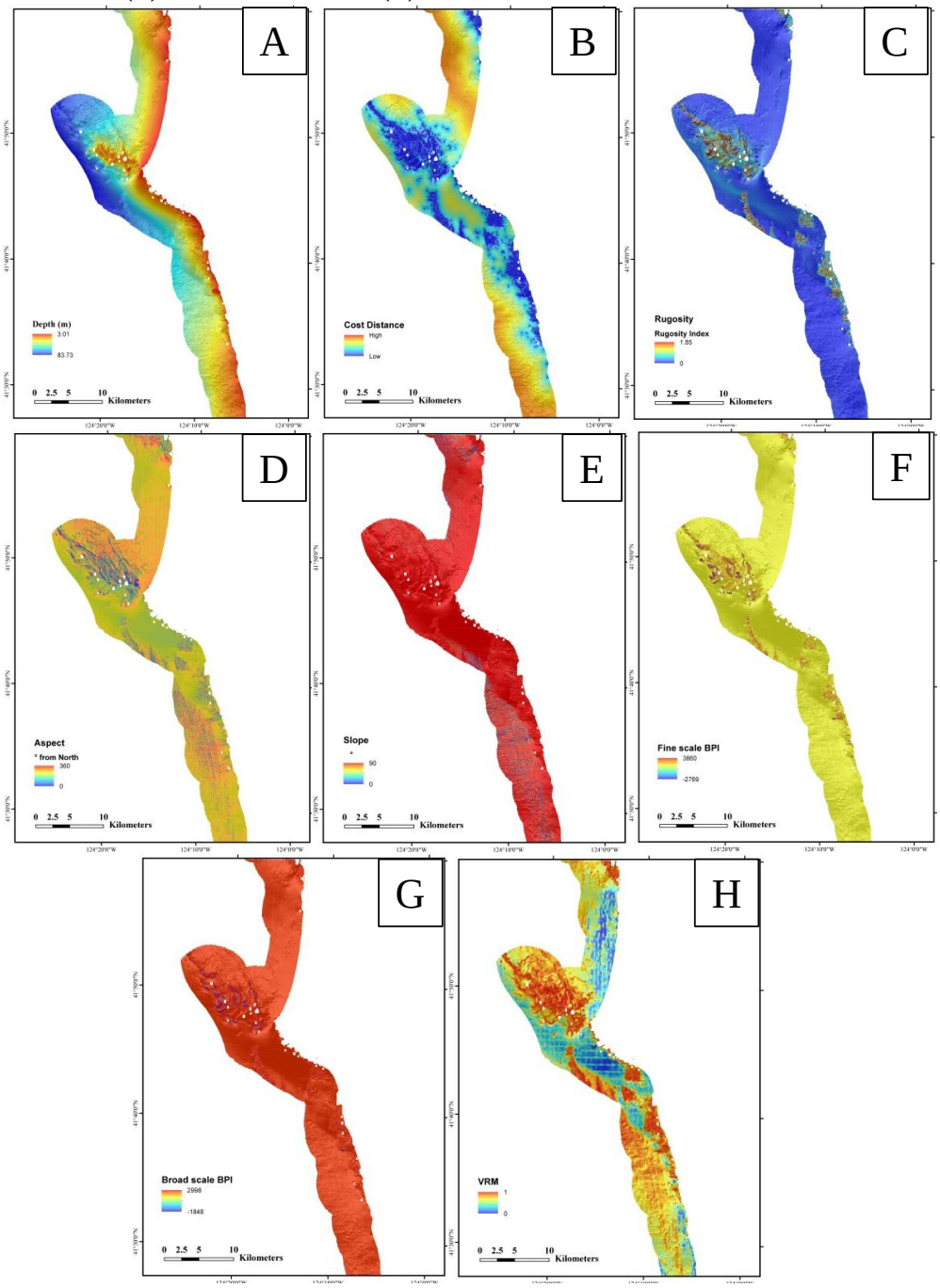

APPENDIX B

Appendix B. All Environmental covariates used in the broad-scale habitat suitability models for the Humboldt County coastline: (A) depth, (B) cost distance, (C) rugosity, (D) aspect, (E) slope, (F) fine-scale BPI, (G) broad-scale BPI, and (H) VRM.

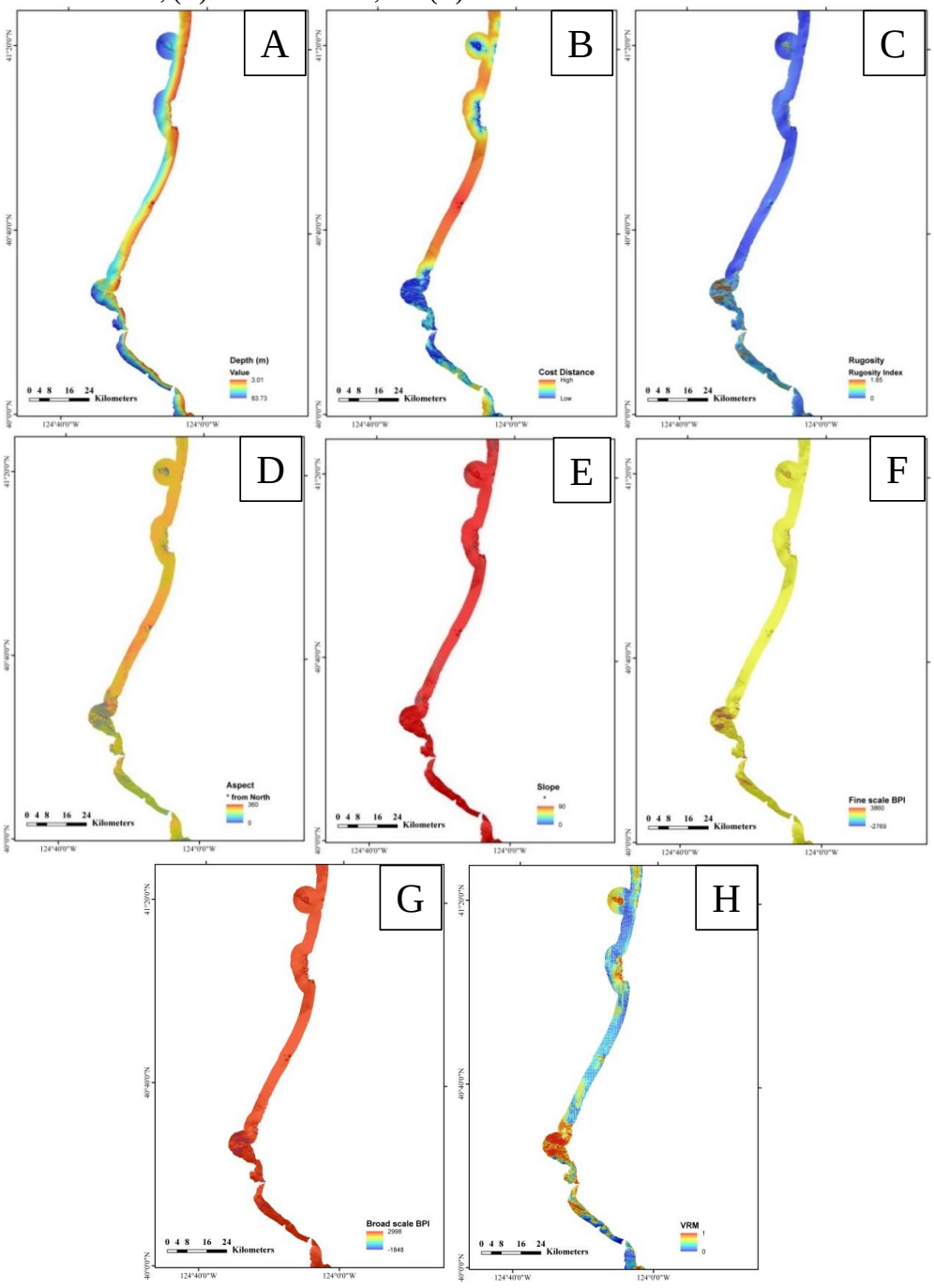

APPENDIX C

Appendix C. All Environmental covariates used in the broad-scale habitat suitability models for the Humboldt Mendocino County coastline: (A) depth, (B) cost distance, (C) rugosity, (D) aspect, (E) slope, (F) fine-scale BPI, (G) broad-scale BPI, and (H) VRM.

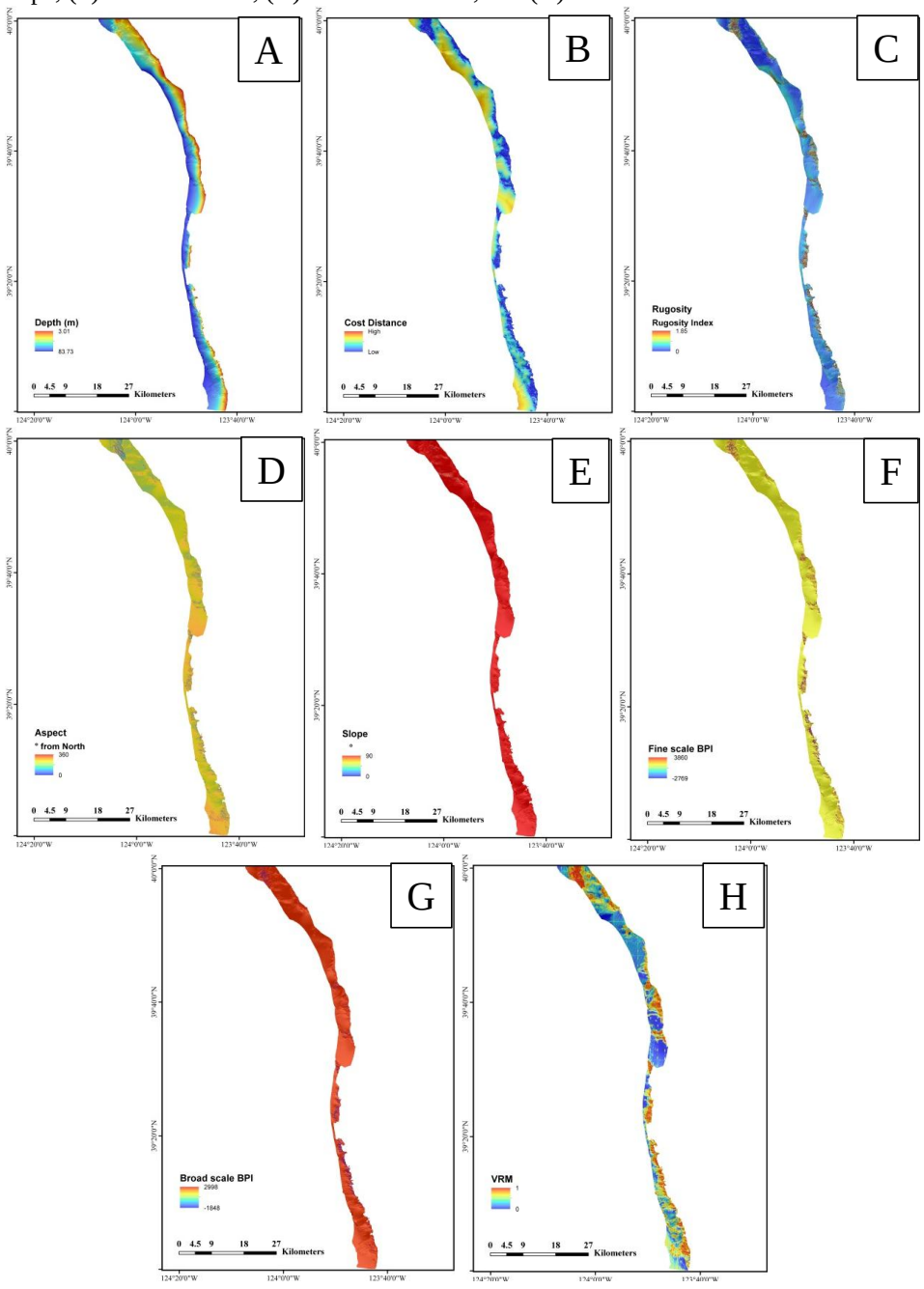

APPENDIX D

Appendix D. All Environmental covariates used in the fine-scale habitat suitability models for the Point Saint George area of the Del Norte County study: (A) Aspect, (B) broad-scale BPI, (C) VRM, (D) fine-scale BPI, (E) cost distance, (F) curvature, (G) rugosity, (H) depth, and (I) slope.

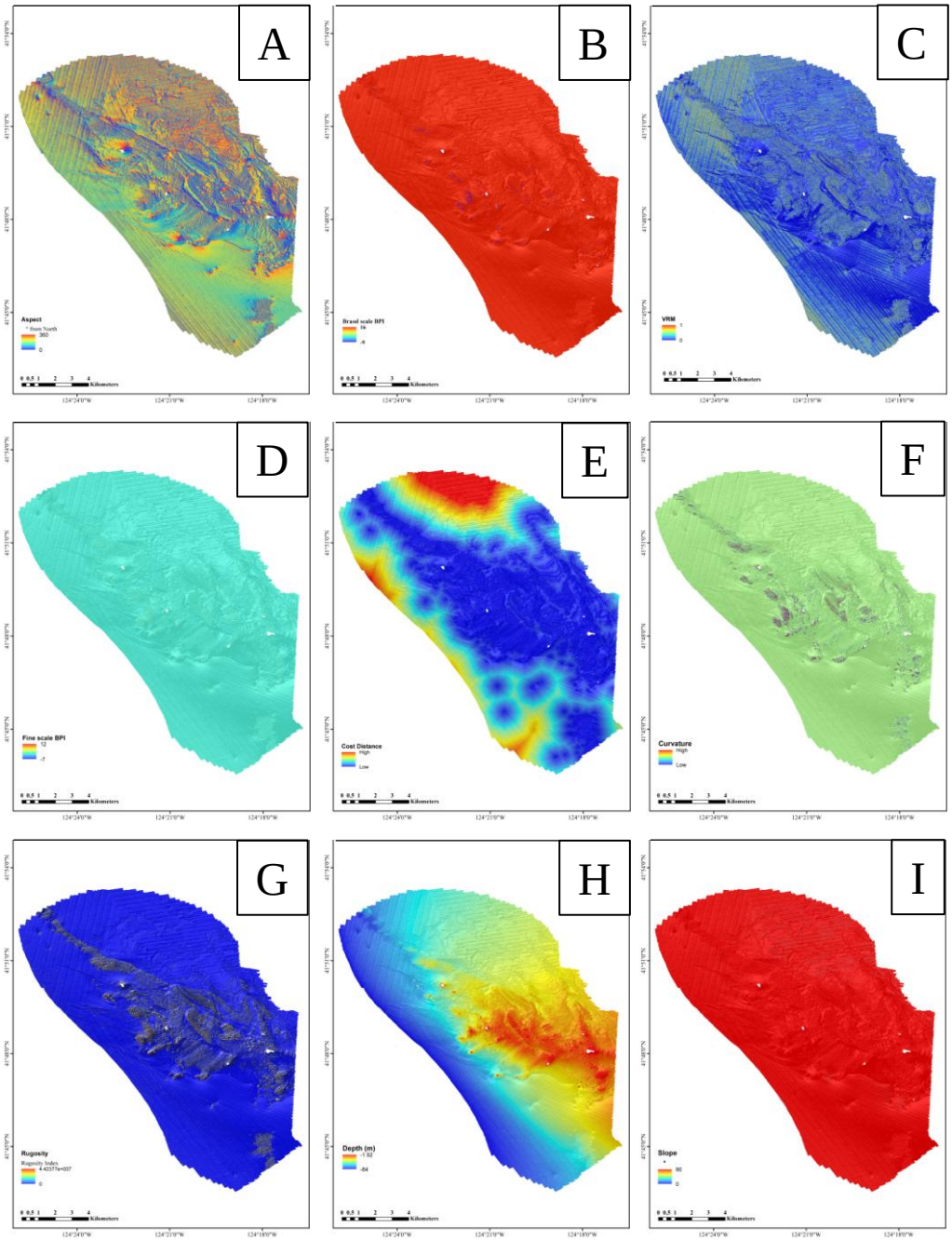

APPENDIX E

Appendix E. All Environmental covariates used in the fine-scale habitat suitability models for the South Cape Mendocino in the Humboldt County study region: (A) Aspect, (B) broad-scale BPI, (C) VRM, (D) fine-scale BPI, (E) cost distance, (F) curvature, (G) rugosity, (H) depth, and (I) slope.

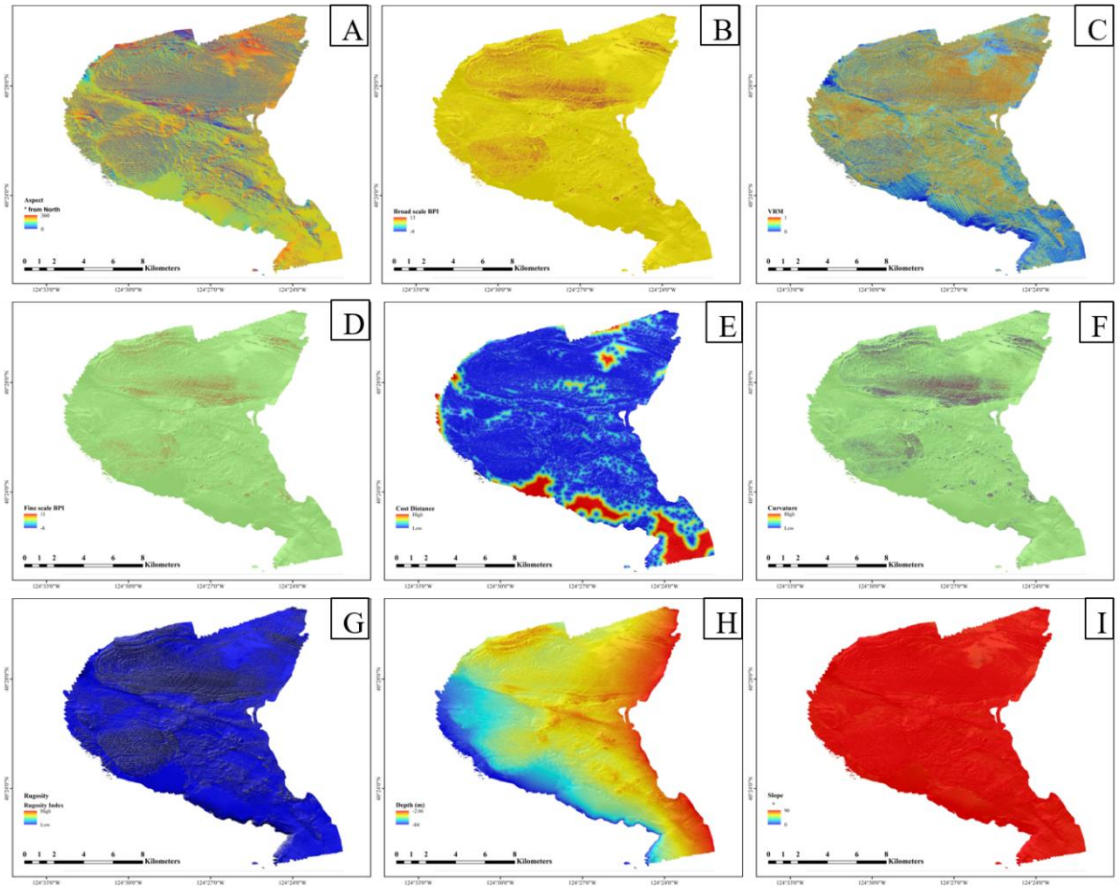

APPENDIX F

Appendix F. All Environmental covariates used in the fine-scale habitat suitability models for the Ten Mile Beach in the Mendocino County study region: (A) Aspect, (B) broad-scale BPI, (C) VRM, (D) fine-scale BPI, (E) cost distance, (F) curvature, (G) rugosity, (H) depth, and (I) slope.